Chapter III

Results

The Evaluations of Chitosan Solution

1. The determination of molecular weight of chitosan

The efflux time and density of deionized water and chitosan solutions are presented in Table 24 in Appendix I.

The relative viscosity of chitosan solutions are presented in Table11,and the plots between ln η_{rel}/concentration and concentration are shown in Figure10. Intrinsic viscosities, the intercepts of the plots, of the solution of chitosan L, M, and H were 6.83, 7.16 and 9.70 respectively. The viscosity average molecular weights (M_V) calculated from the Mark-Houwink equation of chitosan L, M, and H was 994,453.12, 1,046,197.21 and 1,449,978.86 respectively. The method of calculation is described in Appendix I.

2. Viscosity

The apparent viscosities of chitosan solutions at concentration of 0.25, 0.50, 0.75, 1.50, 2.00 and 3.00 %w/w are presented in Table 12 and Figure 11. The steeper curve of the solution of H indicated that it had much higher viscosity than the solution of M and L respectively. From the curve, the same apparent viscosity of 125 mPa.s of the solutions of L, M, and H was obtained at concentration of 2.025, 1.750, 0.825 %w/w respectively. However, the apparent viscosities of the solutions of L, M, and H at the aforementioned concentrations measured with Hakke viscometer were 125.87(±3.67), 129.83(±4.30) and 123.17(±7.68) mPa.s respectively, and that of combined solution of L and H (1:3) was 118.73(±7.05) mPa.s. The apparent viscosities at concentration 1.00%w/w of the solutions of L, M, and H were 27.2, 34.5 and 175.0 mPa.s respectively.

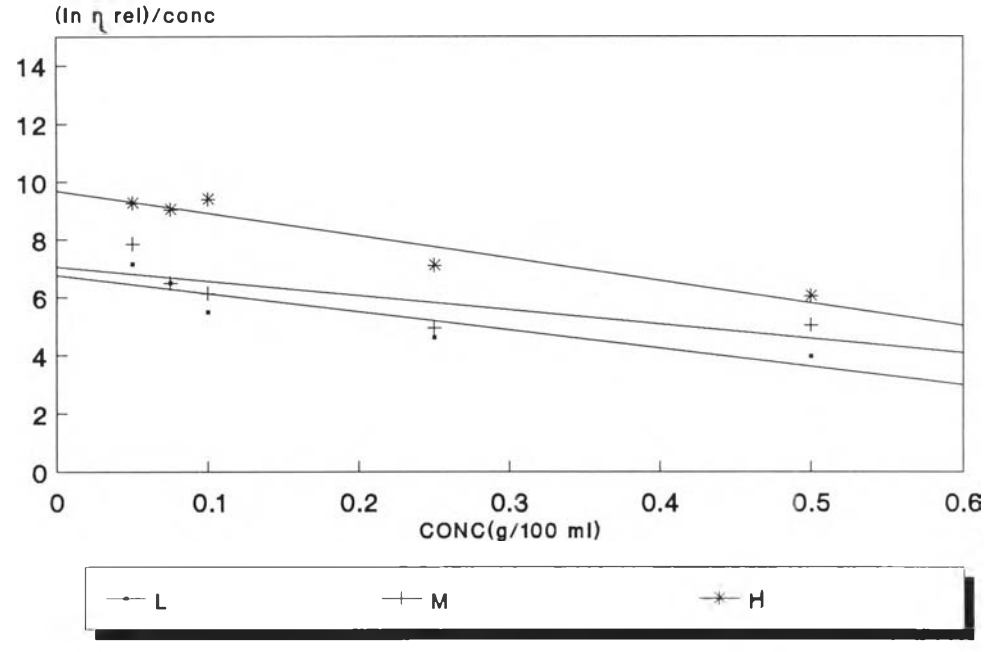

Figure 10 The plots between ln η_{rel}/conc and conc of chitosan solutions.

Table 11 The relative viscosity of chitosan solutions.

CONC. (g/100ml)	CHITOSAN L		CHITOSAN M		CHITOSAN H	
	η rel	(ln η rel)/conc. (100ml/g)	η rel	(ln η rel)/conc. (100ml/g)	η rel	(ln η rel)/conc. (100ml/g)
0.050	1.43	7.15	1.48	7.84	1.59	9.27
0.075	1.63	6.51	1.63	6.51	1.97	9.04
0.100	1.73	5.48	1.85	6.15	2.56	9.40
0.250	3.17	4.61	3.44	4.94	5.91	7.11
0.500	7.20	3.95	12.40	5.04	20.63	6.05

Table 12 The apparent viscosity of chitosan solutions.

VISCOSITY OF CHITOSAN SOLUTIONS				
CHITOSAN L				
CONC		SAMPLE		AVG(SD)
(g/100g)	A	B	C	(mPa.s)
0.250	6.26	6.19	6.07	6.17(0.10)
0.500	13.62	14.65	12.23	13.50(1.21)
0.750	16.74	18.31	19.52	18.19(1.39)
1.500	52.03	56.04	61.87	56.65(4.95)
2.000	124.20	116.90	117.10	119.40(4.16)
3.000	352.20	368.90	369.50	363.53(9.82)
CHITOSAN M				
CONC		SAMPLE		AVG(SD)
(g/100g)	A	B	C	(mPa.s)
0.250	4.55	4.62	4.29	4.49(0.17)
0.500	15.12	15.91	16.04	15.69(0.50)
0.750	25.68	25.34	22.83	24.62(1.56)
1.500	75.58	74.93	74.87	75.13(0.39)
2.000	211.60	200.70	238.00	216.77(19.18)
3.000	781.80	752.90	726.40	753.70(27.71)
CHITOSAN H				
CONC		SAMPLE		AVG(SD)
(g/100g)	A	B	C	(mPa.s)
0.250	18.90	19.62	19.75	19.42(0.46)
0.500	42.99	39.76	40.94	41.23(1.63)
0.750	111.80	105.40	103.40	106.87(4.39)
1.500	389.50	395.20	380.40	388.37(7.46)
2.000	605.70	597.60	593.80	599.03(6.08)

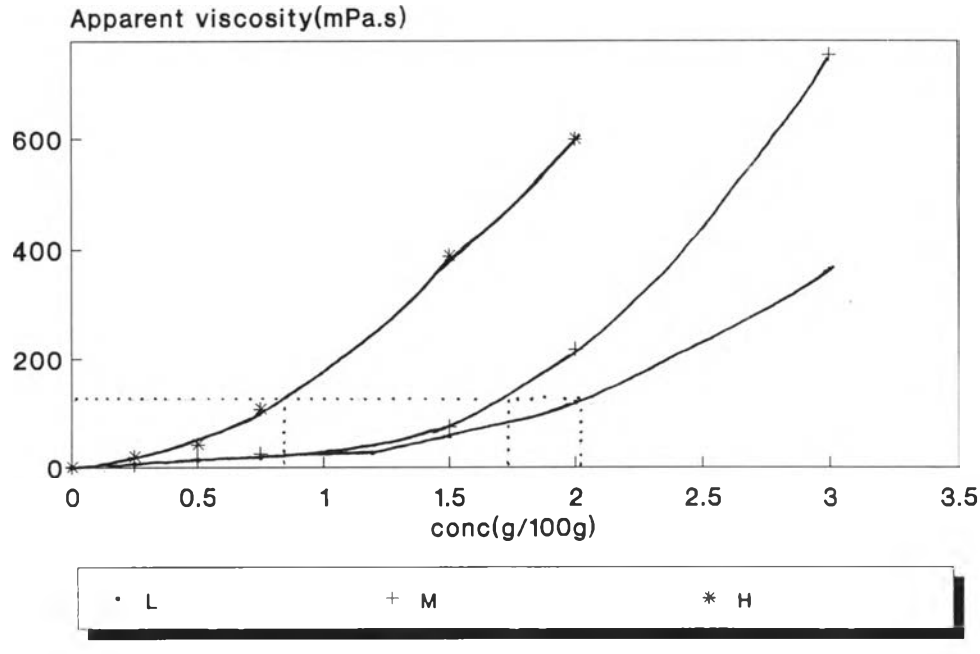

Figure 11 The plot between the apparent viscosity and concentration of chitosan solutions.

3. pH

The pH values of chitosan solutions are shown in Table 13 and are presented in Figrue 12. The pH values of chitosan solutions at the same concentration were nearly equal. The pH profile of the solution M was slightly lower than those of the solutions of L and H, and the pH profile of the solution of L was similar to that of the solution of H, although the pH profile of the solution of L at concentration 0.25-0.5 g/100g was slightly lower than that of the solution of H, and at the concentration 0.5-2.0 g/100g the pH profile of the solution of L was slightly higher than that of solution of H. The pH values of solutions of these three chitosans were between 3.75-5.46, and the pH of the solution of L at concentration 2.025 g/100g was 5.04, the pH of the solution of M at concentration 1.75 g/100g was 4.74 and the pH of the solution of H at concentration 0.825 g/100g was 4.37.

The apparent viscosity and pH value of the solution of chitosan H at concentration 3.00 g/100g could not be measured since it could not be completely hydrated at this concentration and it was too viscous to test.

Tablet Evaluations

1. Weight and thickness increase and tablet appearance

The data of weight and thickness increase and tablet appearence are presented in Table 14.

1.1 Weight variation and weight increase

The mean and standard deviation of the weight of core tablet and coated tablets are shown in Table 25 in Appendix II. They were all within the limit of USP standard. After coating weight of coated tablets was increased between 1.15-1.80 % w/w. The weight of core and coated tablet after kept at room temperature for 1 week was slightly decreased, but after exposure to accelerated condition for 1 week their weights were increased.

1.2 Thickness and thickness increase

Table 13 The pH values of chitosan solutions.

pH OF CHITOSAN L SOLUTION				
CONC		SAMPLE		AVG
(g/100g)	A	B	C	(SD)
0.250	3.73	3.73	3.72	3.73(0.01)
0.500	4.08	4.08	4.08	4.08(0.00)
0.750	4.29	4.30	4.28	4.29(0.01)
1.500	4.70	4.70	4.71	4.70(0.01)
2.000	4.92	4.92	4.93	4.92(0.01)
2.025	5.05	5.05	5.02	5.04(0.02)
3.000	5.47	5.46	5.45	5.46(0.01)
pH OF CHITOSAN M SOLUTION				
CONC		SAMPLE		AVG
(g/100g)	A	B	C	(SD)
0.250	3.73	3.72	3.73	3.73(0.01)
0.500	3.98	4.00	3.99	3.99(0.01)
0.750	4.19	4.19	4.18	4.19(0.01)
1.500	4.58	4.58	4.58	4.58(0.00)
1.750	4.78	4.72	4.73	4.74(0.03)
2.000	4.80	4.71	4.75	4.75(0.05)
3.000	5.10	5.15	5.10	5.12(0.02)
pH OF CHITOSAN H SOLUTION				
CONC		SAMPLE		AVG
(g/100g)	A	B	C	(SD)
0.250	3.81	3.82	3.80	3.81(0.01)
0.500	4.11	4.11	4.12	4.11(0.01)
0.750	4.25	4.29	4.27	4.27(0.02)
0.825	4.38	4.36	4.36	4.37(0.01)
1.500	4.69	4.65	4.70	4.68(0.03)
2.000	4.90	4.91	4.90	4.90(0.01)

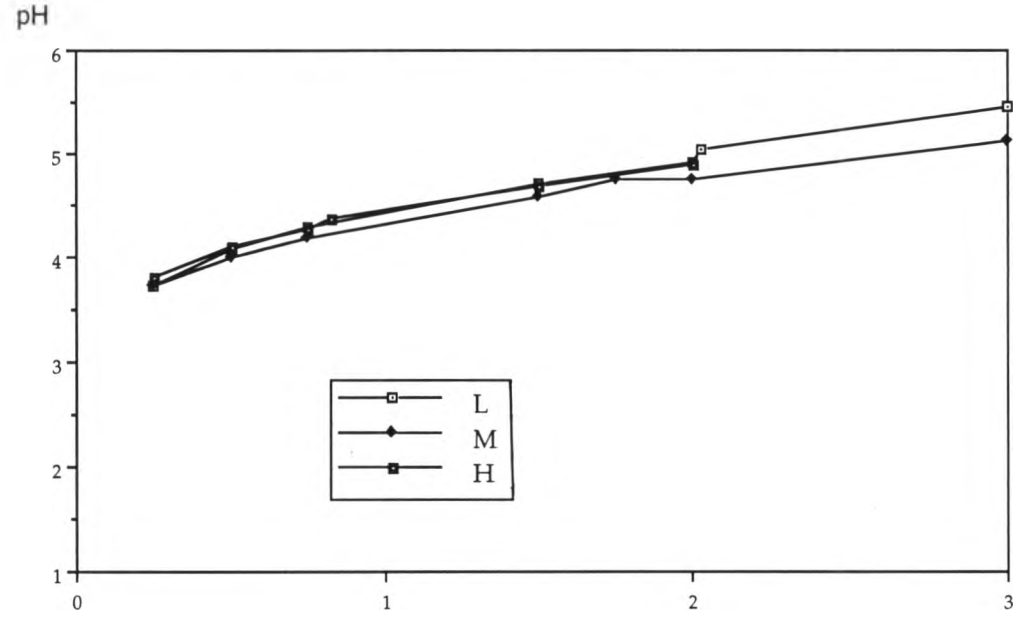

Figure 12 The pH concentration profiles of chitosan solutions.

The thickness of tablets are presented in Table 26 in Appendix II. Their standard deviation never exceeded ± 0.082 mm for all formulations. The range of thickness after coating were between 30-77 μm. The thickness of CORE, L0 and M0 after at room temperature for 1 week (CORE R, L0 R and M0 R) was decreased, but those of H0 R, LA 10 R and LH0 R were slightly increased, whereas the thickness increase of core and coated tablets after exposure to accelerated condition for 1 week was increased.

1.3 The color of tablet

The color of core and coated tablets are presented in Table 14. After preparation, or kept at room temperature for 1 week or exposure to accelerated condition the color of core was white. All formulation of coated tablets had a glossy surface, but with a different shade of color. After coating the color of L0, M0, H0, MA1O, MA20, MA30, MC10, MC20, MC30, was white and that of LA, LB, LC, MB, HA, HB, HC tablets and LH0 tablet was yellowish, and that of LHA system was yellow. After kept at room temperature for 1 week the color of L0 R, M0 R and LA10 R was yellow and that of H0 R and LH0 R was yellowish, whereas the color of coated tablets after exposure to accelerated condition for 1 week of L0 S, M0 S, H0 S and LA10 S tablets was brown, and that of LHO S tablets was yellow.

2. Defect of coated tablet

Some defects of coated tablets are exhibited in Table 14. Variations of defects between formulations could be obviously observed. When using a plasticizer in formulation of chitosan M, H and LH as film former, the cracking and splitting were less than formulations using plasticized chitosan L, except formulations of MC10, MC20, HC10 and HC20. However the picking of plasticized film coated tablet was greater than unplasticized film coated tablets.

The accelerated condition apparently increased the defects, except in LA10 S which the picking was less than in LA10, and the coated tablets which were kept at room temperature for 1 week had more defects than that after preparation.

Table 14 The data of weight and thickness increase, and tablet appearence and defects.

FORMULA	WEIGHT INCREASE(%)	THICKNESS INCREASE(%)	COLOR OF TABLET	% DEFECT		
				CRACKING	SPLIITTING	PICKING
CORE	0.00	0	WHITE			
CORE R	-0.40	-3	WHITE			
CORE S	0.18	13	WHITE			
L0	1.32	55	WHITE	5	6	1
L0 R	0.82	46	YELLOW	5	7	1
L0 S	1.70	60	BROWN	11	9	6
M0	1.25	47	WHITE	7	20	0
M0 R	0.73	43	YELLOW	10	23	0
M0 S	1.74	56	BROWN	8	62	4
H0	1.21	62	WHITE	8	10	1
H0 R	1.06	82	YELLOWISH	8	13	1
H0 S	1.37	93	BROWN	100	41	6
LA10	1.27	74	YELLOWISH	3	12	11
LA10 R	0.91	95	YELLOW	4	12	12
LA10 S	1.49	134	BROWN	7	15	8
LA20	1.80	54	YELLOWISH	2	2	7
LA30	1.47	57	YELLOWISH	9	17	21
LB10	1.64	61	YELLOWISH	4	10	18
LB20	1.43	58	YELLOWISH	7	9	3
LB30	1.69	54	YELLOWISH	0	3	6
LC10	1.71	64	YELLOWISH	9	12	30
LC20	1.15	77	YELLOWISH	9	10	12
LC30	1.31	59	YELLOWISH	2	4	2

Table 14 The data of weight and thickness increase, and tablet appearence and defects (cont.).

FORMULA	WEIGHT INCREASE(%)	THICKNESS INCREASE(%)	COLOR OF TABLET	% DEFECT		
				CRACKING	SPLITTING	PICKING
MA10	1.35	50	WHITE	0	0	2
MA20	1.59	41	WHITE	1	1	7
MA30	1.66	53	WHITE	1	7	2
MB10	1.40	44	YELLOW	0	6	72
MB20	1.38	72	YELLOW	6	4	21
MB30	1.30	55	YELLOW	0	9	31
MC10	1.52	61	WHITE	0	70	0
MC20	1.52	42	WHITE	0	48	0
MC30	1.64	51	WHITE	2	6	9
HA10	1.50	51	YELLOWISH	0	2	1
HA20	1.45	38	YELLOWISH	0	1	1
HA30	1.53	39	YELLOWISH	0	6	7
HB10	1.62	33	YELLOWISH	7	7	35
HB20	1.64	41	YELLOWISH	8	16	26
HB30	1.45	53	YELLOWISH	0	2	47
HC10	1.37	38	YELLOWISH	100	35	7
HC20	1.76	30	YELLOWISH	2	21	3
HC30	1.49	45	YELLOWISH	4	16	5
LH0	1.52	56	YELLOWISH	0	0	0
LH0 R	1.44	60	YELLOWISH	0	1	1
LHO S	2.10	59	YELLOW	0	9	5
LHA10	1.60	47	YELLOW	2	0	3
LHA20	1.38	48	YELLOW	5	8	45
LHA30	1.39	54	YELLOW	2	5	96

3. Friability

The percentage of friability of core tablet and coated tablets (after preparetion, after kept at room temperature for 1 week and after exposure to accelerated condition for 1 week) are shown in Table 27 in Appendix II and depicted in Figure 13(A and B).

From Figure 13 (A), coated tablets were not friable and showed that the weight was slightly more than before test. The percentage of friability of core tablet was 0.25%.

From Figure 13(B), after exposure to the accelerated condition for 1 week or kept at room temperature for 1 week the coated tablets still showed the negative values of percentage of friability, but that of a core tablet after kept at room temperature for 1 week was less than that of core tablet which exposed to the accelerated condition and much less than that of core tablet after preparation.

4. Hardness

The average means of hardness of core and coated tablets are shown in Table 28 in Appendix II and depicted in Figure 14 (A). After coating the hardness of coated tablets was increased.

The average means of hardness of core and coated tablets after kept at room temperature for 1 week and after exposure to accelerated condition are tabulated in Table 28 in Appendix II and portrayed in Figure 14 (B). The hardness of coated tablets after kept at room temperature for 1 week was slightly greater than that after coating. However, their hardness were increased nearly equal to core tablet after kept at the same condition.

5. Disintegration time

The disintegration time of core and coated tablets are presented in Table 29 in Appendix II and illustrated in Figure 15 A and B.

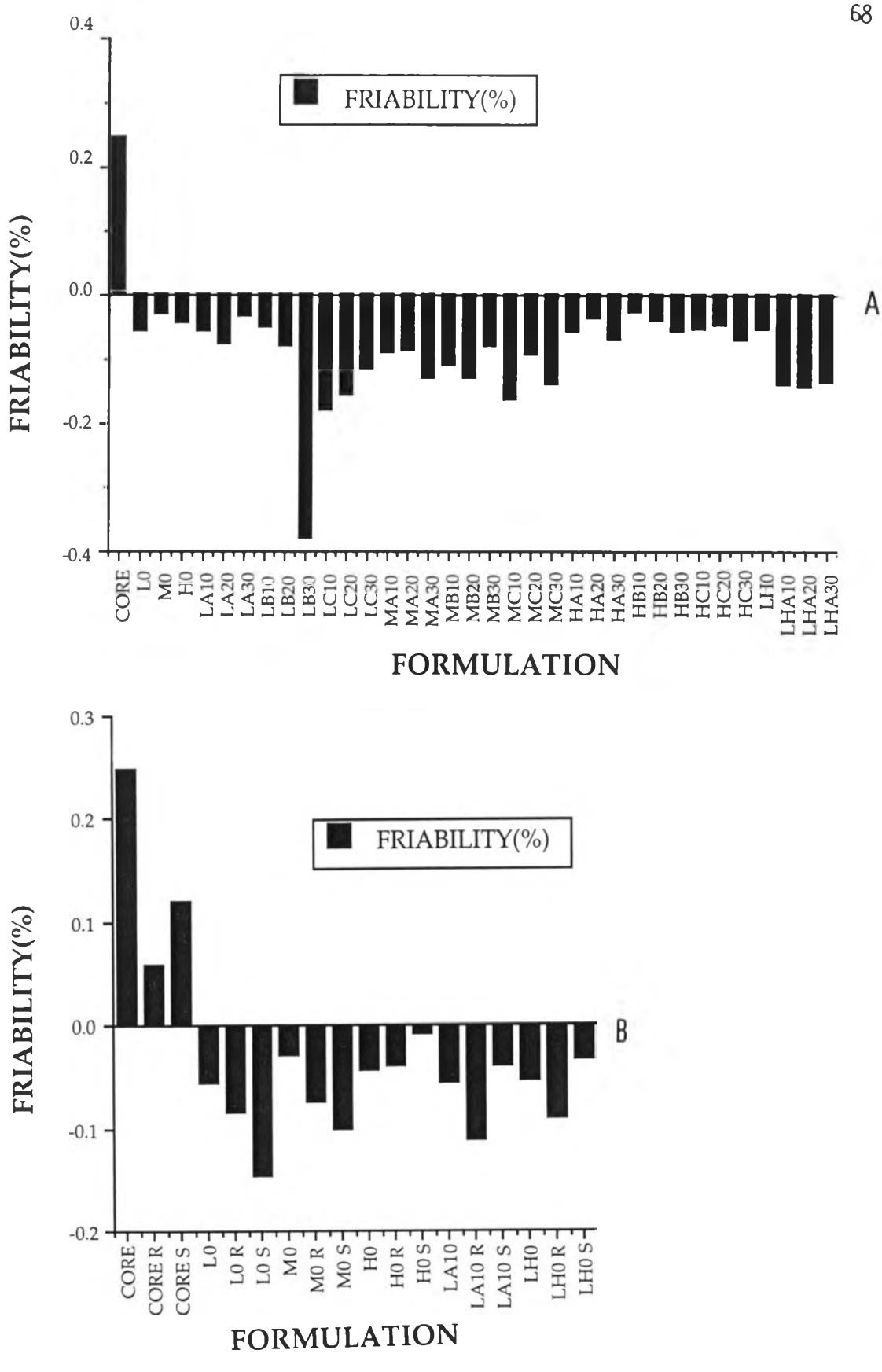

Figure 13 The percentage of friability of core and coated tablets (key:A-After coating, B-After kept at different condition).

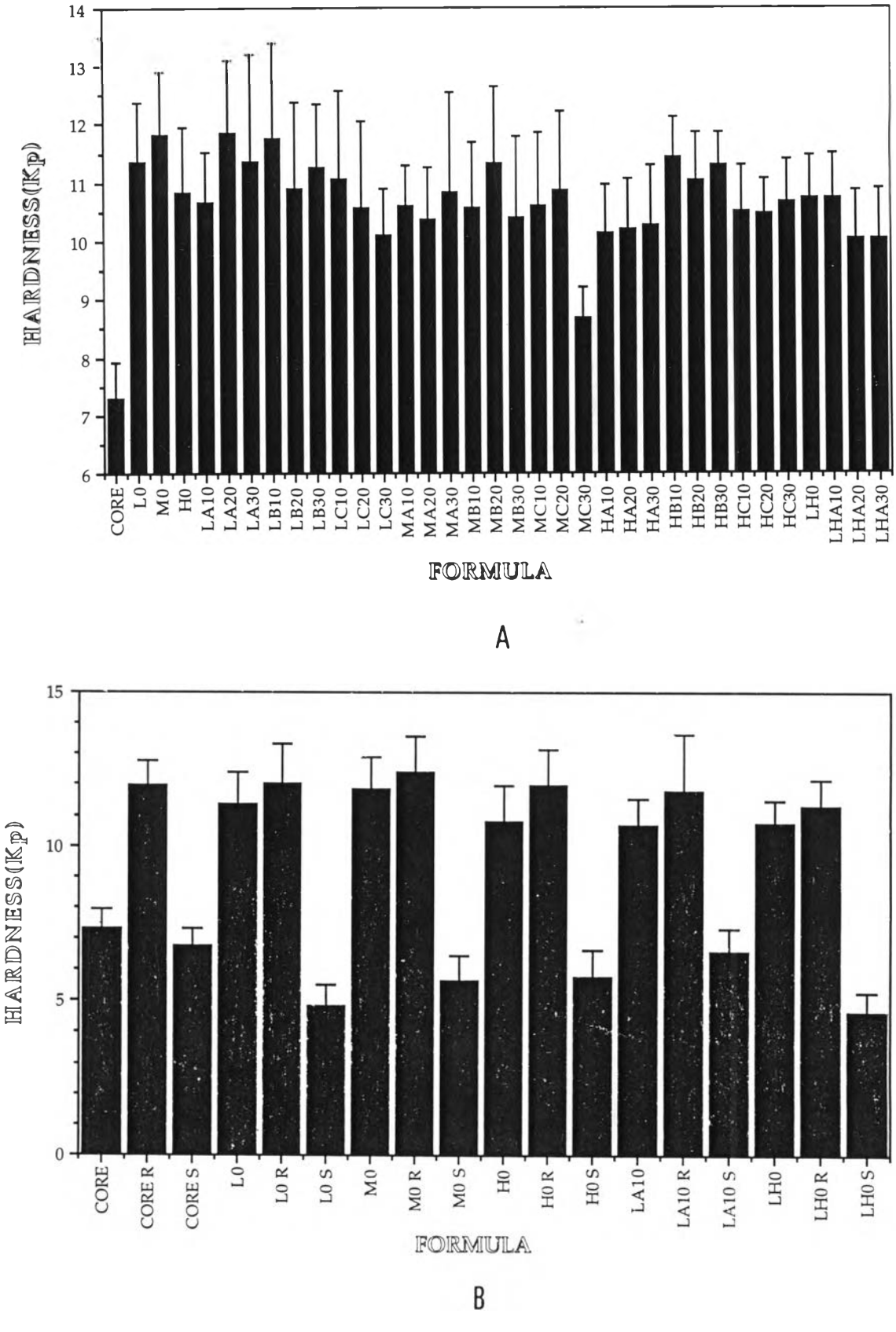

Figure 14 The hardness of core and coated tablets(key:A-After coating, B-After kept at different condition).

The disintegration time of core and coated tablets in dilute HCl(1:100) solution and deionized water is shown in Figure 15A. The disintegration test of L0 and M0 after coating in dilute HCl(1:100) solution was not measured in this study.

The disintegration time of core tablet in dilute HCl solution was slightly higher than that of core tablet in deionized water. The disintegration time of L0 was less than those of M0 and H0, and higher than that of core tablet. In case of using dilute HCl solution as immersion fluid, the disintegration time of H0 was slightly greater than that of core tablet and less than that of H0 in deionized water.

The increasing amount of propylene glycol decreased the disintegration time of coated tablets both in dilute HCl solution and deionized water , and the disintegration time in dilute HCl solution was less than that in deionized water. For LB tablets the increasing the amount of PEG400 increased the disintegration time in dilute HCl solution and the results were reversed in deionized water. For LC tablets, the increasing the amount of triacetin increased the disintegration time in dilute HCl solution which apparently higher than those of LA and LB tablets.

In dilute HCl soltion the disintegration time of M tablets was apparently higher than that in deionized water, except that of MC30. In dilute HCl solution, the disintegration time of MA10 was slightly higher than that of MA30, followed by that of MA20, and that of MB30 was greater than that of MB10, followed by that of MB20, and that of MC20 was apparently higher than that of MC10 and followed by that of MC30. In deionized water, the disintegration time of MA30 was slightly higher than that of MA20, followed by that of MA10. The increase the amount of PEG400 reduced the disintegration time and the result was reversed in MC tablets.

In deionized water, H tablets exhibited the apparently higher disintegration time than in dilute HCl solution. In both immersion fluids, the increase the amount of propylene glycol reduced the disintegration time. For HB tablets, the increasing the amount of PEG400 increased the disintegration time in dilute HCl solution and in deionized water

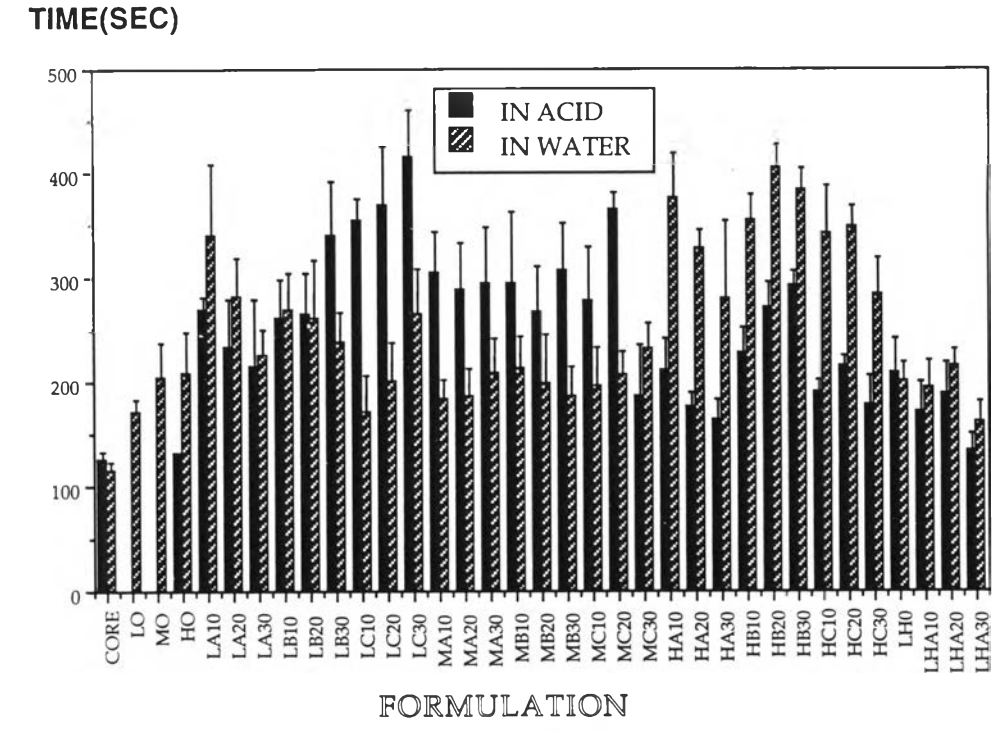

A

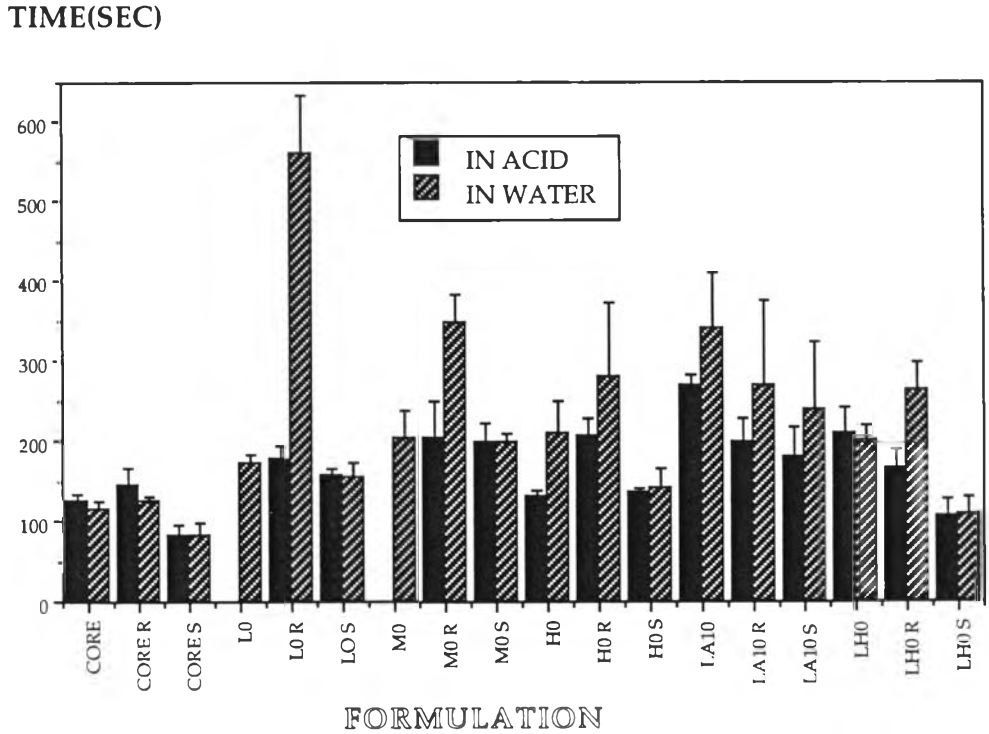

B

Figure 15 The disintegration time of core and coated tablets (key:A-After coating,B-After kept at different condition).

the disintegration time was ranked by HB20>HB30>HB10 repectively. For HC tablets, the disintegration time in deionized water and dilute HCl solution was ranked by HC20>HC10>HC30. In the same immersion fluids, the disintegration time of HC tablets was less than that of HB tablets.The disintegration time of HA tablets in dilute HCl solution was less than that of HB tablets and nearly equal to that of HC tablets.

In case of LH tablets, the disintegration time in dilute HCl solution was ranked by LH0>LHA20>LHA10>LHA30 respectively. and the disintegration time in deionized water was ranked by LHA20>LH0>LHA10>LHA30.

In both immersion fluids, CORE R exhibited slightly higher disintegration time than CORE, followed by CORE S. The disintegration time of L0 R in deionized water was dominantly greater than those of L0 and L0 S, but in dilute HCl solution it was nearly equal to L0 and slightly higher than that of L0 S. M0, M0 R and M0 S showed the same result as presented in L0 tablets. For H0 tablets, the disintegration time of H0 S was less than that of H0 R and that of H0 R in deionized water was higher than that in dilute HCl solution. In both immersion fluids, the disintegration time of LA10 tablets was ranked as LA10>LA10 R>LA10 S, and the disintegration time in dilute HCl solution was less than that in deionized water. For LH0 tablets, the disintegration time of LH0 S in dilute HCl solution was the slowest and nearly equal to that in deionized water. The disintegration time of LH0 R in deionized water was higher than in dilute HCl solution and higher than LH0 after coating, but the disintegration time of LH0 R in dilute HCl soution was less than LH0 after coating.

In the short, the disintegration time of coated tablets was higher than that of core tablet. In dilute HCl solution, L, H and LH tablets exhibited less disintegration time than in deionized water, but the result of M tablets was reversed. An increase in the amount of propylene glycol rather reduced the disintegration time in both immersion fluids, while an increase in the amount of PEG400 increased the disintegration time in dilute HCl solution and reduced in deionized water. In case of using triacetin as plasticizer, it indicated that an increase in the

amount of triacetin rater increased the disintegration time in both immersion fluids.

6. Dissolution studies of propranolol HCl core and coated tablets.

Typical calibration curve for propranolol HCl data as determined by using linear regression is shown in Appendix II (Table 22)and Figure 80.

The dissolution profiles of propranolol HCl from core and coated tablets are presented in Figures 16-31 and experimental data are tabulated in Table 30 in Appendix II.

The dissolution data and profiles were demonstrated in four categories : firstly, showing the effect of molecular weight of chitosan (Figs.16 -19); secondly, showing the effect of type of plasticizer (Figs.20-22); Third, showing the effect of concentration of plasticizer (Figs. 23-26); Finally, showing the effect of accelerated condition (Figs. 27-31). The drug release of each coated formulation was also compared with the drug release of core tablet.

6.1 Molecular weight of chitosan

The variation in dissolution profiles of propranolol HCl from LO, MO, HO, LHO and core tablets are depicted in Figure 16. These profile, showed that core tablet exhibited the highest drug release at each time interval. For HO, the percentage of drug dissolved was higher than LO, MO and LHO during the first 12 minutes and then slightly less than that of LHO. For LO, MO and LHO, the similar pattern of dessolution profile and the amount of drug released were obtained except that after 12 minutes which the drug released of LHO was higher than the others. For LO, the percentage of drug dissolved was slightly greater than MO.

Figure 17(A) illustrated the dissolution profiles of drug from coated tablets using different grades of chitosan with 10% propylene glycol. The drug release from core tablet was the fastest followed by LA10, LHA10, MA10, HA10

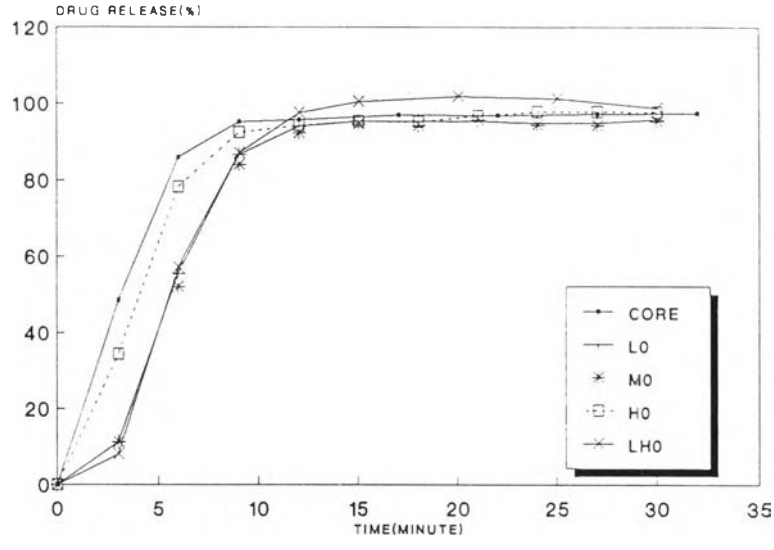

Figure16 The dissolution profiles of propranolol HCl from core, LO, M0, H0 and LH0.

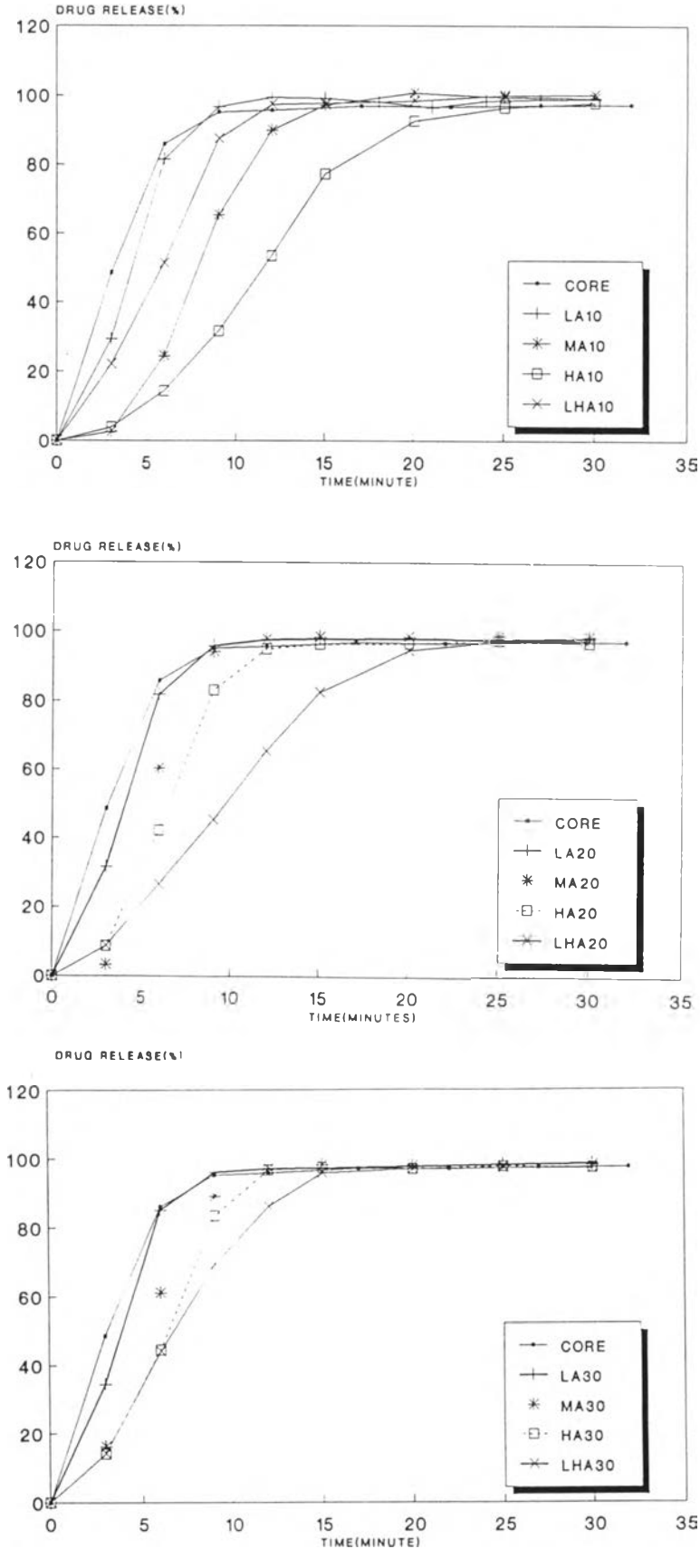

Figure 17 The dissolution profiles of propranolol HCl from coated tablets plasticized with propylene glycol (key:A-10%, B-20%, C-30%).

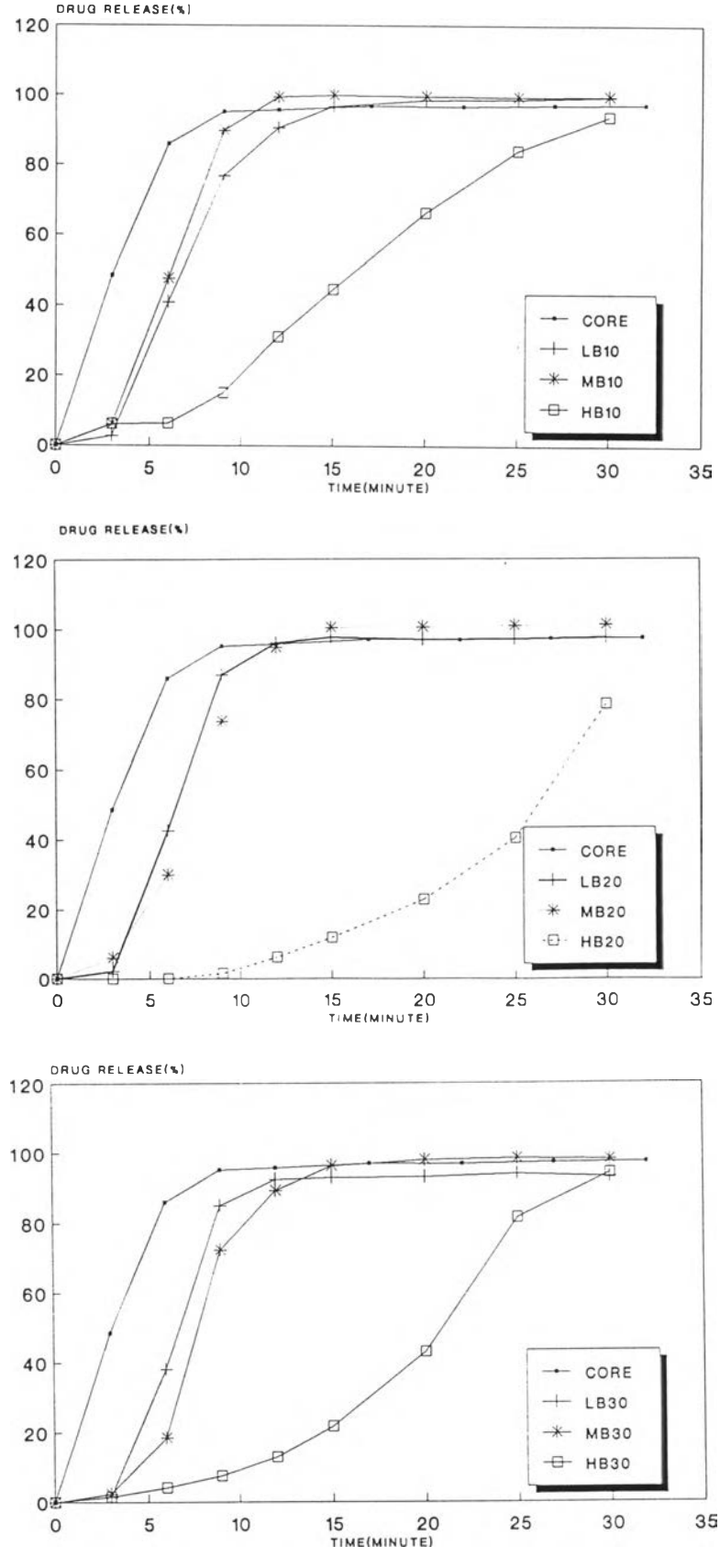

Figure 18 The dissolution profiles of propranolol HCl from coated tablets plasticized with PEG 400(key:A-10%, B-20%, C-30%).

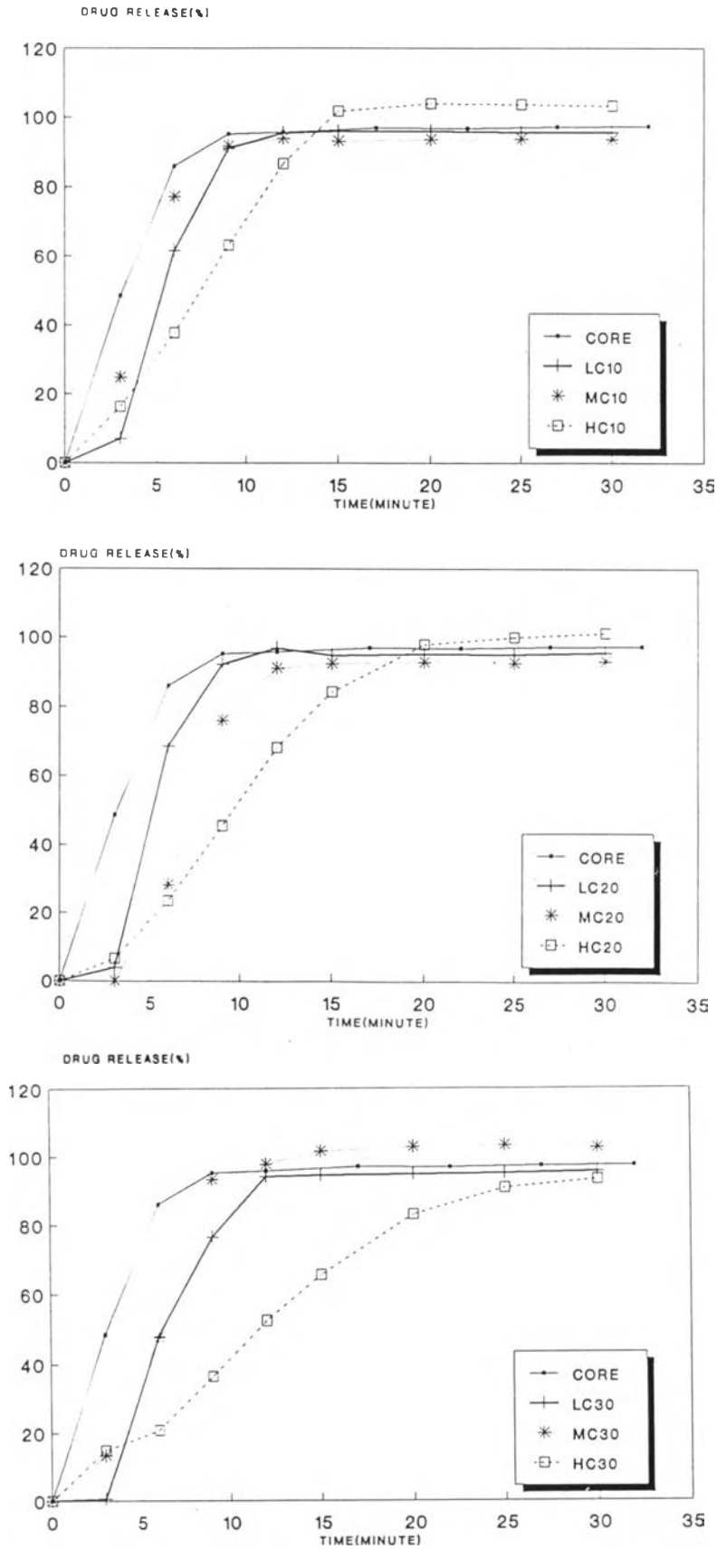

Figure 19 The dissolution profiles of propranolol HCl from coated tablets plasticized with triacetin (key:A-10%, B-20%, C-30%).

respectively. For HA10, the drug dissolution was higher than that of MA10 during the first 3 minutes and then less than MA10 at each time interval. When using propylene glycol at concentration 20 % w/w , as depicted in Figure17(B), the drug release of LA20 was higher than those of MA20, HA20 and LHA20 respectively. MA20 showed the slowest drug released during the first 3 minutes, but after that it exhibited the drug released greater than HA20 and LHA20. LHA20 showed the slowest drug release after the first 3 minutes. While increasing the concentration of propylene glycol to 30 % w/w, as shown in Figure 17(C), the pattern of drug released was similar to when using 20 % w/w except the first 3 minutes the drug released of MA30 was greater than HA30 and LHA30, and the drug released of HA30 was very equal to LHA30 during the first 6 minutes.

The drug released profiles of coated tablets using three concentrations of PEG400 as plasticizer and using different grades of chitosan as film former are graphically shown in Figures18 (A, B and C). HB tablets showed dominantly slower drug release than the others. When using 20 and 30 % w/w of PEG400 , the drug release of HB tablets exhibited much slower than those of the others and LB tablets showed greater the drug release than MB tablets. When using 10 % w/w of PEG400, the drug released of MB system was slightly greater than LB system.

The dissolution profiles of coated tablets using triacetin as plasticizer and using different grades of chitosan as film former are presented in Figure 19 (A, B and C). Figure19 (A), the drug released of LC 10 was less than the others during the first 3.5 minutes and then gradually increased to greater than that of HC10, but still less than that of MC10. After 9.5 minutes the drug released of LC10 showed slightly higher than MC10. From figure 19(B). The amount of drug released of LC20 was between MC20 and HC20 during the first 3 minutes and then was greater than MC20 and HC20 except that after 19 minutes; HC20 produced slighly higher dissolution than the others. From figure 19 (C), LC30 showed the lag time and slowest release during the first 3 minutes and then suddenly increased the drug released to greater than HC30 at 4 minutes and equal to MC30 at 6 minutes and then less than MC30 at each

time interval. The drug released of HC30 was lower than the others during after the first 4 minutes.

6.2 Type of plasticizer

Figures 20 (A, B and C) are dissolution profiles of drug from coated tablets using chitosan L as film former and of different concentration of three plasticizers . LA coated tablets exhibited markedly higher drug released than LB and LC coated tablets, however they were still less than that of core tablet. The percentage of drug released of LC10 was greater than LB10, as same as the drug released of LC20 was more than LB20 during the first 12 minutes and then nearly equal to the others during after 12 minutes. For LC30, the dissolution profile exhibited the slowest drug release which nearly equal to that of LB30 during the first 3 minutes then gradually slightly greater than LB30 during 3 to 6 minutes and then less than LB30 during 6 to 11.5 minutes, and nearly equal to the others during after 11.5 minutes.

The dissolution profiles of drug from coated tablets using chitosan M as film former and added three plasticizers at 10, 20 and 30 % w/w of chitosan are displayed in Figure 21 (A, B and C). The drug released during the first 10 minutes MB10 was greater than that of MA10, but less than that of MC10. At 20 % w/w of plasticizers, Figure 21 (B), The drug release of MB20 was slightly greater than that of MA20 and that of MA20 was greater than that of MC20 at the first 3 minutes. During 3 to 12.5 minutes, the drug dissolved of MA20 was apparently higher than MB20 and MC20 and the drug dissolved of MB20 was nearly equal to MC20. Figure 21(C), revealed that MB30 produced dominantly slower drug release than MA30 and MC30 during the first 15 minutes and MA20 exhibited slightly greater drug release than MC30 during the first 7.5 minutes.

In the case of using chitosan H as film former and added plasticizers at concentration 10, 20 and 30 % w/w of polymer, the dissolution profiles are portrayed in Figure 22. HB tablets exhibited the drug gradually release and produced the tremendously slower dissolution than HA and HC tablets. Figure 22(A), the drug released of HC10 was apparently greater than those of HA10 and HB10 tablets. The drug dissolution

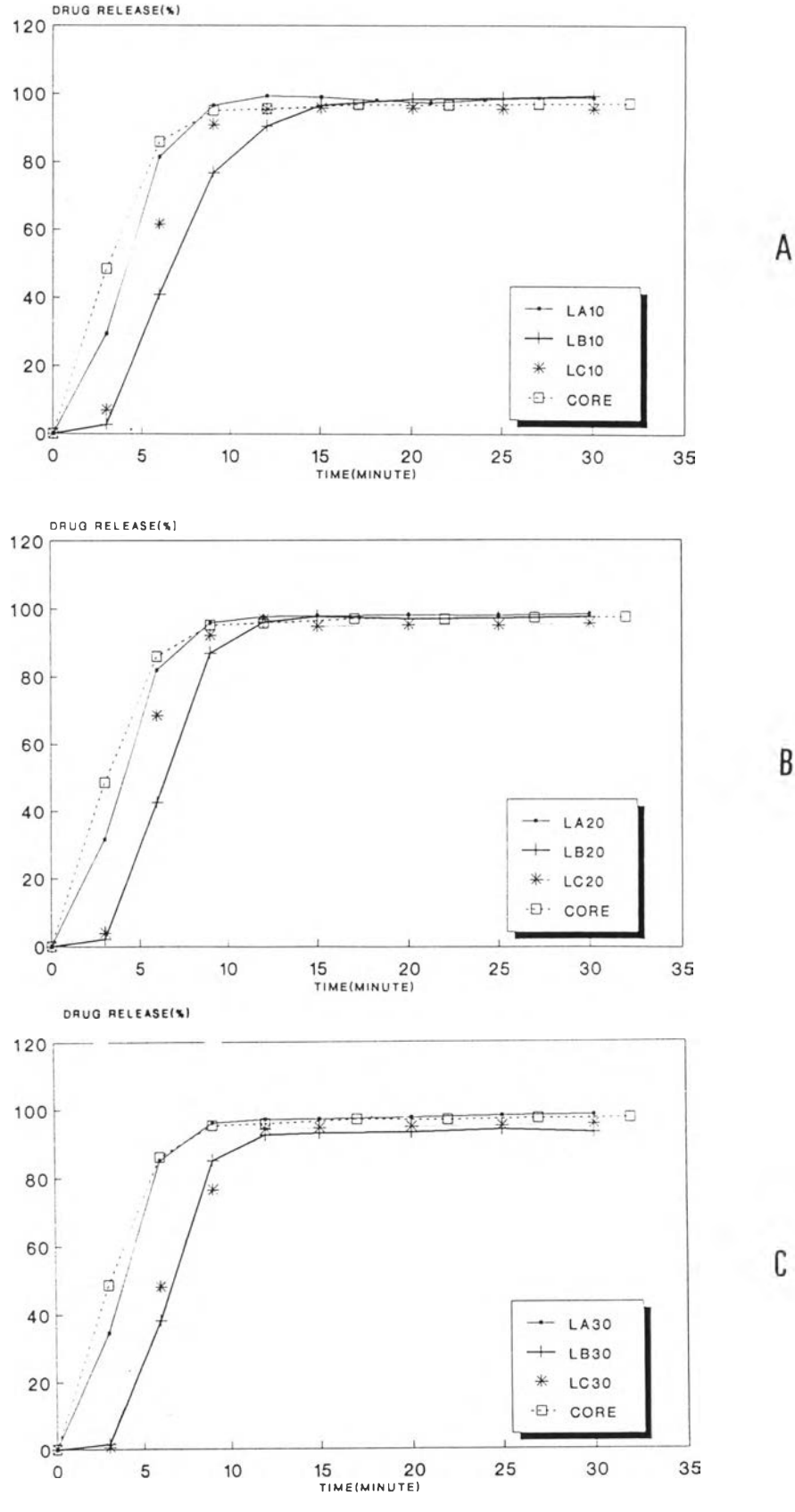

Figure 20 The dissolution profiles of propranolol HCl from tablets coated with plasticized chitosan L (key:A-10%, B-20%, C-30%).

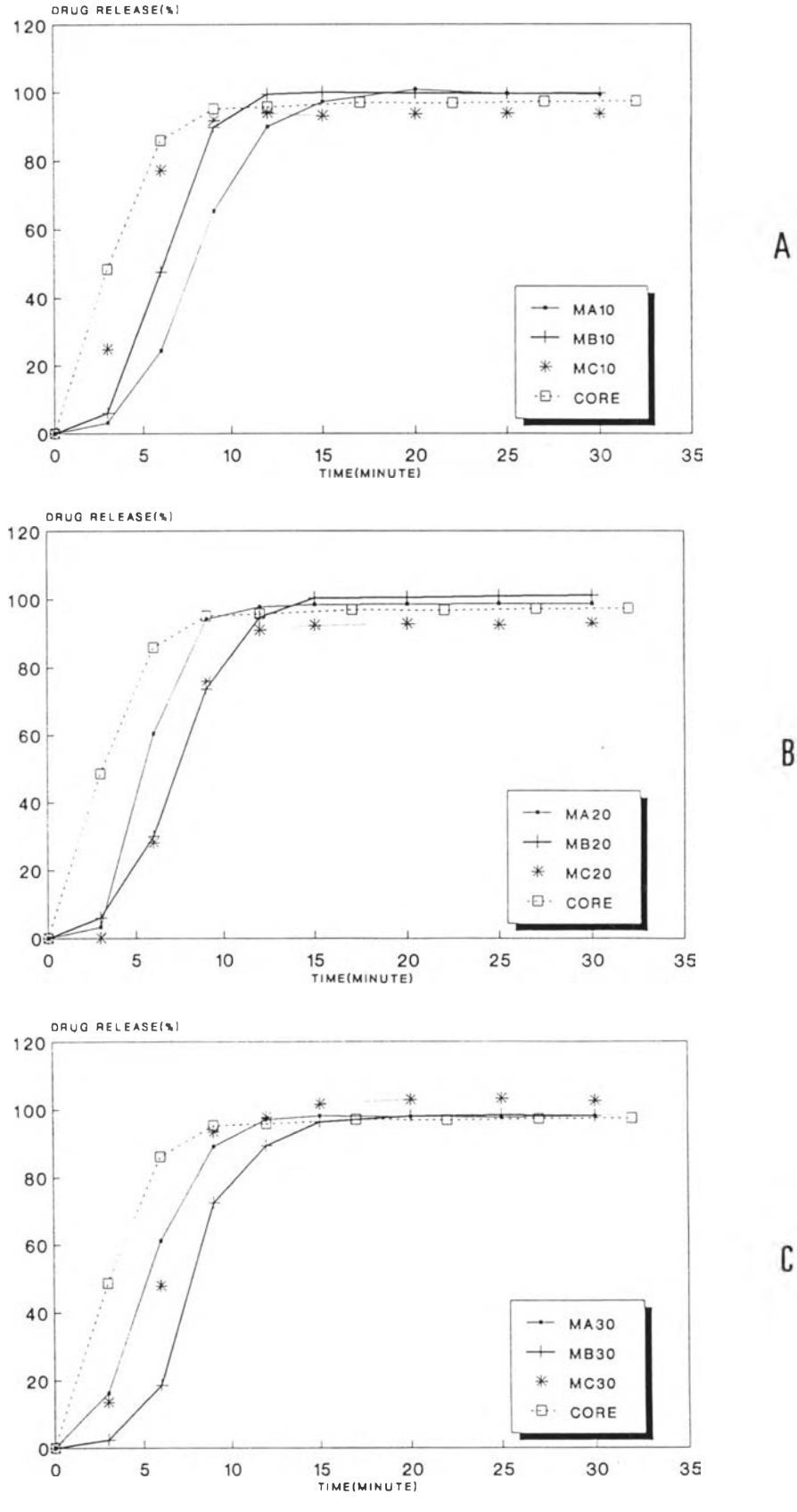

Figure 21 The dissolution profiles of propranolol HCl from tablets coated with plasticized chitosan M (key:A-10%, B-20%, C-30%) .

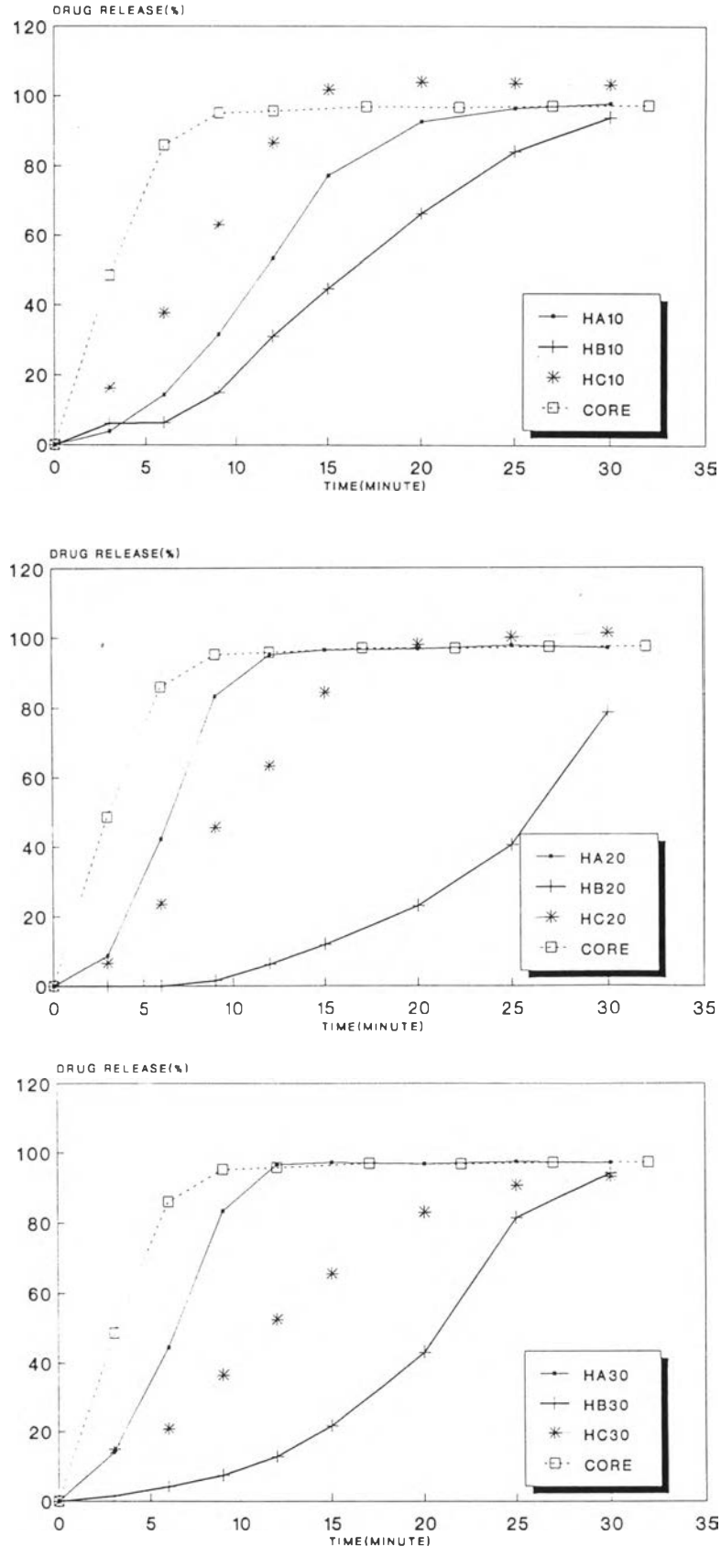

Figure 22 The dissolution profiles of propranolol HCl from tablets coated with plasticized chitosan H (key:A-10%, B-20%, C-30%).

profile in Figrue 22(B) showed that HA20 could release the drug greater than HC20 and HB20 as same as the drug released of HA30 was higher than HC30 and HB20 as shown in Figure 22(C), except that during the first 3 minutes the drug dissolved of HA30 was nearly equal to that of HC30. The drug released of HA30 was dominantly greater than that of HB30.

6.3 Concentration of plasticizer

The comparison of dissolution profiles of propranolol HCl from coated tablets using three concentrations (10, 20 and 30 % w/w of polymer) of three plasticizers was demonstrated as following remarks.

For chitosan L as film former, The plasticized film coated tablet with three concentrations of propylene glycol (LA10, LA20 and LA30) exhibited the faster drug dissolution than unplasticized coated tablet (LO), as illustrated in Figure 23(A). These three formulars showed the same drug release pattern which the fastest drug release was from LA30, followed by LA20 and LA10 respectively, however, drug released from these three profiles was very nearly equal. The dissolution profilles of plasticized film coated tablet with PEG400, as shown in Figure 23(B), displayed the slower drug dissolution than LO. All these plasticized formulas exhibited the lag time during the first 3 minutes and showed the same drug release pattern which the drug dissolved was very nearly equal during the first 7.5 minutes. The dissolution profiles of plasticized coated tablet with triacetin, as depicted in Figure 23(C), showed that these three formulas had the lag times during the first 3 minutes which LC30 showed the lowest drug released, followed by those of LC20 and LC10 respectively. LC30 produced slower drug release than LO, and LC20 slightly higher than LC10 during 4 to 12 minutes.

For chitosan M, the drug released of coated tablets which used propylene glycol as plasticizer is illustrated in Figure 24(A). The drug dissolutoin of M0 was slightly greater than MA20 during the first 9 minutes and higher than that of MA10 during the first 12 minutes, but exhibited lower than that of that of MA30 at each time interval. The lag times were apparently seen in dissolution profiles of MA10 and MA20 during

the first 3 minutes. When using PEG400 as plasticizer, as illustrated in Figure 24(B), the drug released of MB30 were less than that of M0 during the first 13.5 minutes and less than those of MB10 and MB20 at each time interval. The profiles also exhibited the lag times of MB tablets which the slowest drug release during the first 3 minutes was from MB30, followed with those of MB20, MB10 and M0 respectively. The dissolution profiles of the system using triacetin are shown in Figure 24(C). The drug released of MC20 was less than those of the others at each time interval and clearly showed the lag time during the first 3 minutes. The drug released of MC10 was greater than that of MC30 during the first 8 minutes and greater than that of M0 during the first 12 minutes.

For chitosan H, the dissolution profiles of coated tablet prepared by using three plasticizers at different concentrations are comparable. When using propylene glycol as plasticizer (Figure 25(A)), the slowest drug dissolution was obtained from HA10 and the drug released of HA20 was slightly greater than HA30. All plasticized film coated formulas using propylene glycol had the drug release slower than H0 during the first 12 minutes. For HB tablets, as depicted in Figure 25(B), the slowest drug release was obtained from HB20, followed by those of HB30, HB10 and H0. All these plasticized formulas displayed the lag time in the early stage about the first 6 minutes. After the lag time, HB20 and HB30 gradually released the drug which was slower than HB10. The dissolution profiles of HC tablets (Fig. 25(C)) showed that all plasticized film coated formulas produced the drug release slower than core tablet and H0. HC10 produced faster drug release than HC20 and HC30. During the first 5 minutes, the drug release of HC20 was the slowest and that of HC10 was nearly equal to that of HC30. The drug release of HC30 was slower than HC20 at each time interval after 5 minutes.

For chitosan LH, the dissolution profiles of formulas prepared by using propylene glycol as plasticizer are depicted in Figure 26. The slowest dissolution profile was obtained form LHA20, and during the first 3 minutes the profile of LH0 showed the slowest drug release which was nearly equal to that of LHA20, followed by LHA30 and LHA10 respectively.

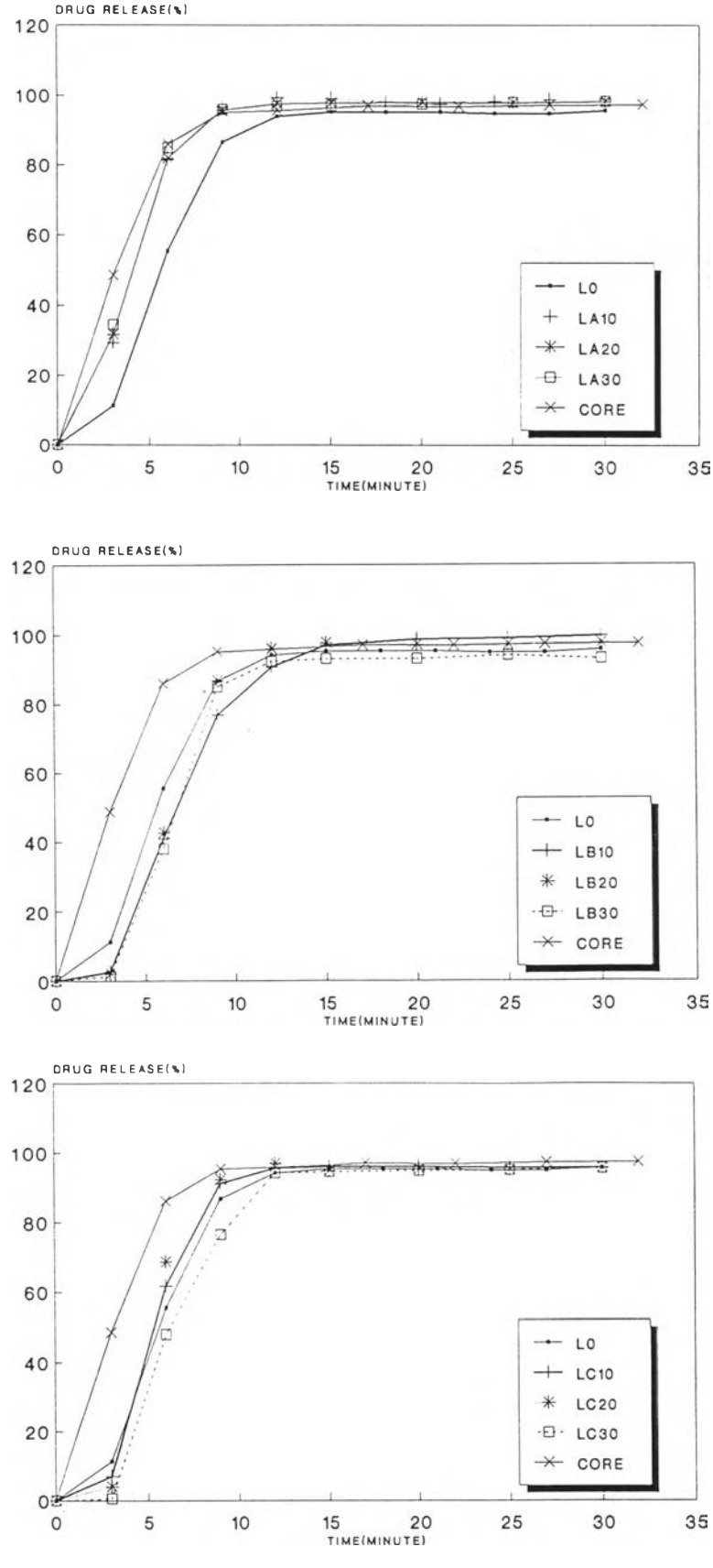

Figure 23 The dissolution profiles of propranolol HCl from tablets coated with unplasticized and plasticized chitosan L (key:A-propylene glycol, B-PEG400, C-triacetin).

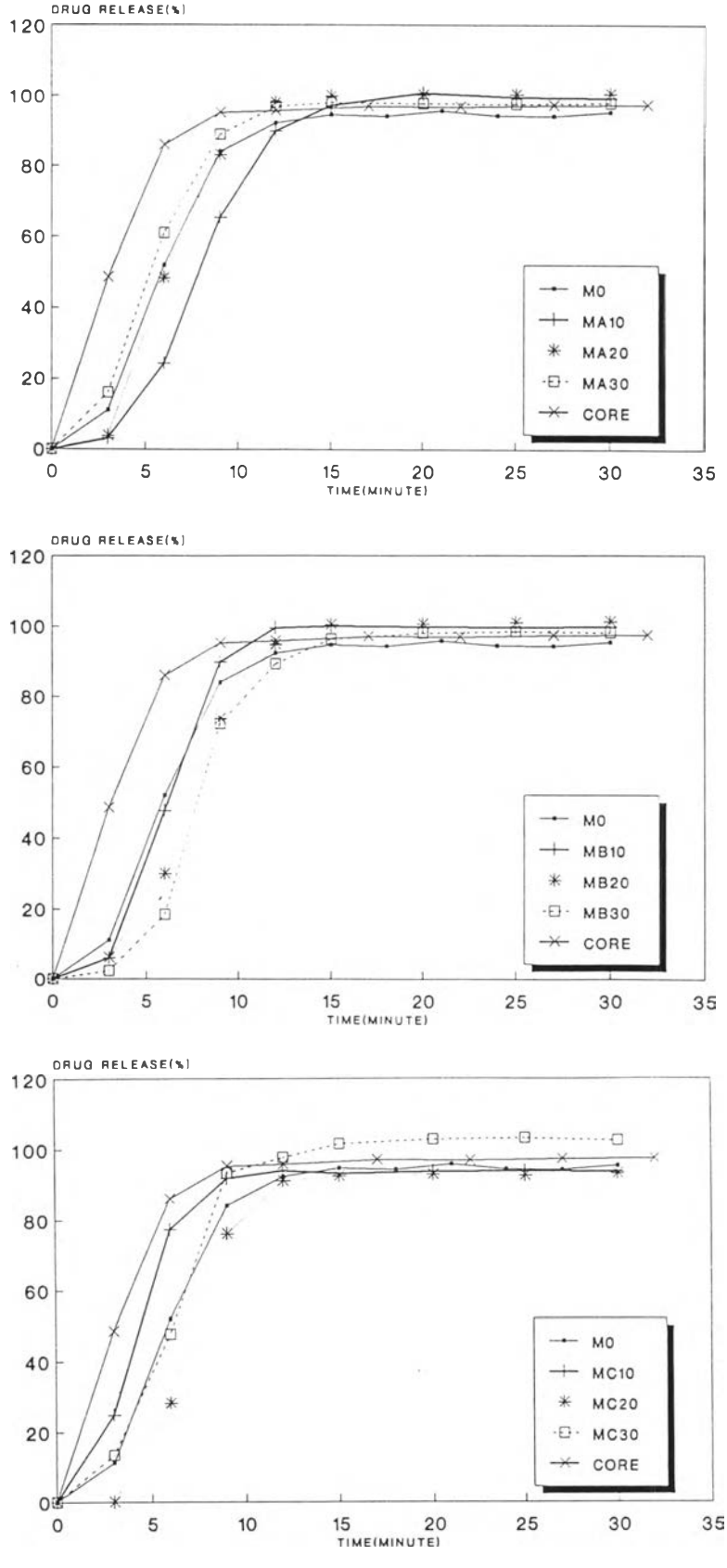

Figure 24 The dissolution profiles of propranolol HCl from tablets coated with unplasticized and plasticized chitosan M (key:A-propylene glycol, B-PEG400, C-triacetin).

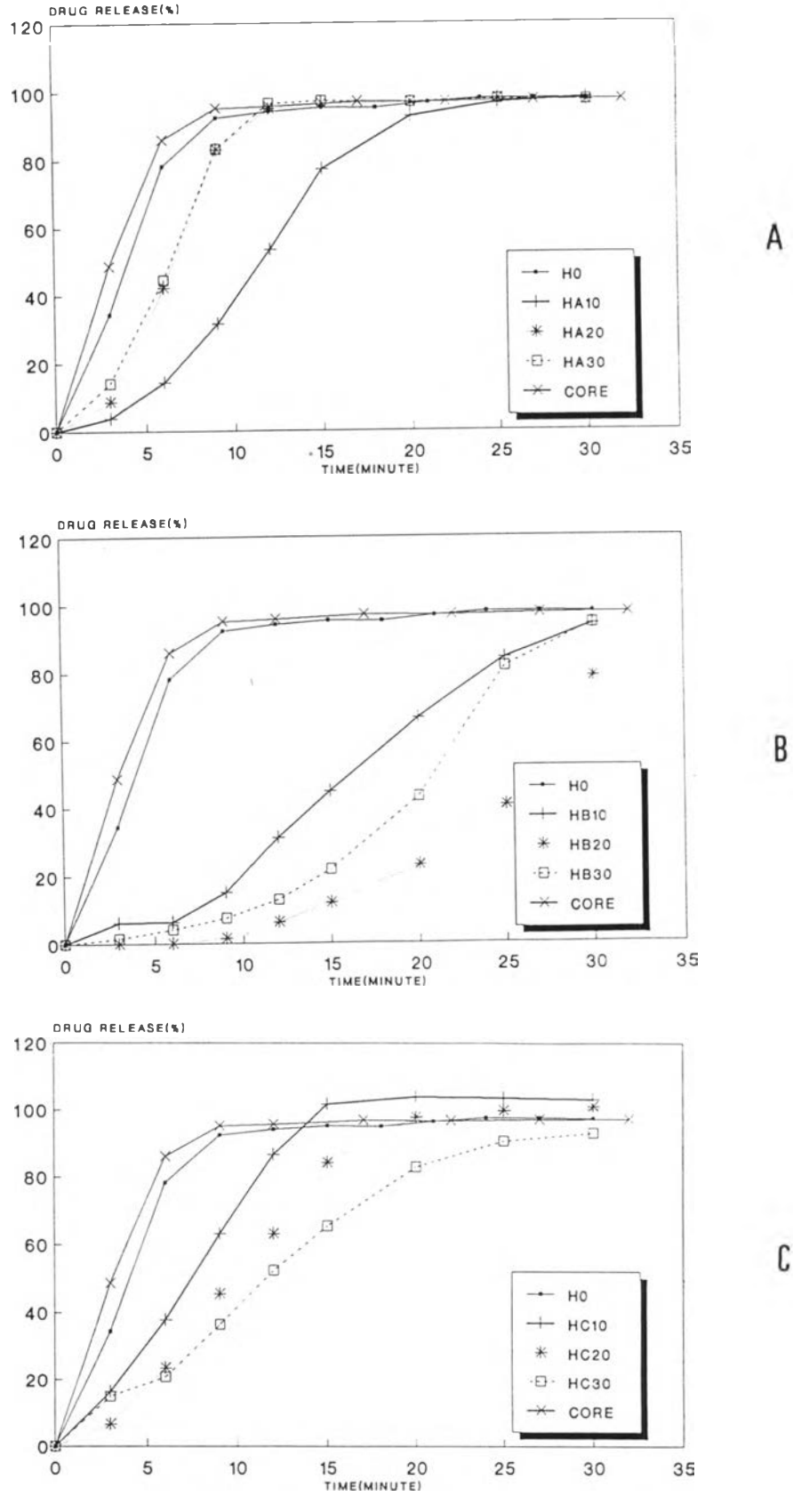

Figure 25 The dissolution profiles of propranolol HCl from tablets coated with unplasticized and plasticized chitosan H (key:A-propylene glycol, B-PEG400, C-triacetin).

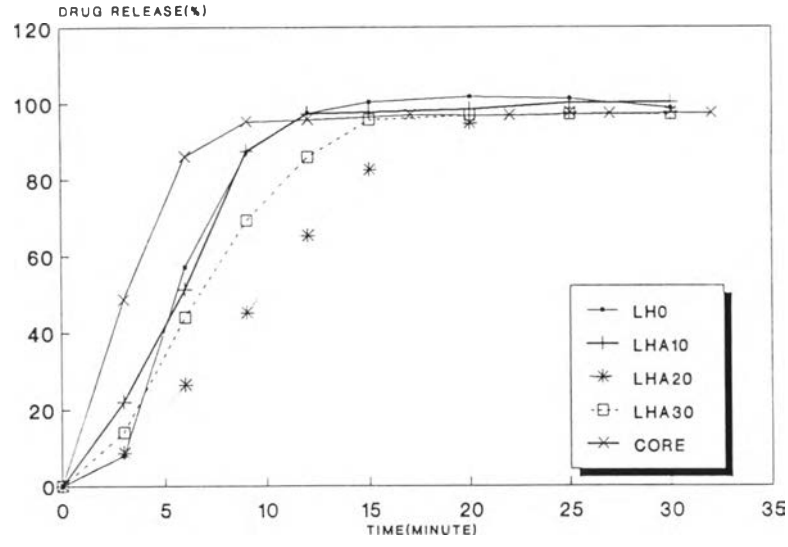

Figure 26 The dissolution profiles of propranolol HCl from tablets coated with unplasticized and plasticized chitosan LH.

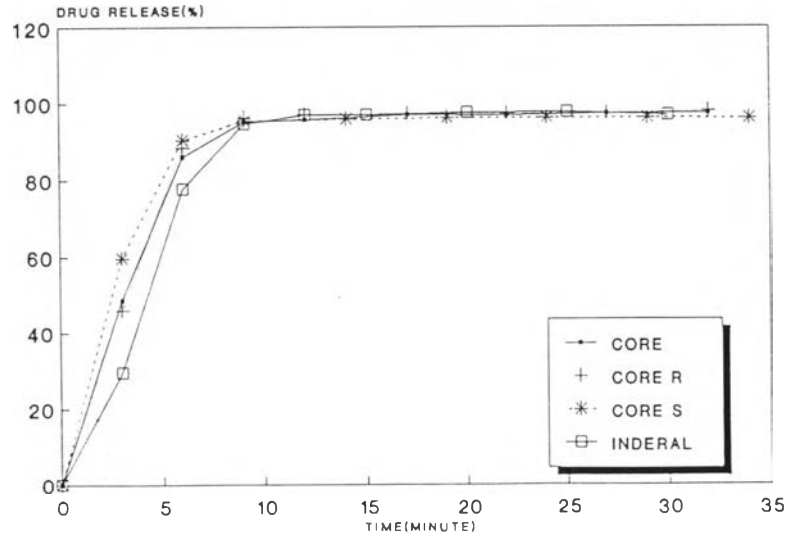

Figure 27 The dissolution profiles of propranolol HCl from INDERAL and core tablet after kept at different condition.

The drug released at each time interval of LHA10 was greater than LHA30 and followed by that of LHA20 respectively.

6.4 After exposure to accelerated condition.

The comparison of drug dissolution after preparation, kept at room temperature for 1 week and after contacted with accelerated condition for 1 week are graphically illustrated in Figures 27-30.

The dissolution profile in Fig.27 of core tablet after preparation was nearly equal to that after kept for 1 week at room temperature (CORE R), but slightly slower than that after exposure to accelerated condition (CORE S) and the drug release of commercial tablet (Inderal®) was slightly slower than the others during the first 9 minutes, and then all dissolution profiles displayed nearly equal.

The drug dissolution profile of L0 after exposure to accelerated condition indicated that the drug release was dramatically slower than L0 and L0 R, as shown in Figure 28 (A). The drug released of L0 R was also markedly lower than L0, and also showed the lag time during the first 6 minutes and then the dissolution profile was to be a straight line during 6Û¥-□+@ minutes and then reached to the plateau phase. The lag time of L0 R was longer than L0. The released profile of L0 S showed nearly to be a straight line.

The drug dissolution profiles of M0 and H0 after exposure to accelerated condition in Figure 28(B) and Figure 28(C) respectively, showed the dramatically reducing the drug dissolution and were also nearly to be a straight line. The dissolution profiles of M0 R and H0 R were nearly to be a linear during the first 21 minutes and then gradually to the plateau phase, and could not observed the lag time of H0 R , but could see a small lag time from M0 R during the first 3 minutes.

The drug release of LH0 S as shown in Figure 29(A) was also dominantly slower than that of LH0 and slihgtly slower than that of LH0 R. LH0 R provided a maximum drug released only 57.57 % at 30 minutes. The dissolution profiles of LH0 R and LH0 S were nearly to be a linear during 9 to 30

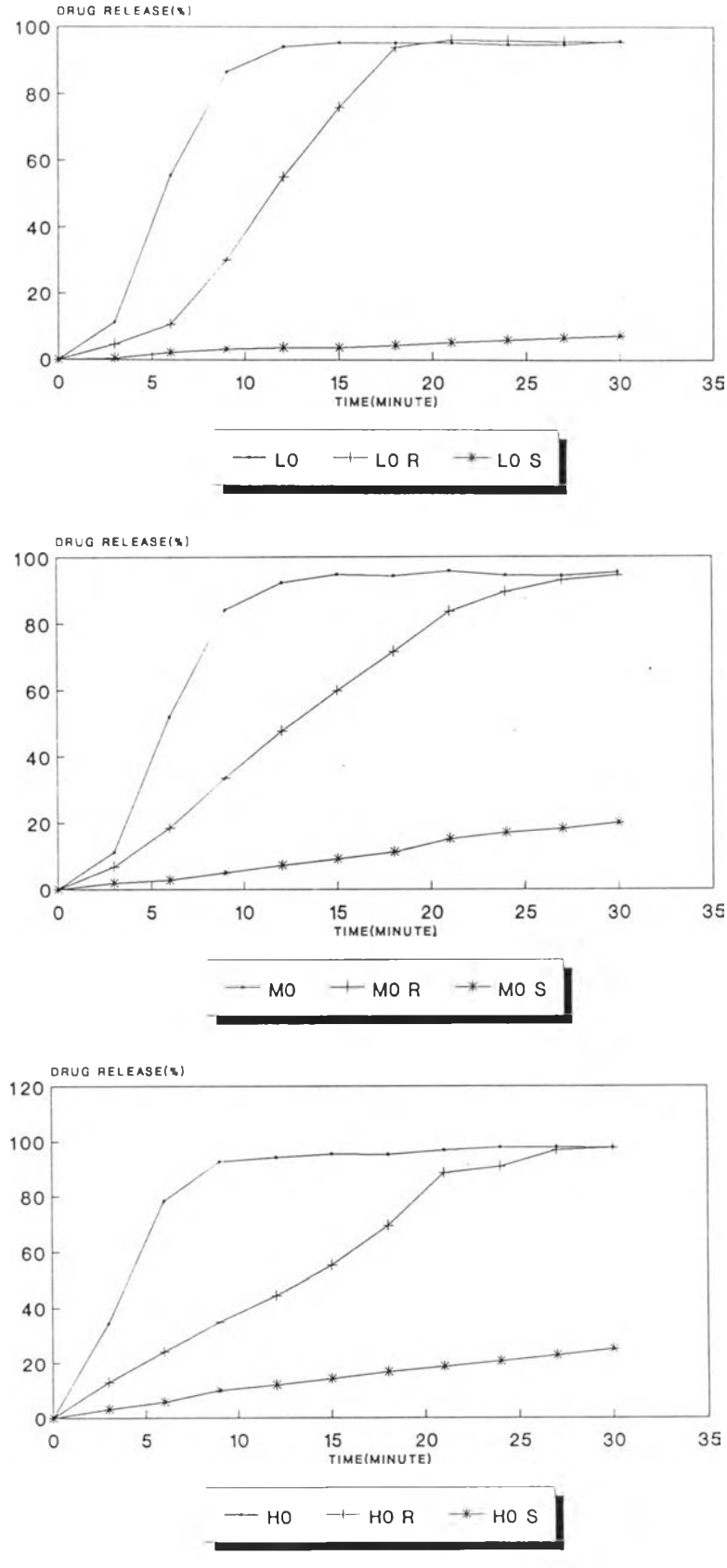

Figure 28 The dissolution profiles of propranolol HCl from coated tablet after kept at different condition(key: A-L0, B-M0, C-H0).

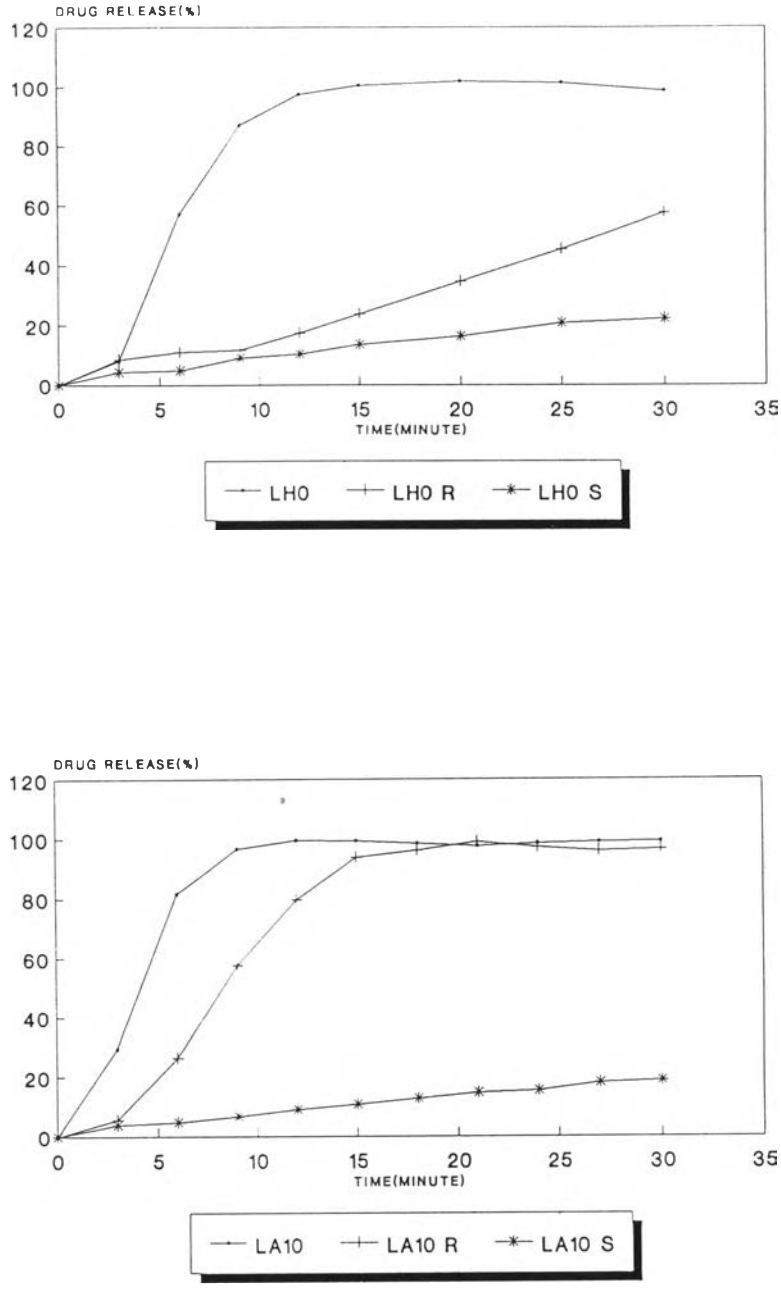

Figure 29 The dissolution profiles of propranolol HCl from coated tablet after kept at different condition(key:A-LH0, B-LA10).

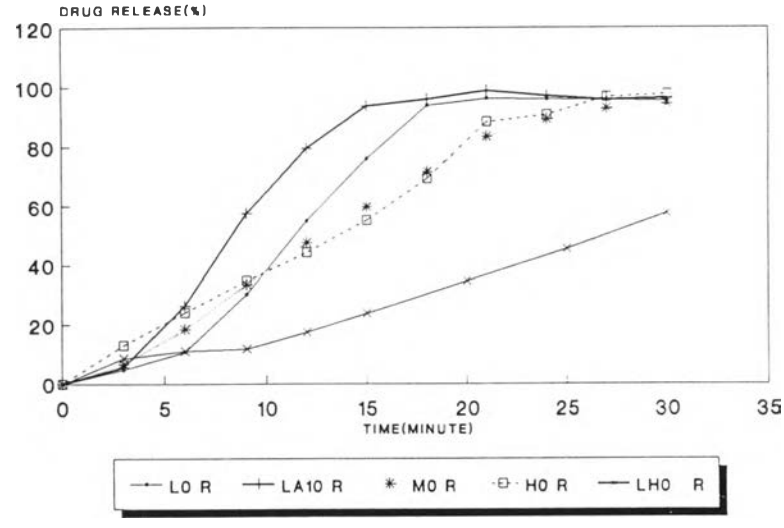

Figure 30 The dissolution profiles of propranolol HCl from coated tablet after kept at room temperature for 1 week.

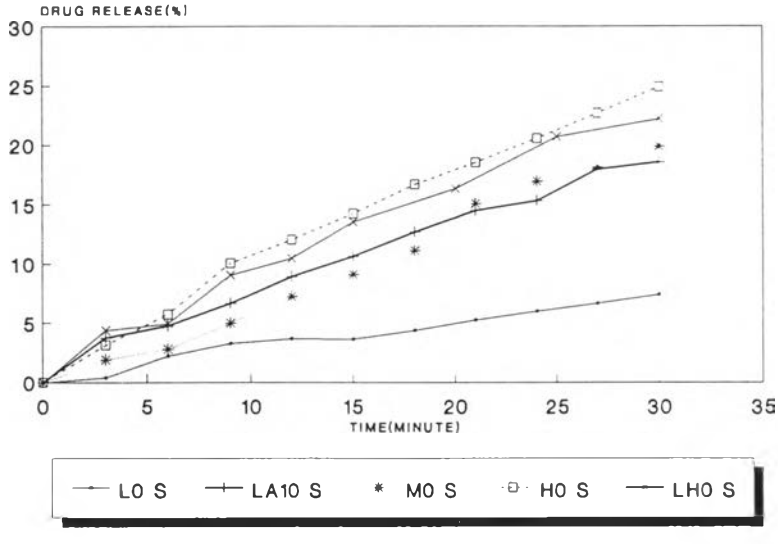

Figure 31 The dissolution profiles of propranolol HCl from coated tablet after exposure to accelerated condition.

minutes. The slopes of dissolution profiles of LH0 R and LH0 S during the first 9 minutes were slightly less than during 9 to 30 minutes, but LH0 apparently showed the lag time during the first 3 minutes.

The drug release of LA10 R as presented in Figure 29(B) showed the lag time during the first 3 minutes and exhibited the drug release which was slower than LA10, and the dissolution profile of LA10 S indicated that the drug release was apparently slower than those of LA10 R and LA10.

The dissolution profiles of film coated tablets which were kept at room temperature for 1 week are depicted in Figure 30. The amount of drug released of only LH0 R could not reach the plateau stage in the first 30 minutes. The drug released of LA10 R was greater than that of L0 R, and M0 R was nearly equal to H0 R.

The dissolution profiles of coated tablets after exposure to accelerated condition are illustrated in Figure 31. The profile of L0 S exhibited the slowest drug released, followed by that of M0 S during the first 20 minutes and then the drug released of M0 S was higher than LA10 S. The drug released of LH0 S during the first 6 minutes was closely equal to those of LA10 S and H0 S, and then was greater than that of LA10 S but lower than that of H0 S.

7. The appearance of coated tablets.

The picture of LH0 as displayed in Figure 32 showed that coated tablets were yellowish and glossy and after submersion in deionized water for 5 minutes as depicted in Figure 32(C) the coating layer swelled and a transparent gel layer around the core tablet was obtained. After kept at room temperature for 1 week the color of coated tablets was more yellowish as depicted in Figure 33(1)(A) and after exposure to accelerated condition as illustrated in Figure 33(1)(B) its color was changed to brown, and after dissolution test of coated tablets exposed to accelerated condition it still showed brown, glossy undissolved film coated tablet as shown in Figure 33(1)(C). Similar results were exhibited in tablets of L0, M0, H0 and LA10 as shown in Figure 33(2)(A, B, C and D) except the tablet of M0

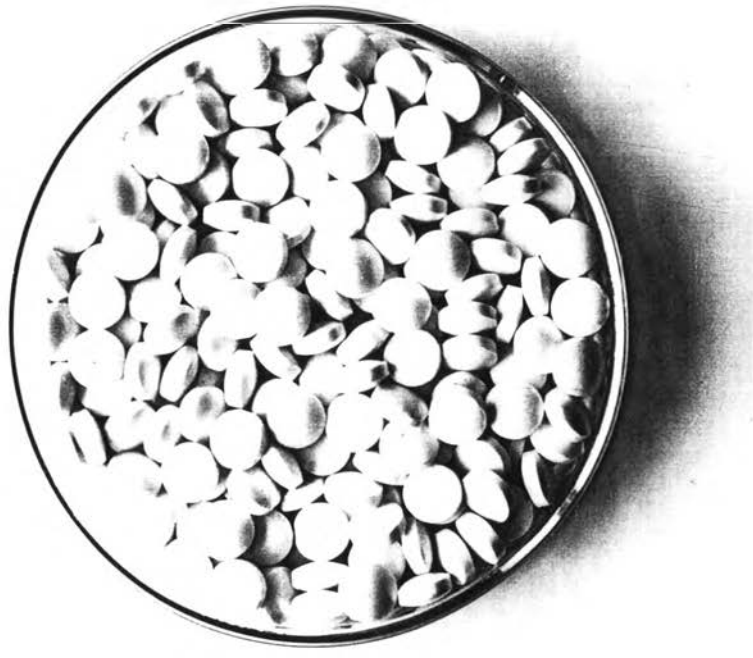

A

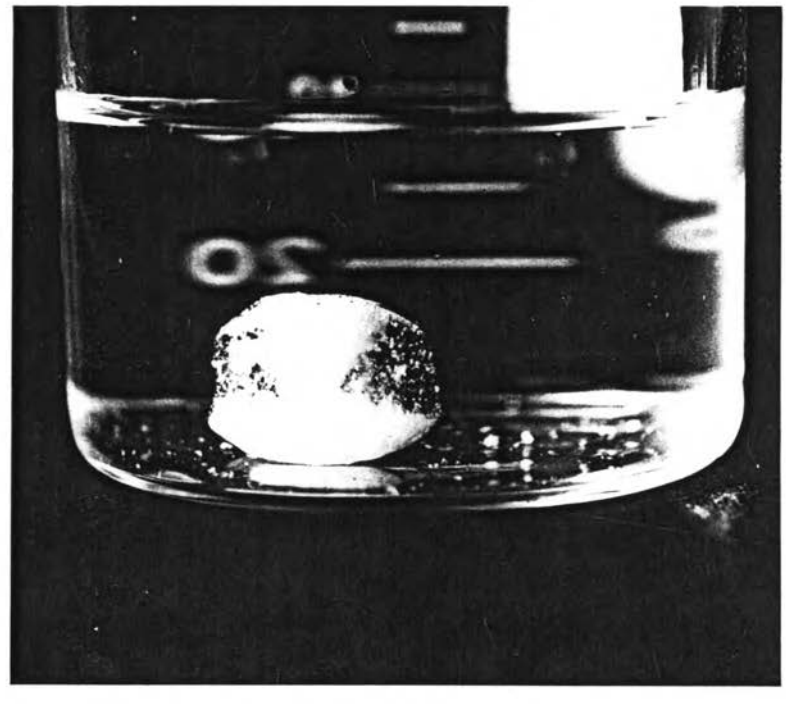

B C

Figure 32 The appearance of coated tablet(LHO)(key:A-low magnification, B-high magnification, C-in deionized water for 5 minutes).

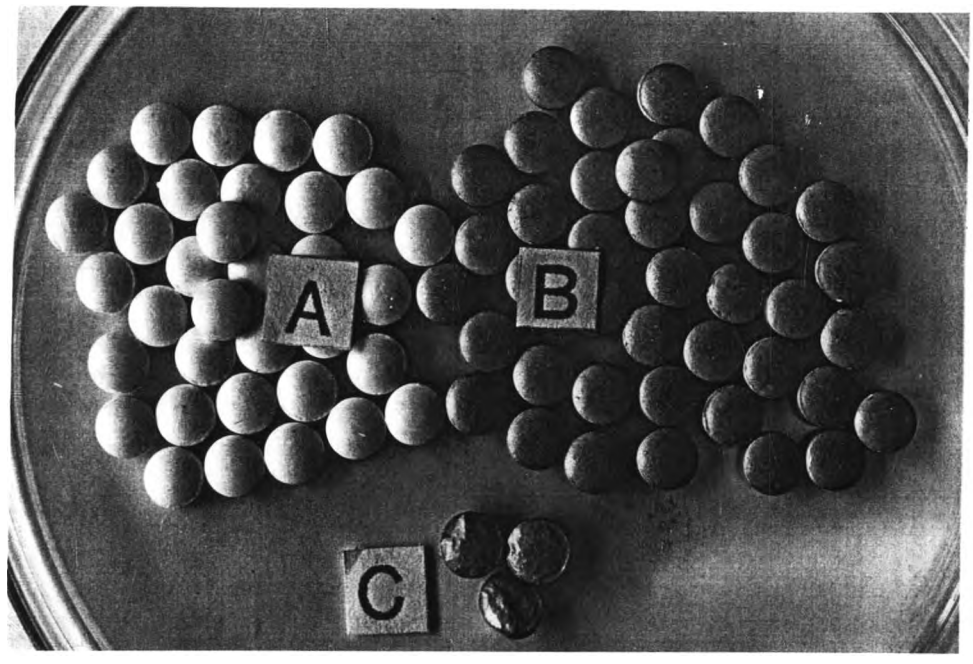

Figure 33(1) The appearance of coated tablet(LH0)(key:A-after kept at room temperature for 1 week, B-after exposure to accelerated condition, C-after exposure to accelerated condition and dissolution test).

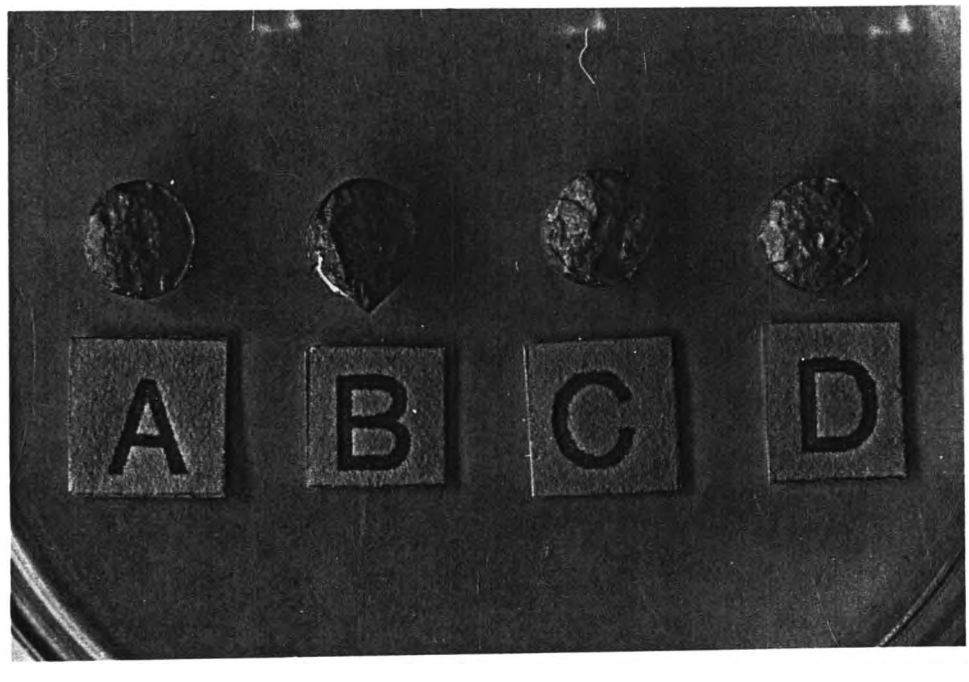

Figure 33(2) The appearance of coated tablets after exposure to accelerated condition and dissolution test(key:A-L0, B-M0, C-H0, D-LA10).

S after dissolution test had the edge splitting showing the inside tablet.

8. Surface topography

Scanning electron micrographs showing the surface topography of core and coated tablets are illustrated in Figures 34-56. The surfaces at crown area at magnification 75 and 2000, and edge areas at magnification 75 of the tablets are depicted.

8.1 Core tablet

The surface topography of the core tablet is illustrated in Fig 34 (A,B and C). The rough surface containing the compressed structure of granules and other added additives was clearly depicted.

8.2 Coated tablet

Areas of coated tablet were sampled and photographed. Figures 35-39, 40-44, 45-49, and 50-51 are illustrations of coated tablets using chitosan L, M, H and LH as film former respectively,and Figures 52-55 are illustrations of coated tablets when exposed to accelerated condition with and without subjected to dissolution test.

8.2.1 Chitosan L

The photomicrographs of L0 exhibited rather smooth surface and a few of very small pores on surface. For LA10, LA20 and LA30, their surfaces had degree of smoothness less than that of L0. LA10 had slightly more some moderate and very small pores on surface than LA20 and LA30.

The SEM photomicrographs of LB10 and LB20 illustrated many white needle shaped crystal in the film texture. The length of the particle was about 5-100 micron. By means of comparison, LB20 composed of more particles than LB10. The photomicrographs of LB20 and LB30 showed that there were white mold-like spots which occurred in LB30 more than in LB20. In addition, no needle shaped crystal could be observed in LB30. These tablets composed of medium to very

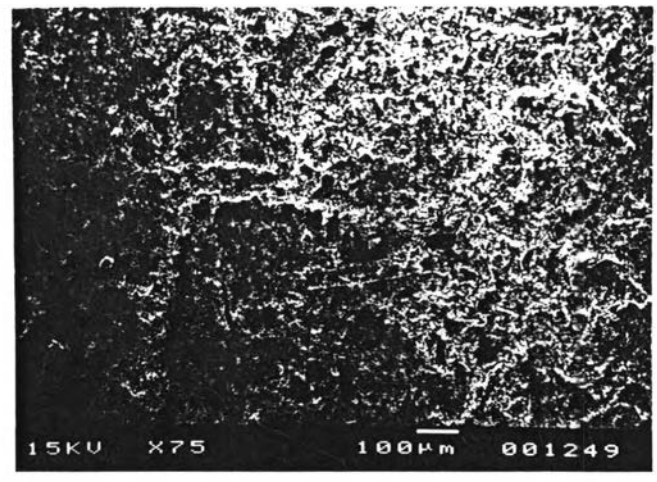

A

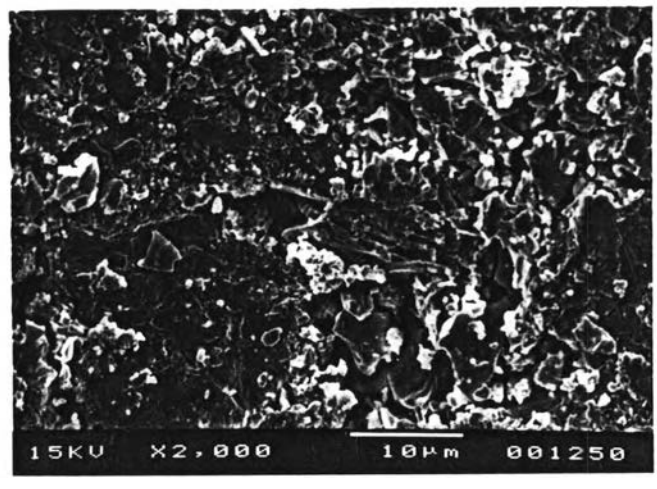

B

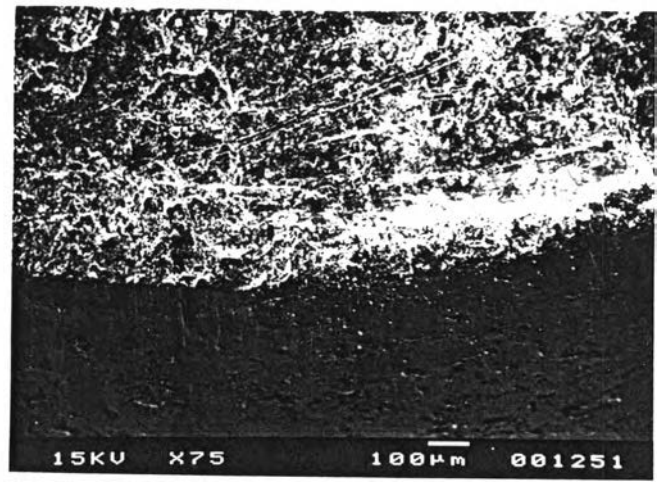

C

Figure 34 The photomicrographs of core tablet(key:A-crown*75, B-crown*2000, C-edge*75)).

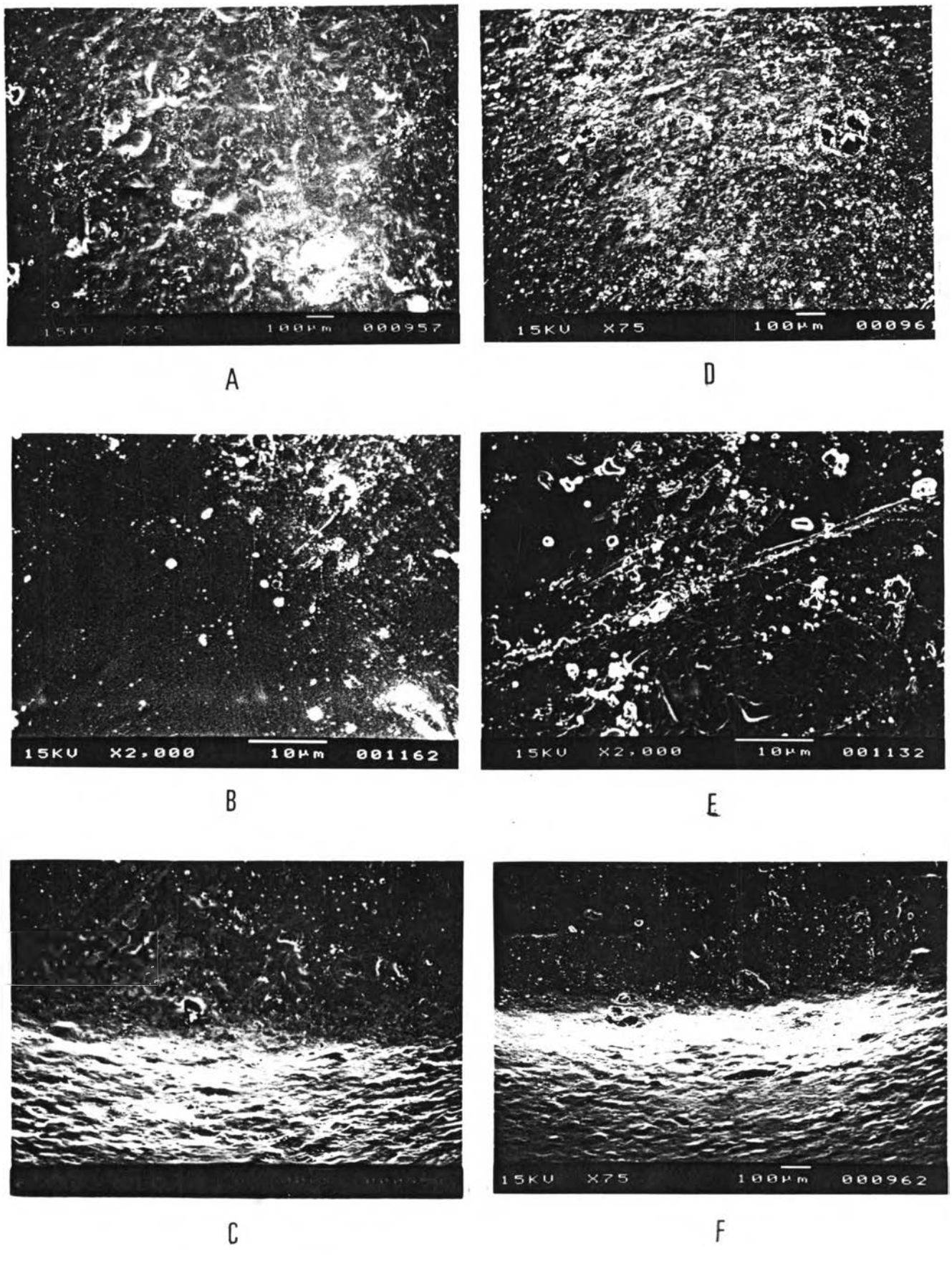

Figure 35 The photomicrographs of coated tablet(key:A-C(L0) (A-crown*75, B-crown*2000, C-edge*75), D-F(LA10) (D-crown*75, E-crown*2000, F-edge*75)).

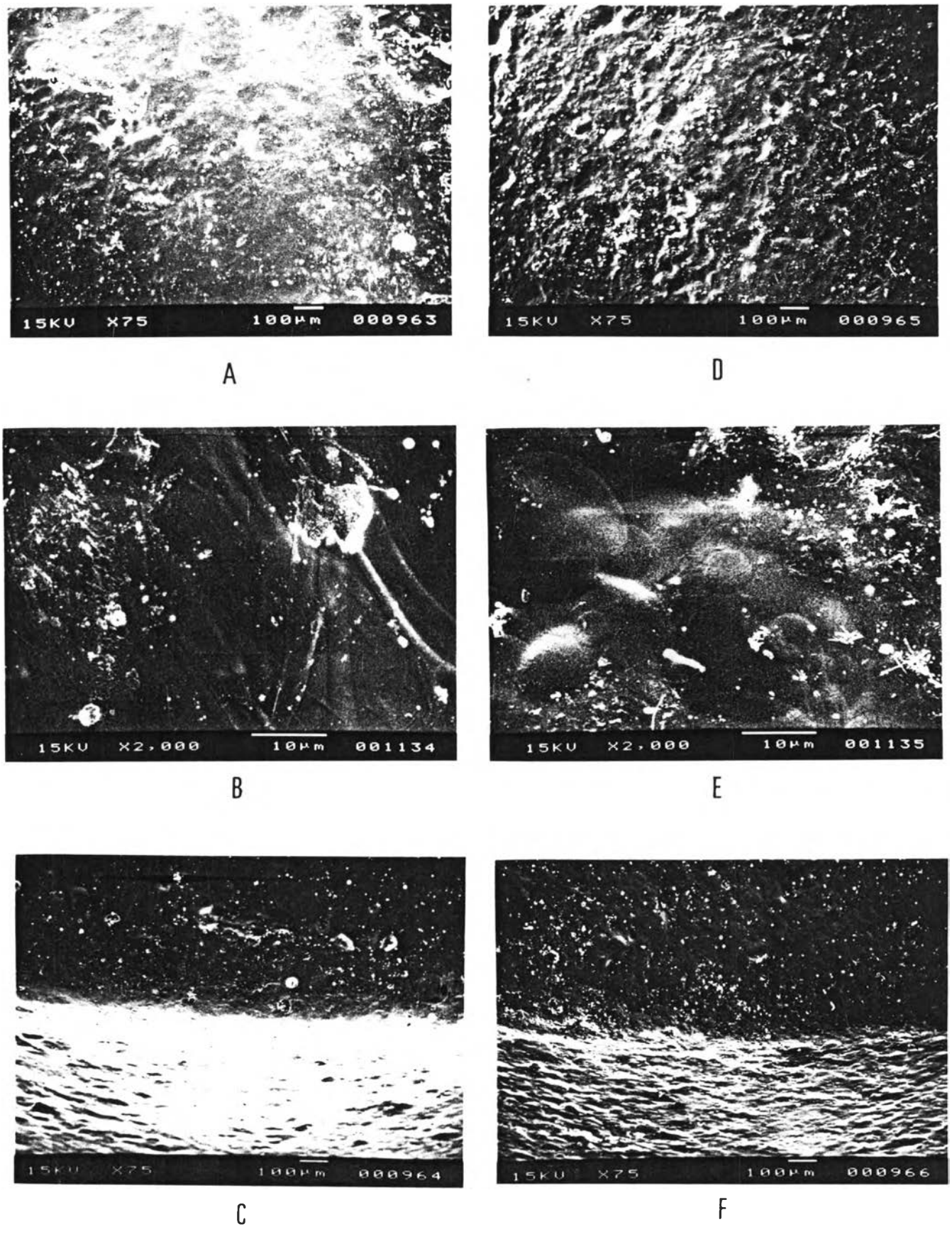

Figure 36 The photomicrographs of coated tablet(key:A-C(LA20) (A-crown*75, B-crown*2000, C-edge*75), D-F(LA30) (D-crown*75, E-crown*2000, F-edge*75)).

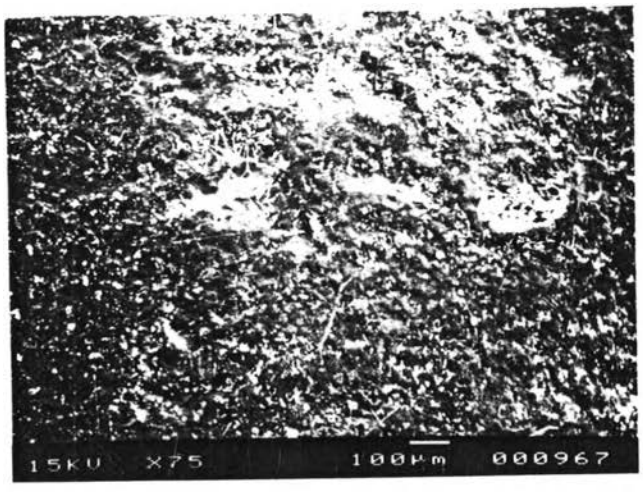

A

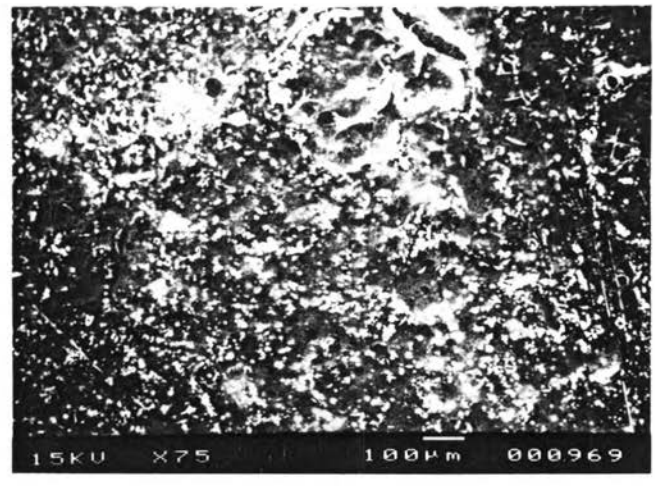

D

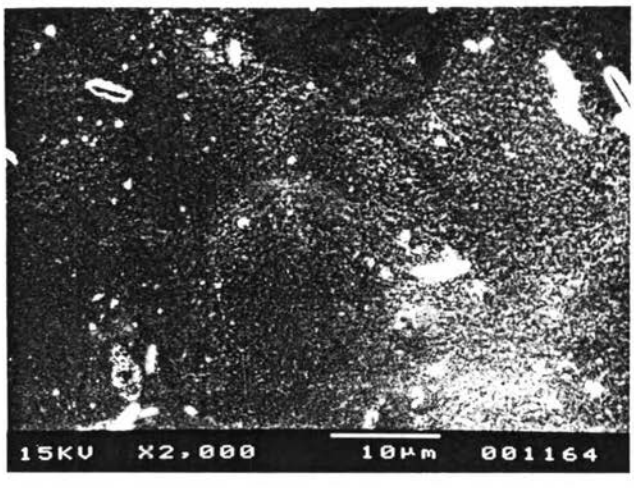

B

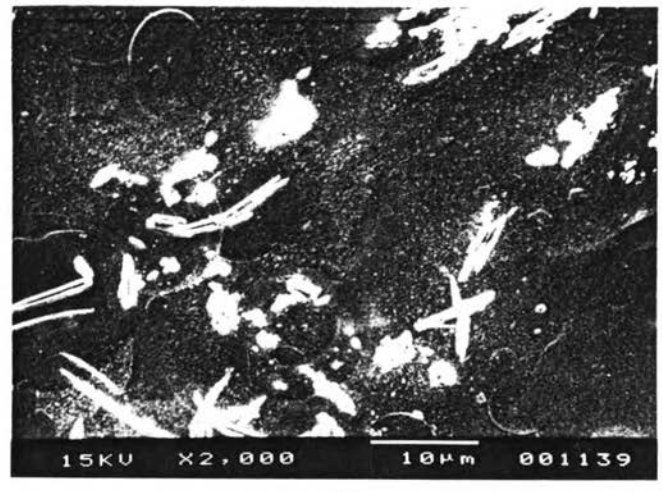

E

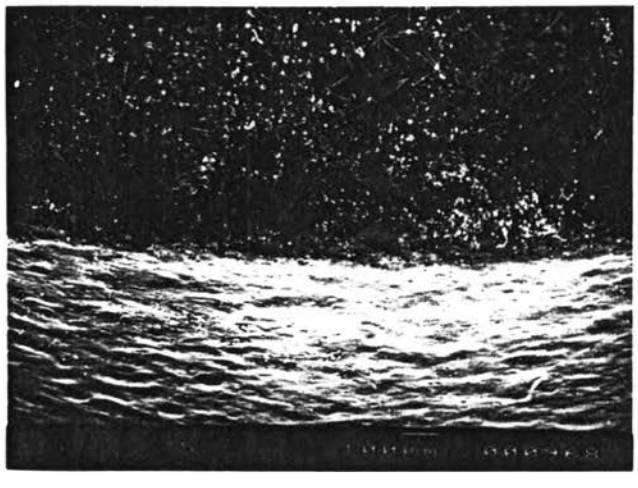

C

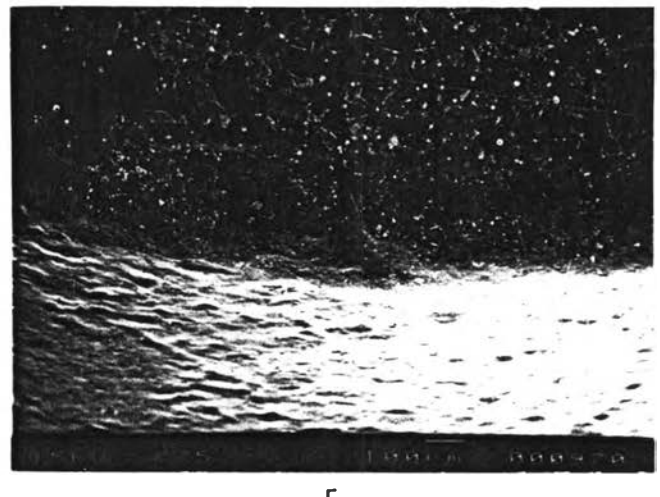

F

Figure 37 The photomicrographs of coated tablet(key:A-C(LB10) (A-crown*75, B-crown*2000, C-edge*75), D-F(LB20) (D-crown*75, E-crown*2000, F-edge*75)).

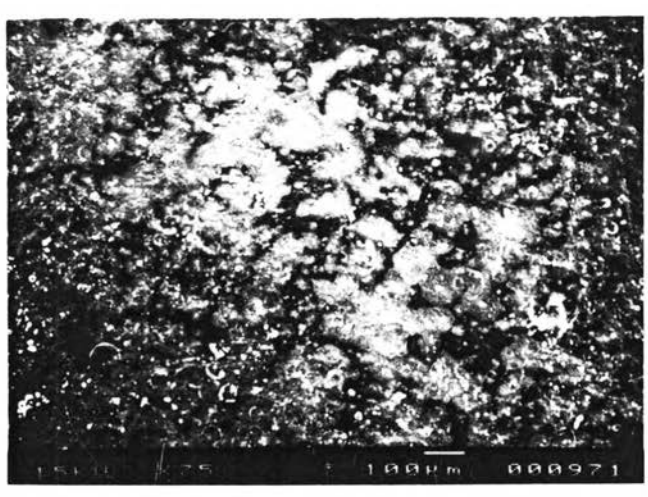

A

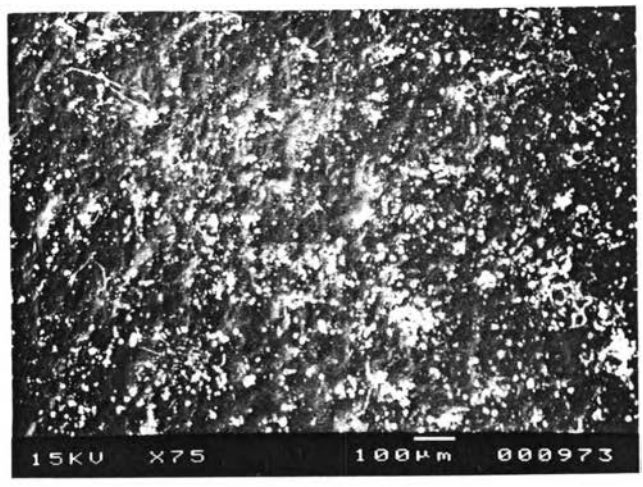

D

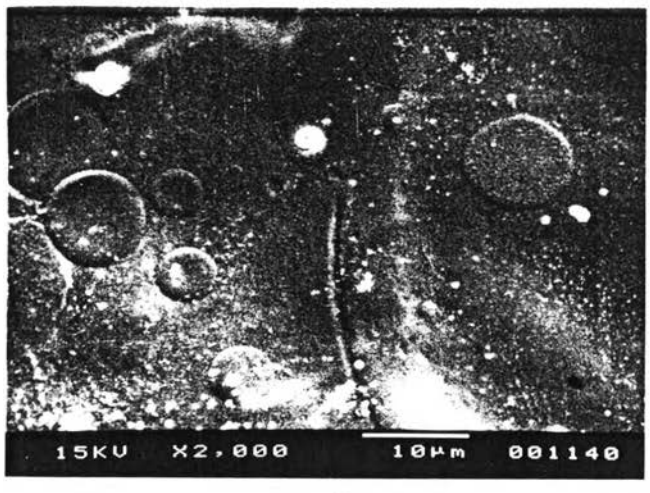

B

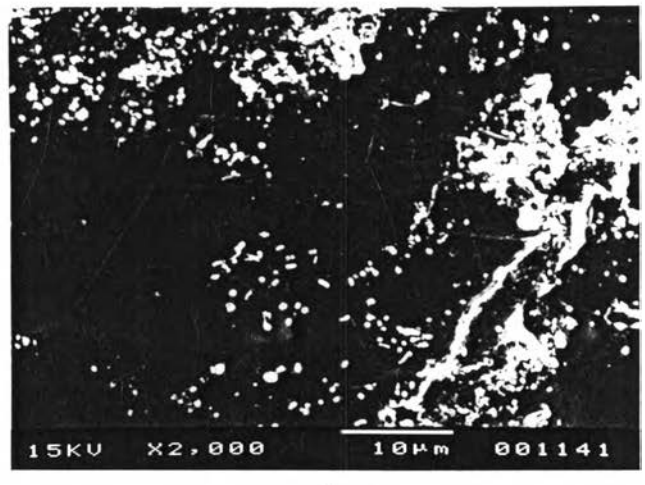

E

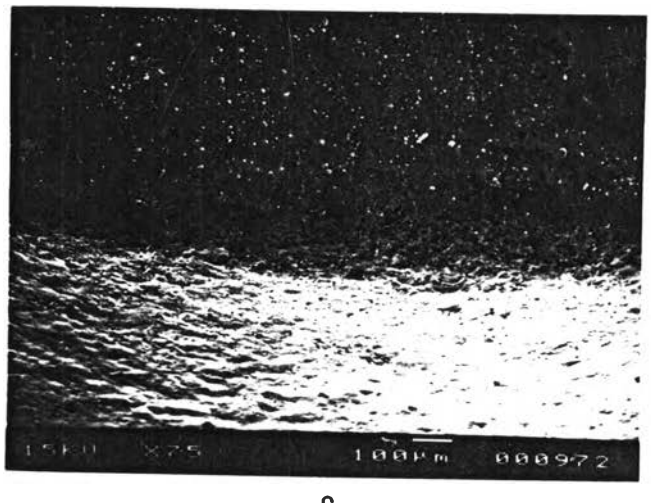

C

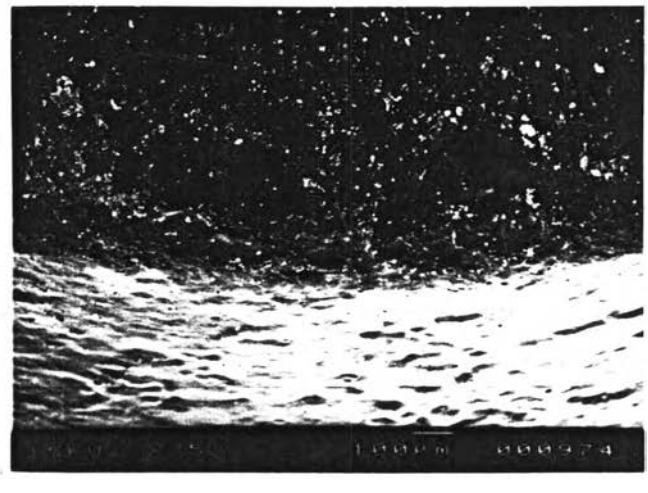

F

Figure 38 The photomicrographs of coated tablet(key:A-C(LB30) (A-crown*75, B-crown*2000, C-edge*75), D-F(LC10) (D-crown*75, E-crown*2000, F-edge*75)).

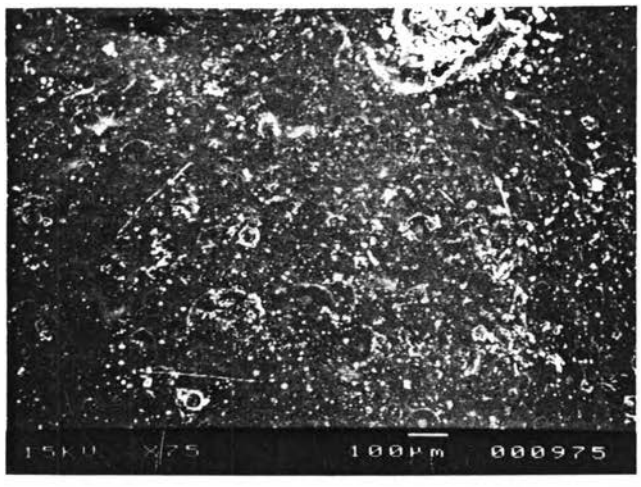

A

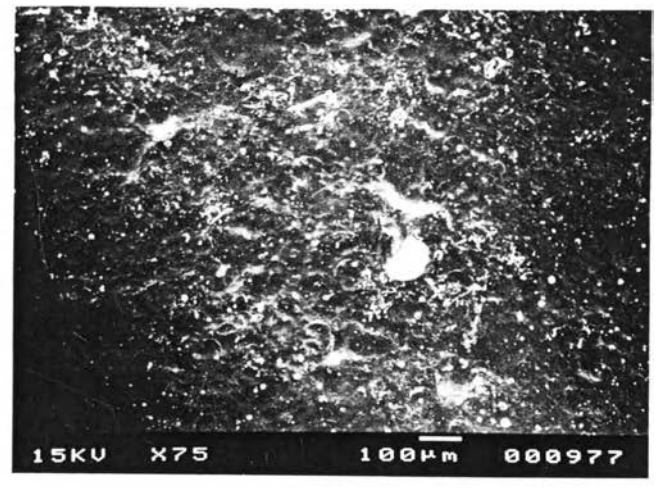

D

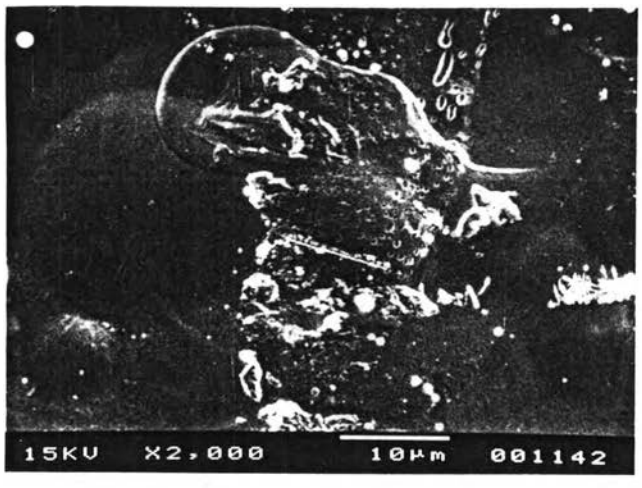

B

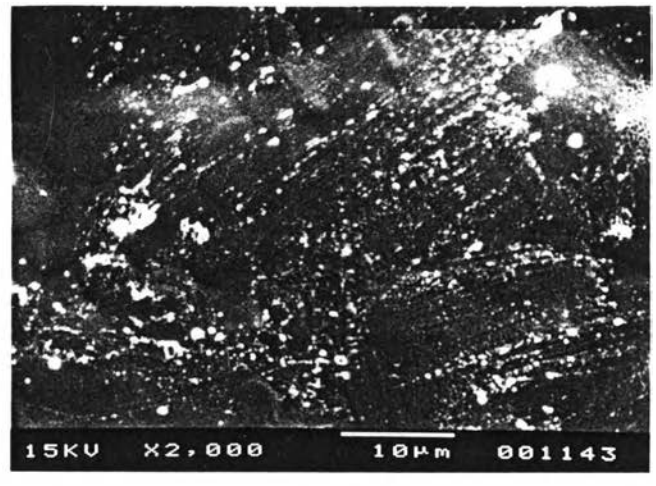

E

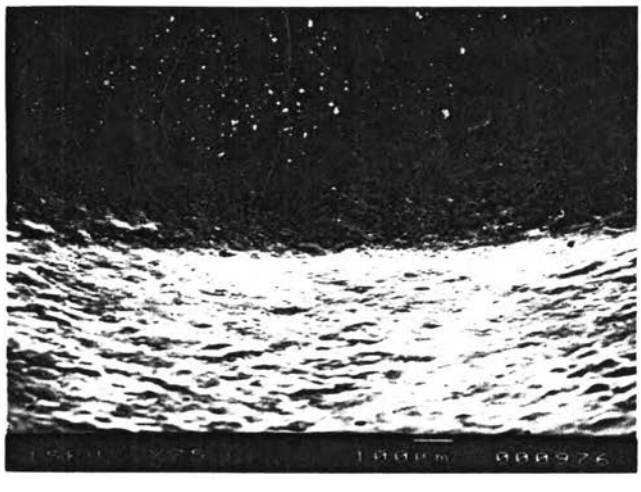

C

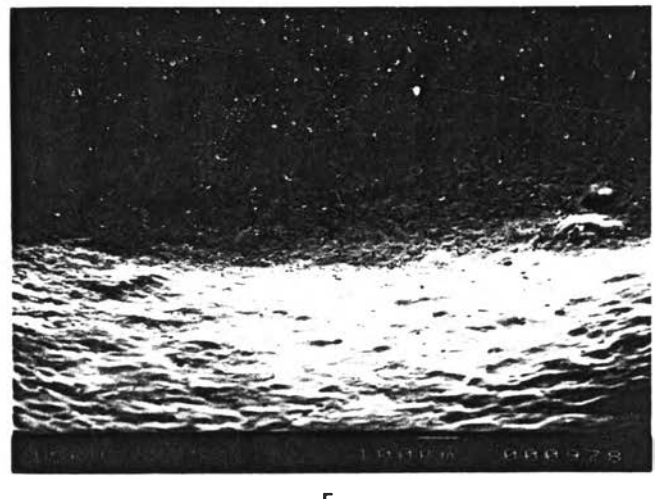

F

Figure 39 The photomicrographs of coated tablet(key:A-C(LC20) (A-crown*75, B-crown*2000, C-edge*75), D-F(LC30) (D-crown*75, E-crown*2000, F-edge*75)).

small pores on surface liked in tablet of LA20 and LA30, but the degree of smoothness was rather less than LA tablets.

The surfaces of LC10, LC20 and LC30 tablets were rather smooth with some small pores at the crown area. The amount of pores could be ranked as : LC30>LC20>LC10. Morever, there were irregular and rod shaped particles of 0.5-3 micron on the film surface. The amount of particles could be ranked as LC10>LC30>LC20.

8.2.2 Chitosan M

The surface of M0 (Fig 40 A,B and C) was rather smooth, but showed less degree of smoothness than that of surface of L0 at high magnification. In addition there were many medium-sized pores presented on the crown and edge of coated tablet.

By means of comparison, the degree of smoothness of MA30 was higher than MA10 and MA20. These three tablets composed of some pores which the amount could be ranked as : MA30<MA20<MA10.

The microscopic apperance of tablets coated with M containing PEG400 as plasticizer showed that there were a few particles and white mold-like spots on the surface of MB10, but the surfaces of MB20 and MB30 mainly exhibited only white mold-like spots as occurred in LB20 and LB30. The amount of white mold-like spots could be ranked as followed : MB30>MB20>MB10. The surface of these three tablets were rather smooth with some small creeks on the edge of the tablet.

The pictures showed that the surface was rather rough in MC10. There were many pores on surface of MC10 and MC30, especially at the edge of the latter tablet. The degree of smoothness could be ranked as : MB20>MB10>MB30. Some particles were deposited on the surface of the film which the amount of particles could be ranked as : MB30>MB20>MB10.

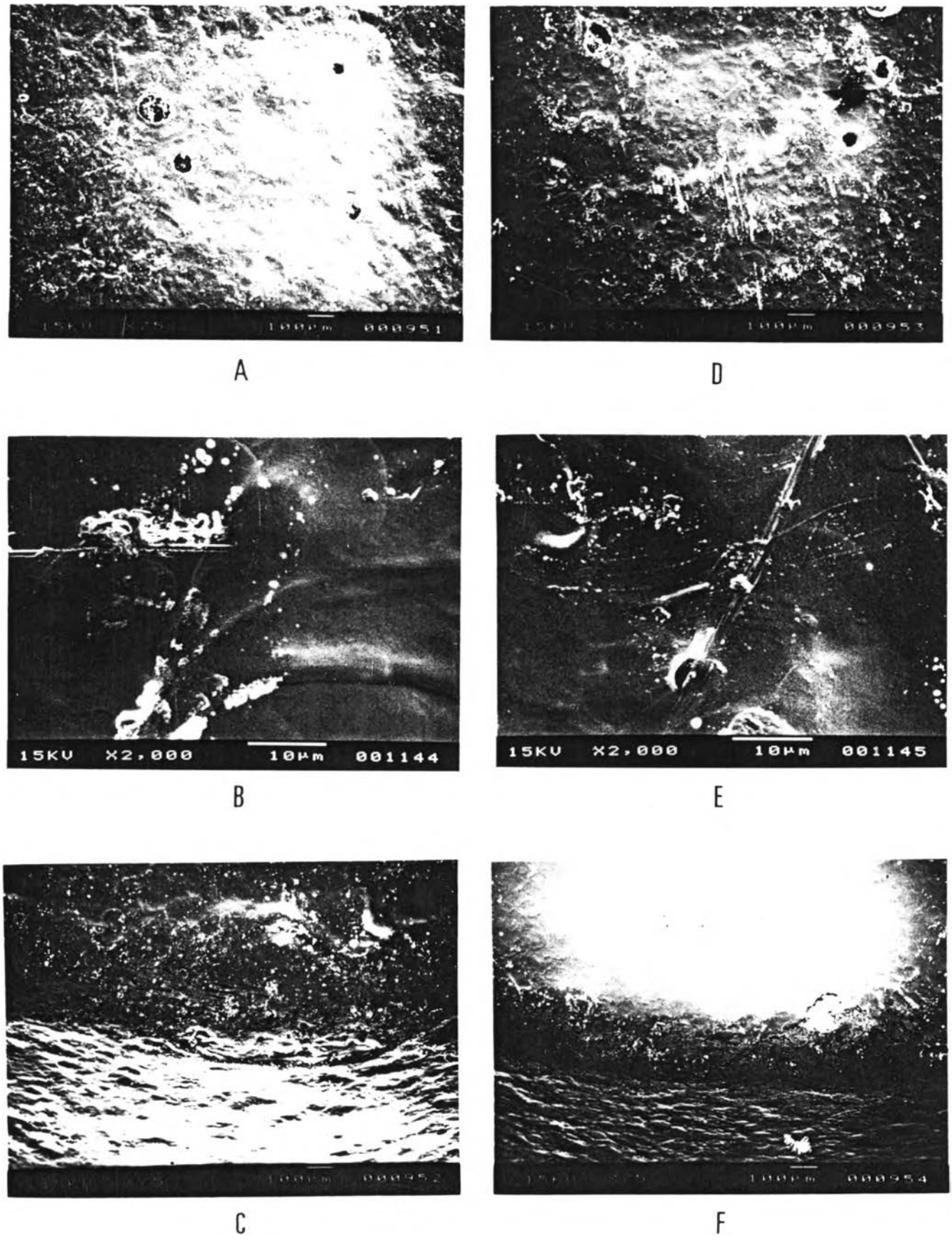

Figure 40 The photomicrographs of coated tablet(key:A-C(M0) (A-crown*75, B-crown*2000, C-edge*75), D-F(MA10) (D-crown*75, E-crown*2000, F-edge*75)).

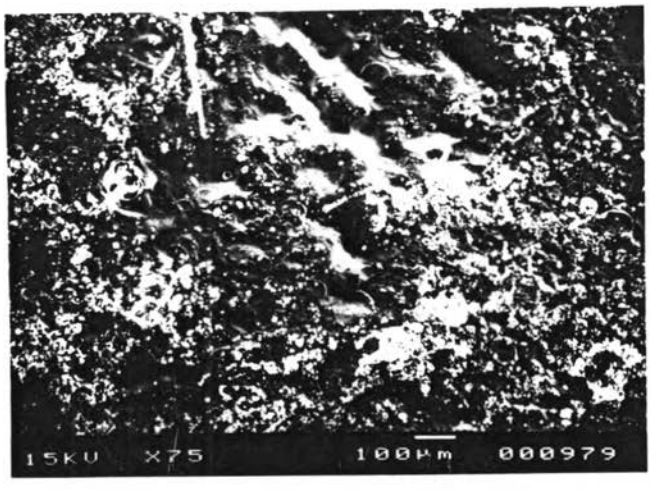

A

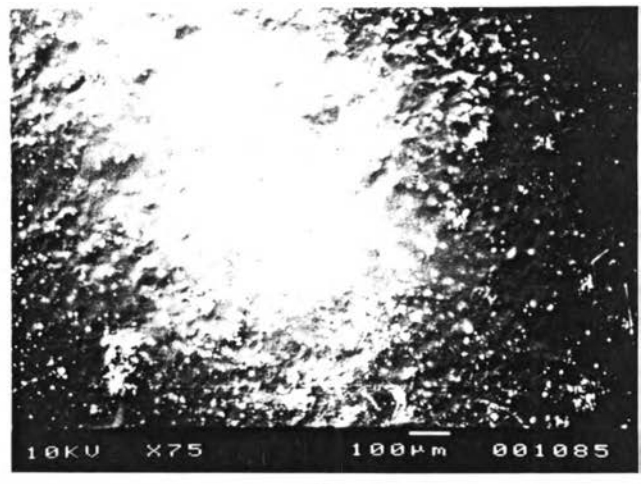

D

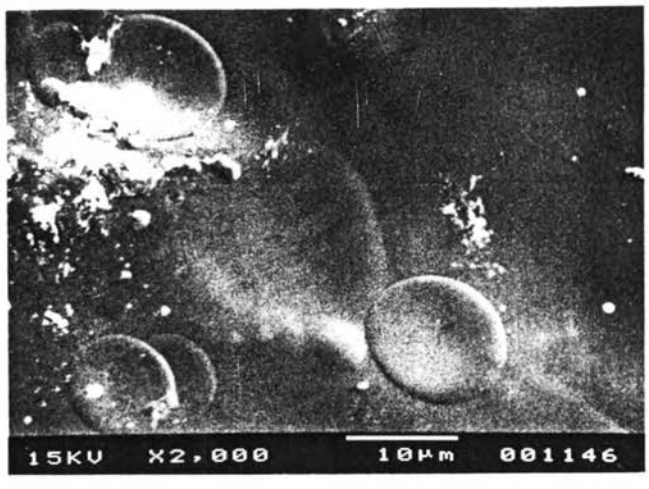

B

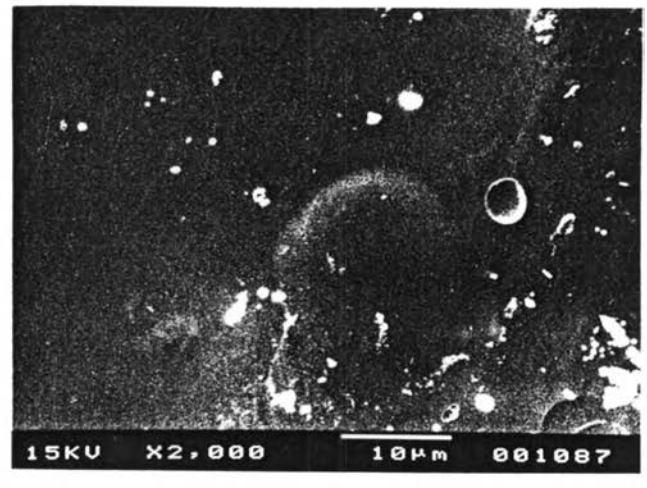

E

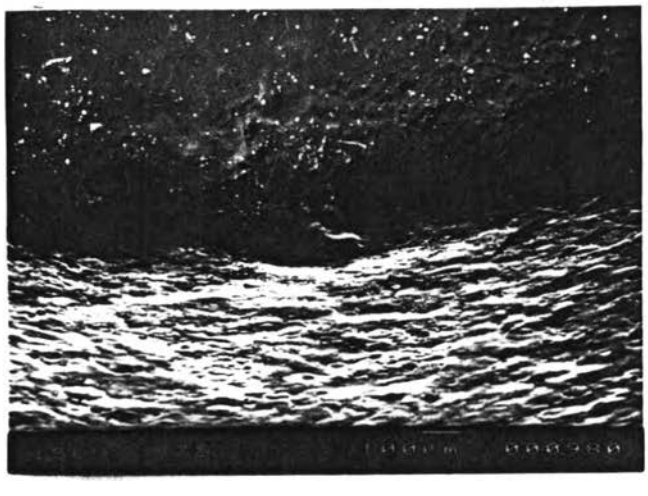

C

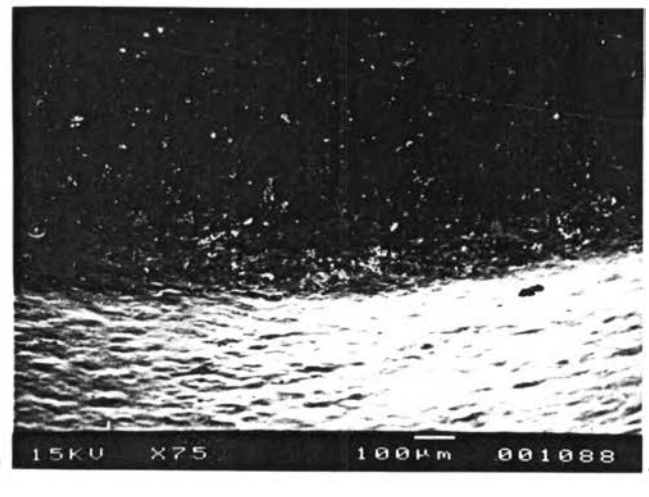

F

Figure 41 The photomicrographs of coated tablet(key:A-C(MA20) (A-crown*75, B-crown*2000, C-edge*75), D-F(MA30) (D-crown*75, E-crown*2000, F-edge*75)).

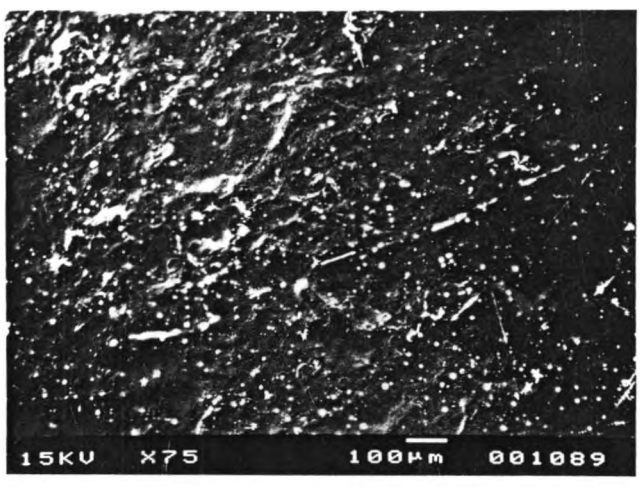

A

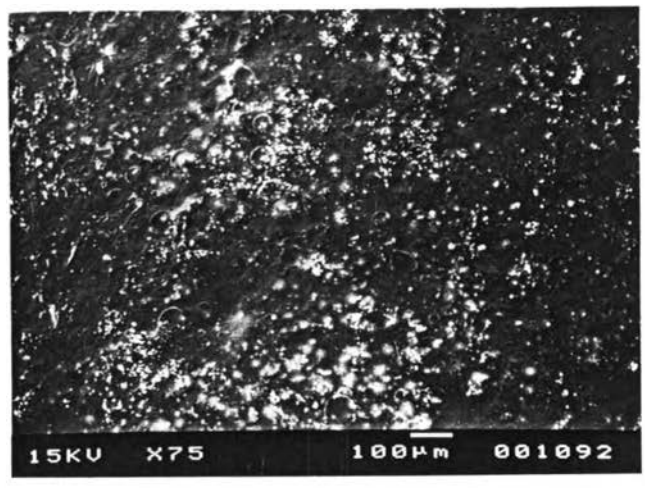

D

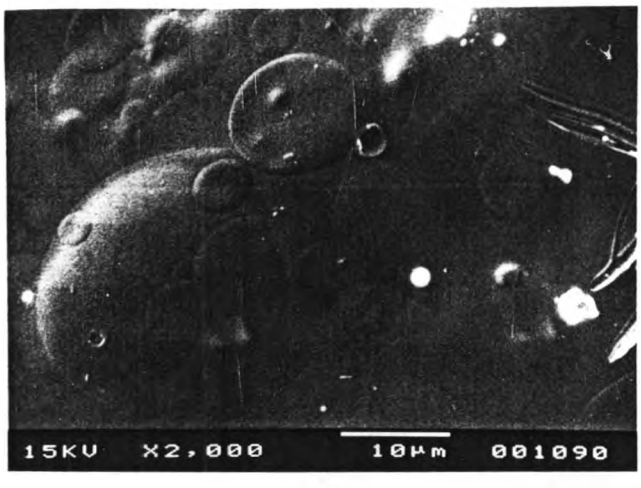

B

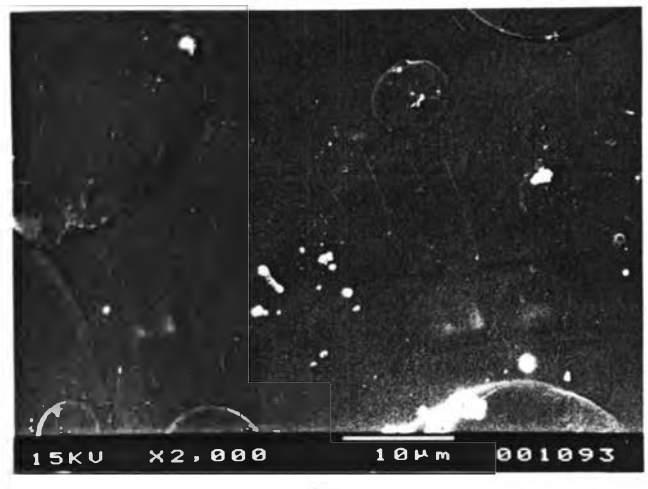

E

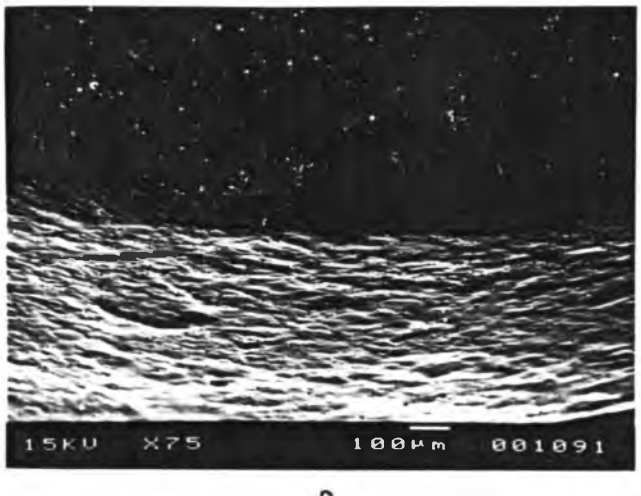

C

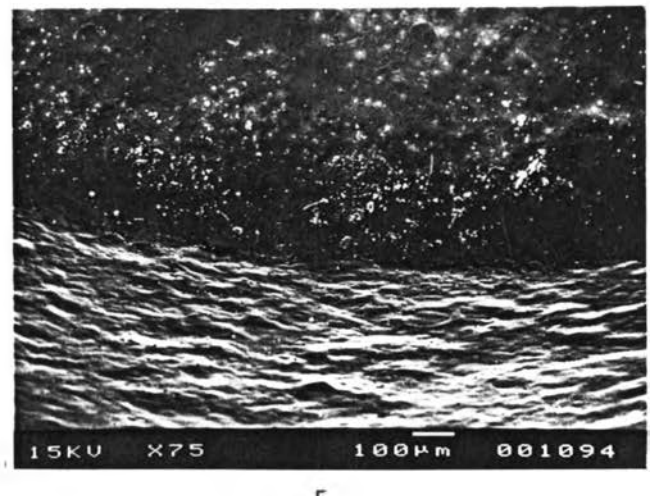

F

Figure 42 The photomicrographs of coated tablet(key:A-C(MB10) (A-crown*75, B-crown*2000, C-edge*75), D-F(MB20) (D-crown*75, E-crown*2000, F-edge*75)).

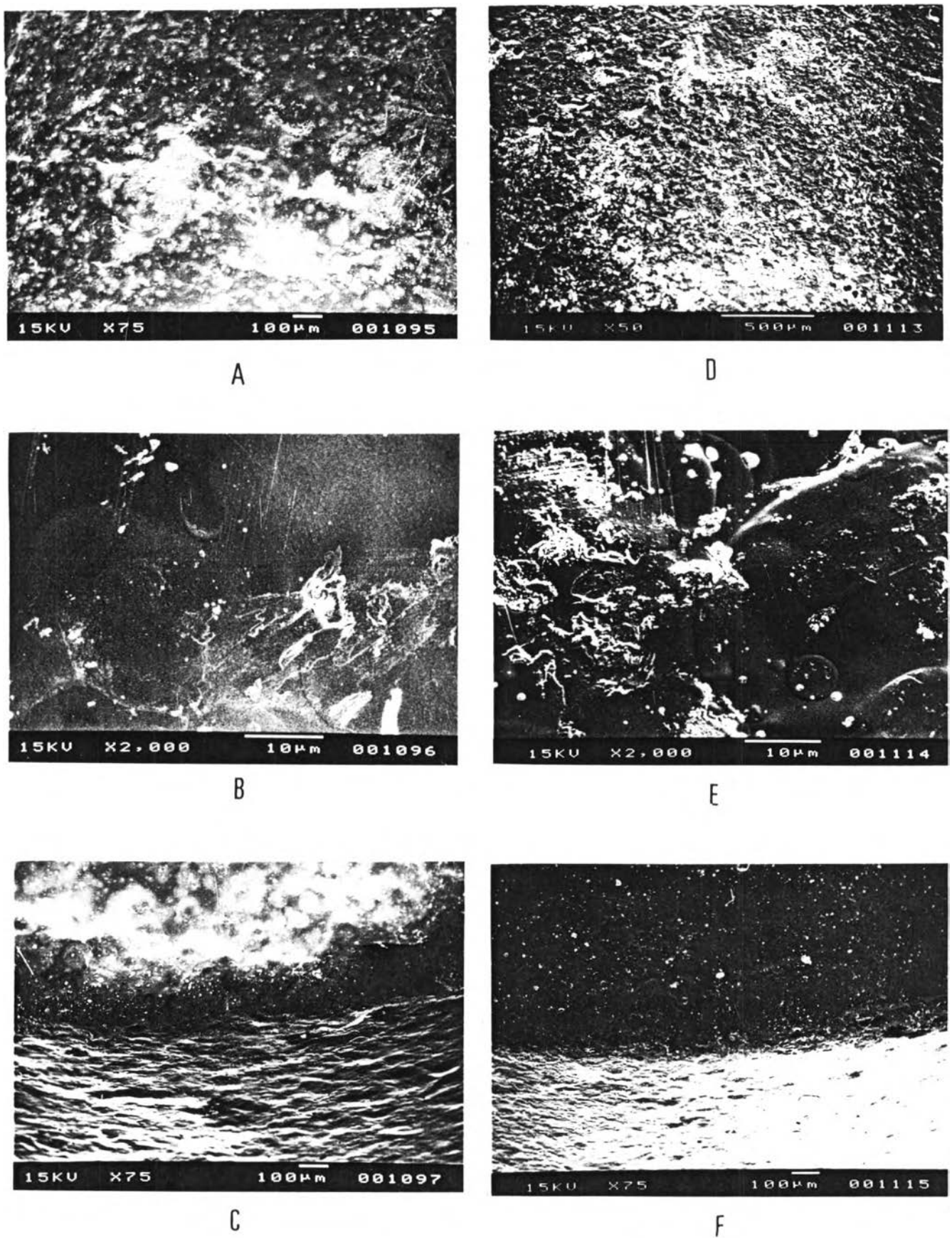

Figure 43 The photomicrographs of coated tablet(key:A-C(MB30) (A-crown*75, B-crown*2000, C-edge*75), D-F(MC10) (D-crown*75, E-crown*2000, F-edge*75)).

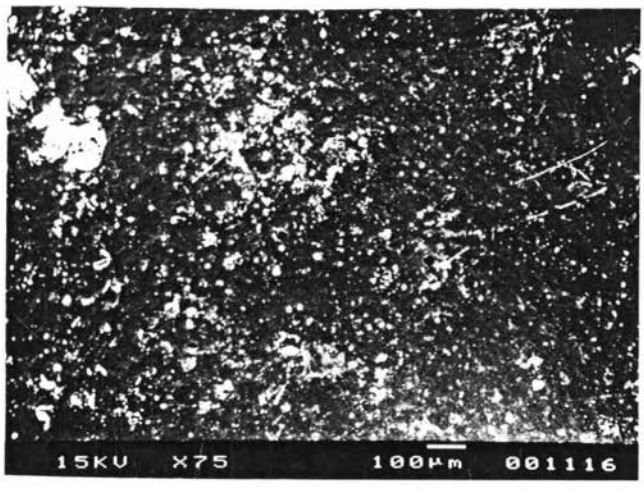

A

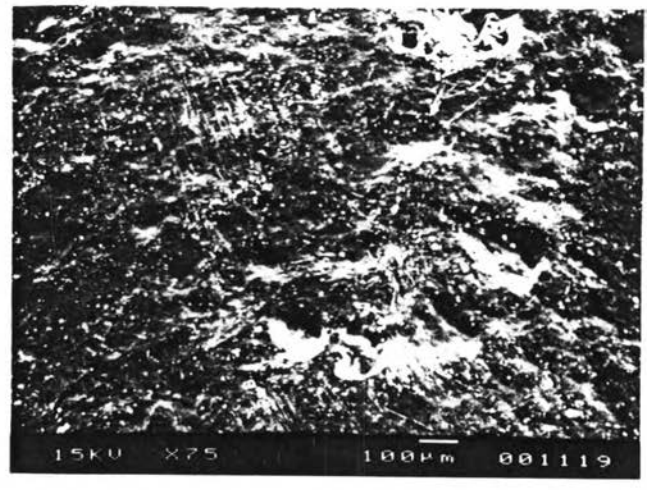

D

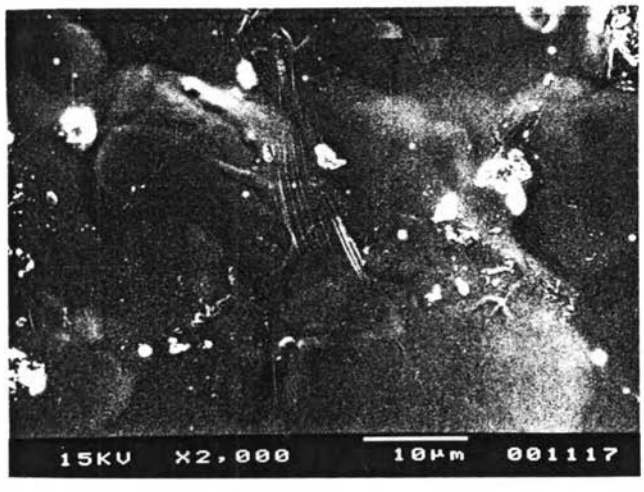

B

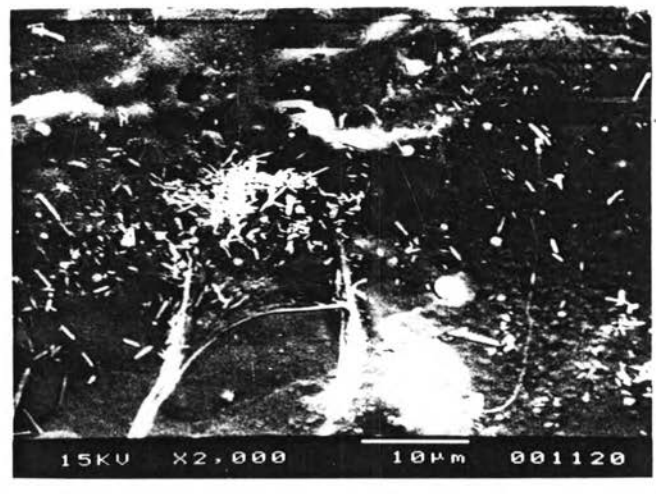

E

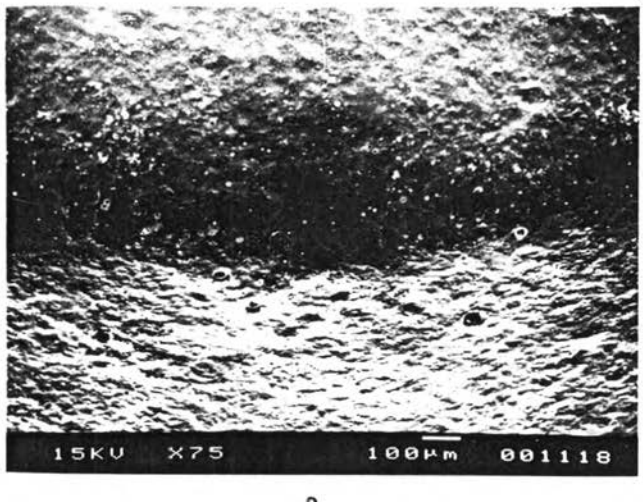

C

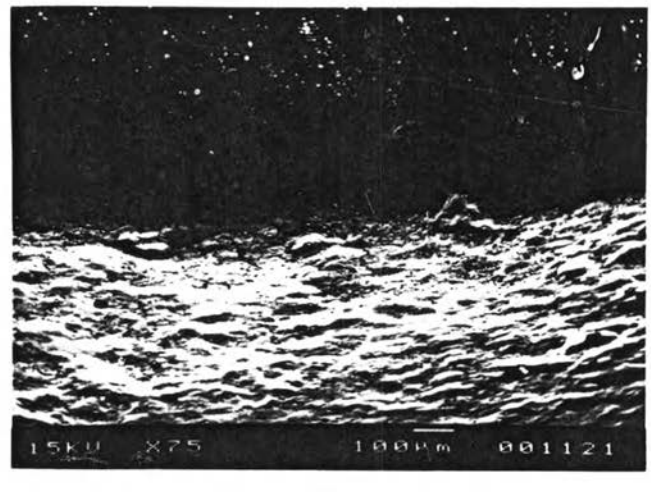

F

Figure 44 The photomicrographs of coated tablet(key:A-C(MC20) (A-crown*75, B-crown*2000, C-edge*75), D-F(MC30) (D-crown*75, E-crown*2000, F-edge*75)).

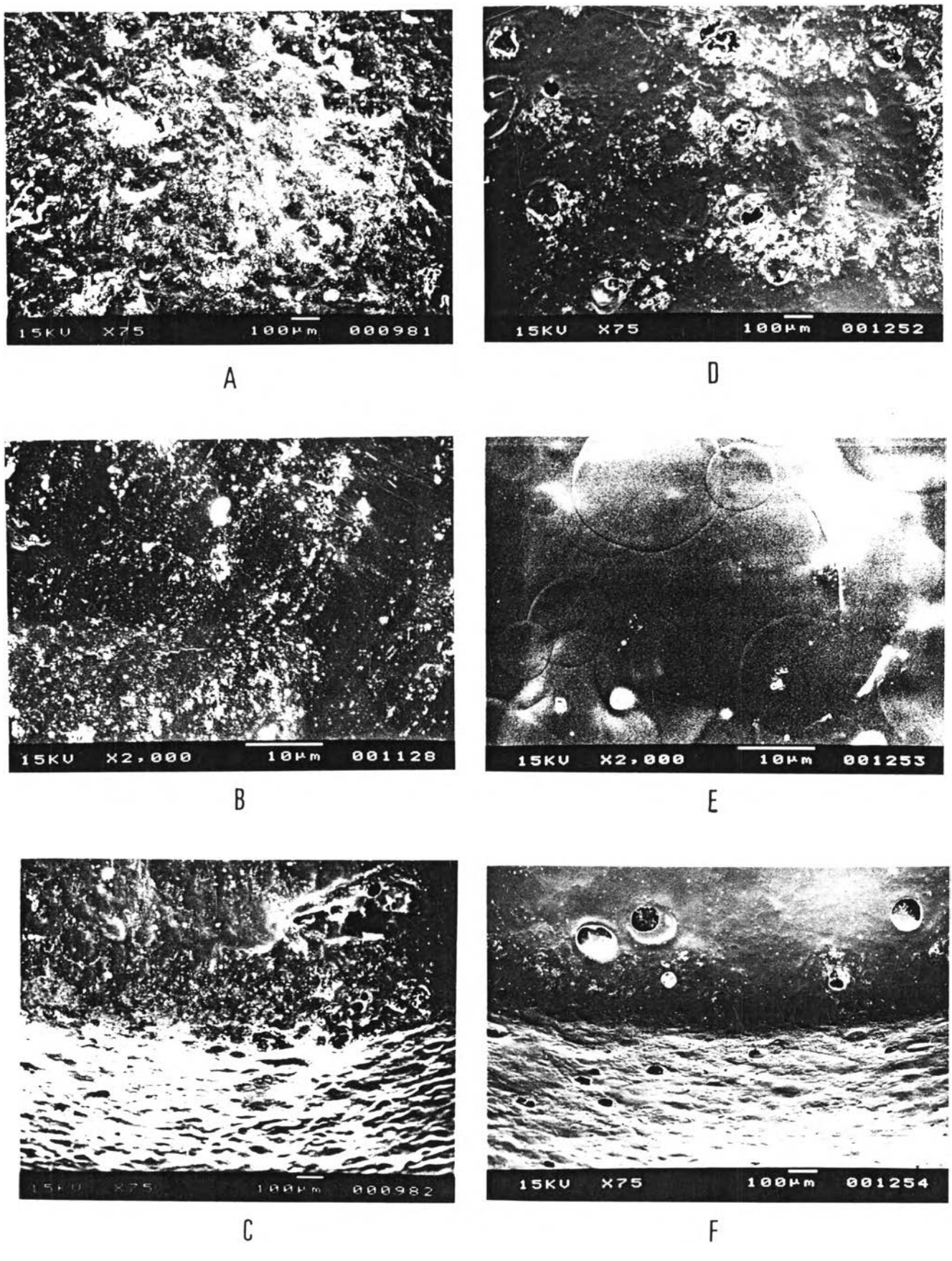

Figure 45 The photomicrographs of coated tablet(key:A-C(H0) (A-crown*75, B-crown*2000, C-edge*75), D-F(HA10) (D-crown*75, E-crown*2000, F-edge*75)).

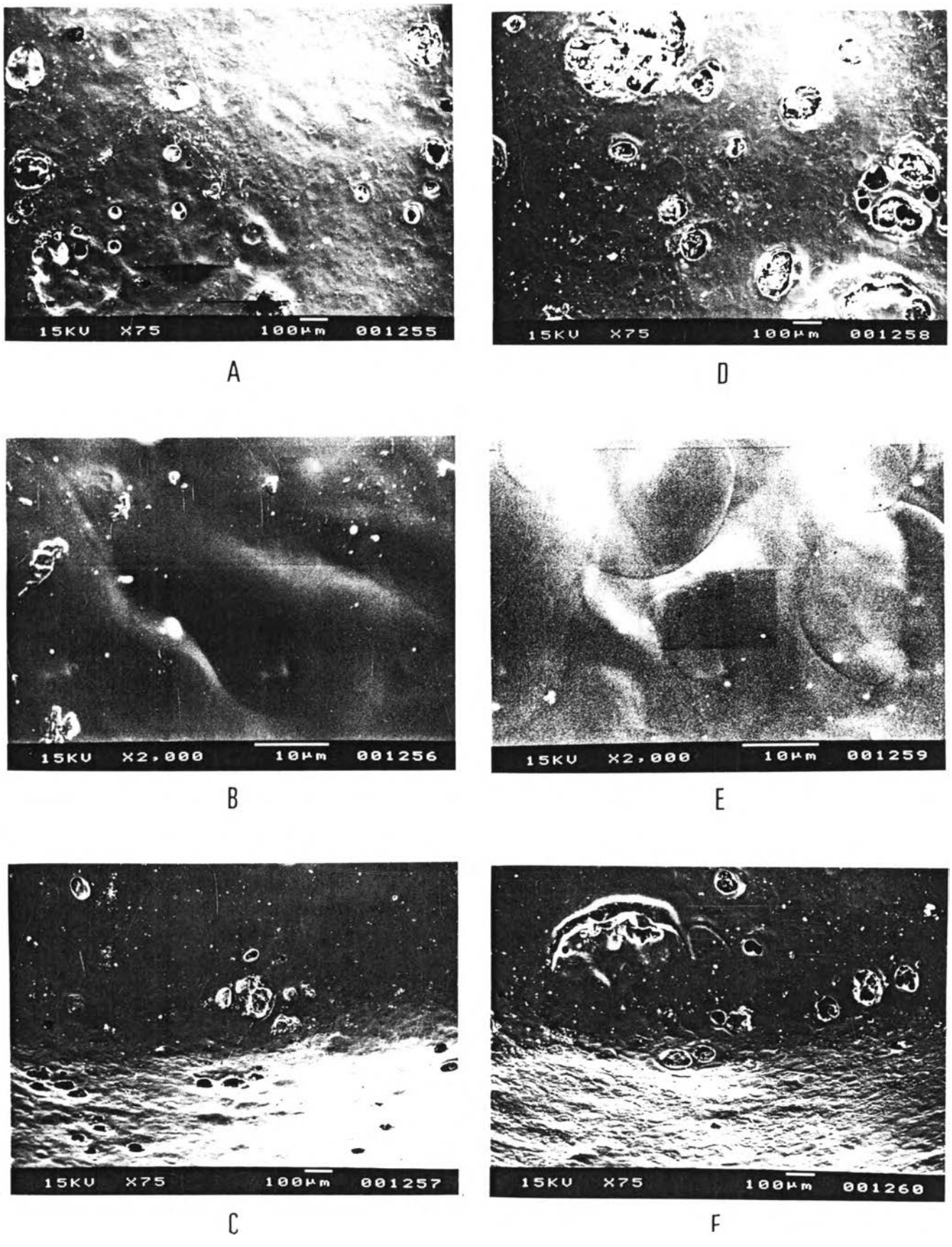

Figure 46 The photomicrographs of coated tablet(key:A-C(HA20) (A-crown*75, B-crown*2000, C-edge*75), D-F(HA30) (D-crown*75, E-crown*2000, F-edge*75)).

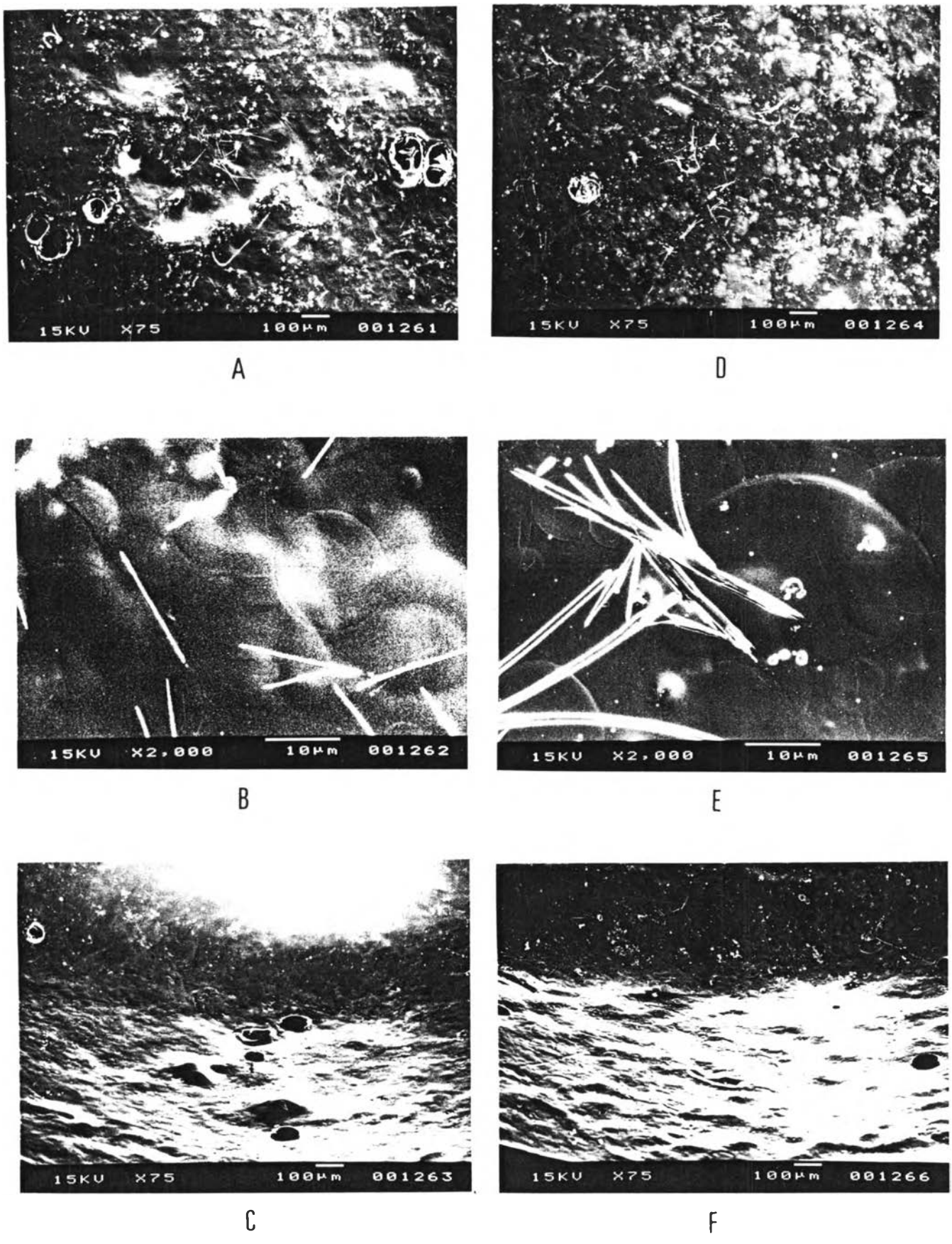

Figure 47 The photomicrographs of coated tablet(key:A-C(HB10) (A-crown*75, B-crown*2000, C-edge*75), D-F(HB20) (D-crown*75, E-crown*2000, F-edge*75)).

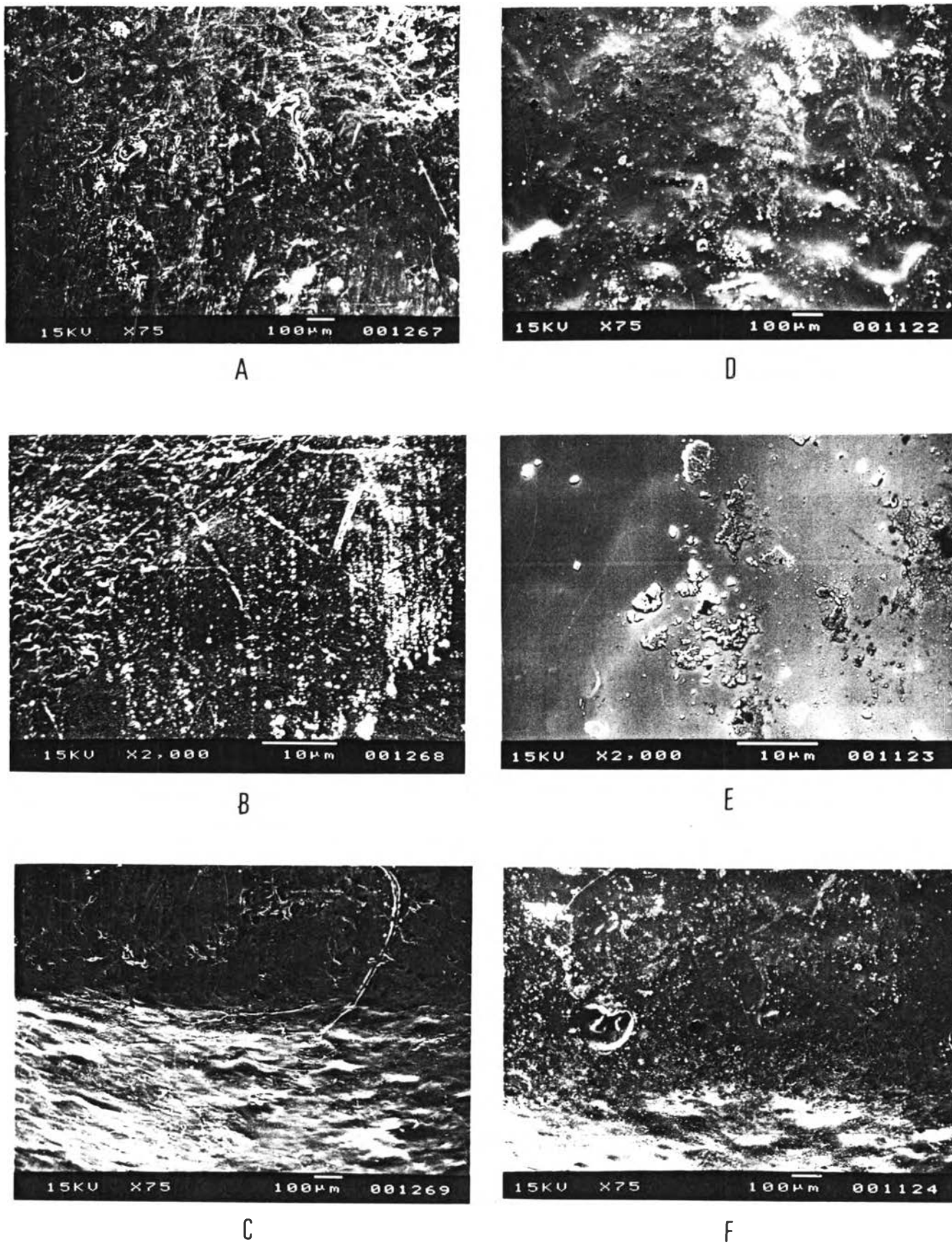

Figure 48 The photomicrographs of coated tablet(key:A-C(HB30) (A-crown*75, B-crown*2000, C-edge*75), D-F(HC10) (D-crown*75, E-crown*2000, F-edge*75)).

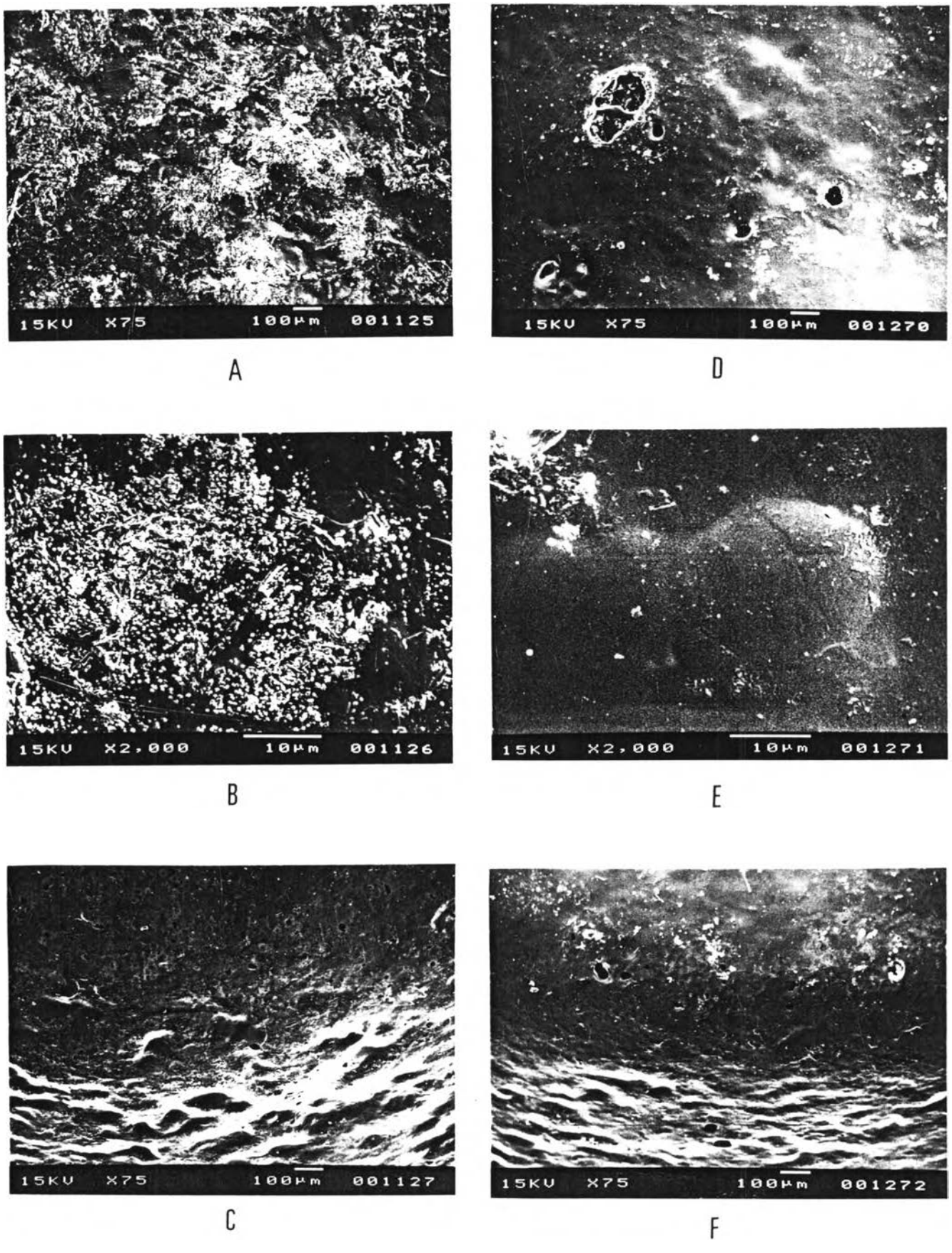

Figure 49 The photomicrographs of coated tablet(key:A-C(HC20) (A-crown*75, B-crown*2000, C-edge*75), D-F(HC30) (D-crown*75, E-crown*2000, F-edge*75)).

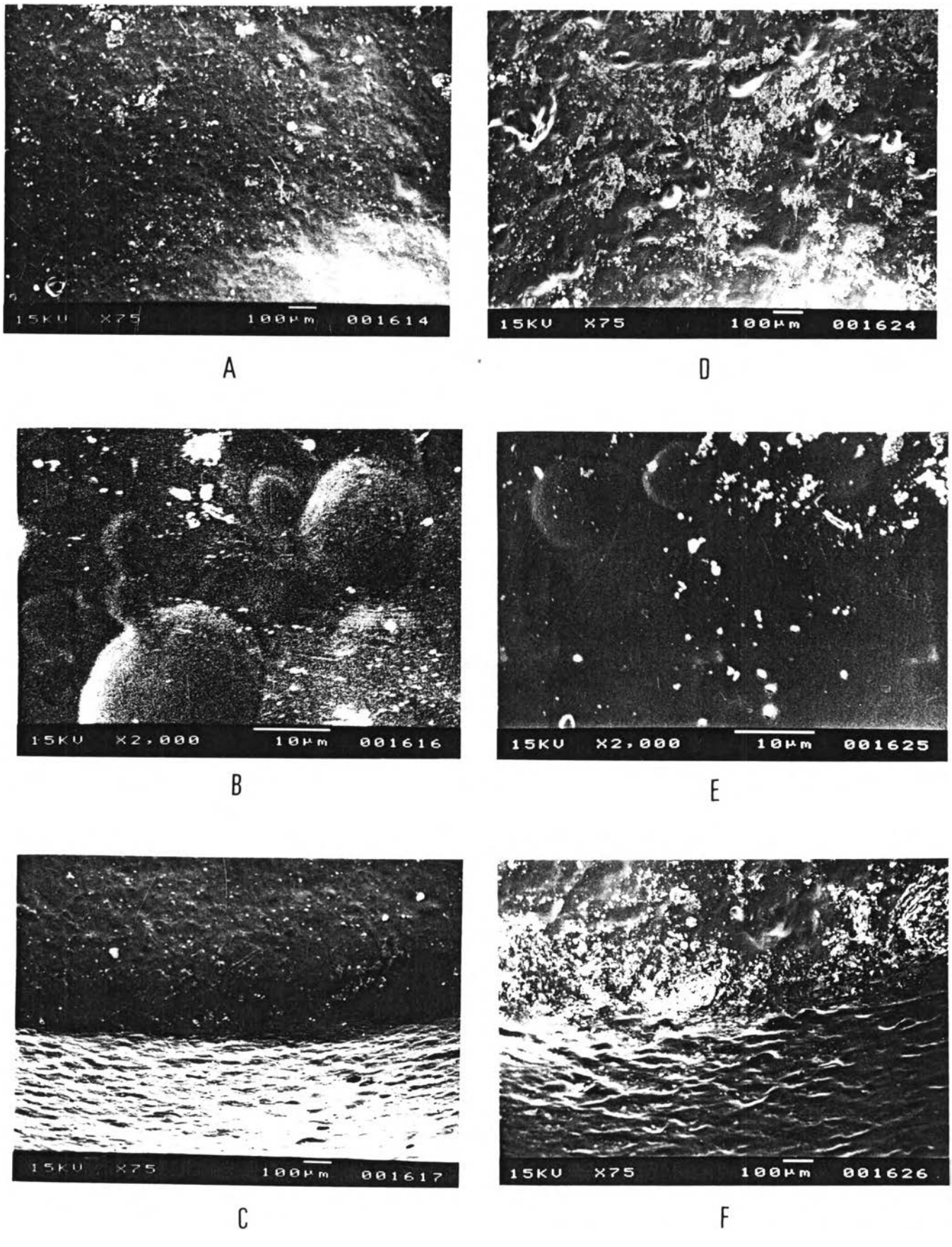

Figure 50 The photomicrographs of coated tablet(key:A-C(LH0) (A-crown*75, B-crown*2000, C-edge*75), D-F(LHA10) (D-crown*75, E-crown*2000, F-edge*75)).

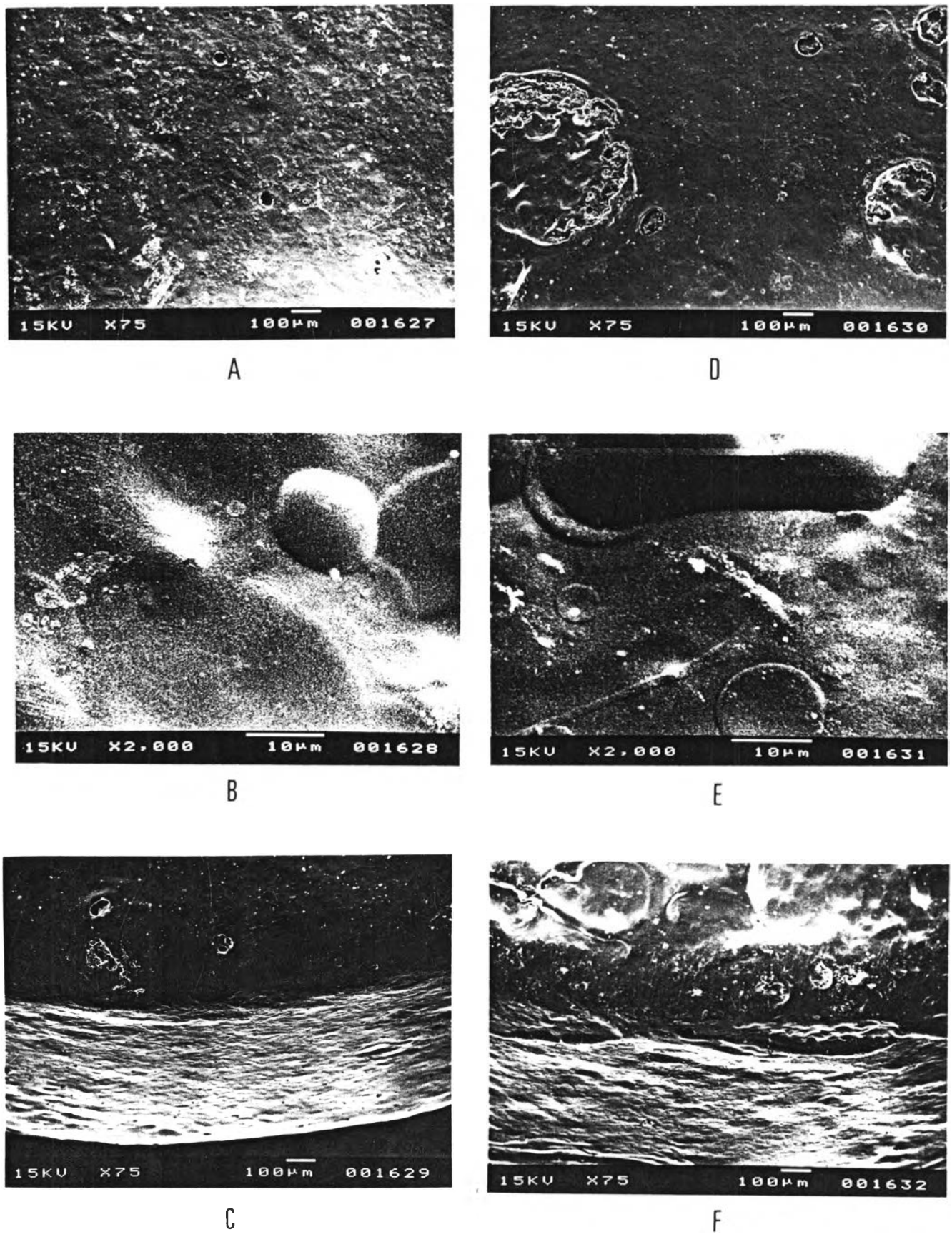

Figure 51 The photomicrographs of coated tablet(key:A-C(LHA20) (A-crown*75, B-crown*2000, C-edge*75), D-F(LHA30) (D-crown*75, E-crown*2000, F-edge*75)).

8.2.3 Chitosan H

The SEM photomicrographs of H0 showed that the surface was rather rough with some medium-sized pores on the crown and very small pores at the edge of tablet.

The surface of all these tablets was smoother than H0. The number of defect on the surface could be ranked as : HA30>HA10>HA20.

Many needle shaped crystals of about 5-200 micron were occurred in the film texture. These particles were longer than those found in LB and MB systems. The number of particles could be ranker as : HB10>HB20>HB30 and the amount of white mold-like spots found on film surfaces could be ranked as : HB20>HB30>HB10. All tablets composed of some medium sized pore which the amount could be ranked : HB30>HB10>HB20 and degree of smoothness could be ranked as :HB0>HB10>HB30.

There were many small pores and some medium sized pores on surface of HC tablets. The amount of particles could be ranked as : HC20>HC10>HC30. The surface of HC system was rather rough. The lowest degree of smoothness was found in HC20.

8.2.4 Combined chitosan L and H

The rather smooth surface of LH0 had some particle deposited. These particles were irregular sphape and narrow size range of 0.2-50 micron. The very small pores were mainly observed in the surface.

The surface of LHA10 was rather rough deposited with some irregular shaped particles and some defects were also clearly seen. The surface of LHA20 was rather smooth composed of some pores . There were many defects in surface of LHA30 and the surface was rather rough.

8.3 Coated tablet after exposure to accelerated condition and coated tablet after exposure accelerated condition after dissolution test.

The SEM photomicrographs of L0 after exposure to accelerated condition (L0 S) showed a small crack on surface. The degree of smoothness of L0 and L0 S was alike, but the amount of pores of L0 S was fewer than L0. The surface of L0 S after dissolution test at low magnification was smoother than that of L0, but at high magnification there were many particles which imbeded in the surface. These particles were irregular and rod shapes which the length was about 2-100 micron. The surface was also seen many pores occurred between particles.

The surface of LA10 S was smoother than LA10. The amount of pores was fewer than that of LA10 and there was a small crack at the edge of the tablet. The microscopic apperance of LA10 S after dissolution test showed the irregular and rod shapes particles imbeded in the surface. The length of the particles was about 0.5-250 micron. Most particles were larger than found in L0 S after dissolution test. The amount and size of pores of LA10 and LA10 S after dissolution test were alike.

The surface of M0 S was smoother than M0. The surface of M0 S after dissolution test had the irregular and rod shapes particles imbeded in the surface; the length of these particles was about 0.5-80 micron. The amount of small pores was fewer than found in M0 and M0 S.

The surface of H0 S had many cracks occurrence and could be observed some crystals deposited near the crack which might be the crystal of some substance in core tablet component. The degree of smoothness of H0 S after dissolution test was more than that of H0 S. The irregular and rod particles were found imbeded in surface. The length of these particles was about 0.5-30 micron and long scratchs could be observed near the defect of the film surface as shown in Figure 55 D. The length of these scratchs was about 30-350 micron.

Large cracks on surface of LH0 S were clearly seen and some wrinkles were also observed at higher magnification. The surface of LH0 S after dissolution test composed of many long scratchs and some irregular particles. The length of the scratchs was about 75-350 micron and the length of particle was about 0.3-75 micron. There was little long cracks occurred inside some scratchs. Some wrinkles also could

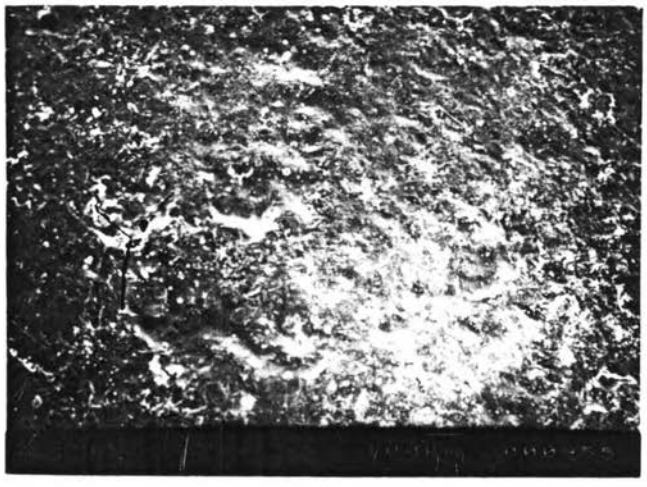

A

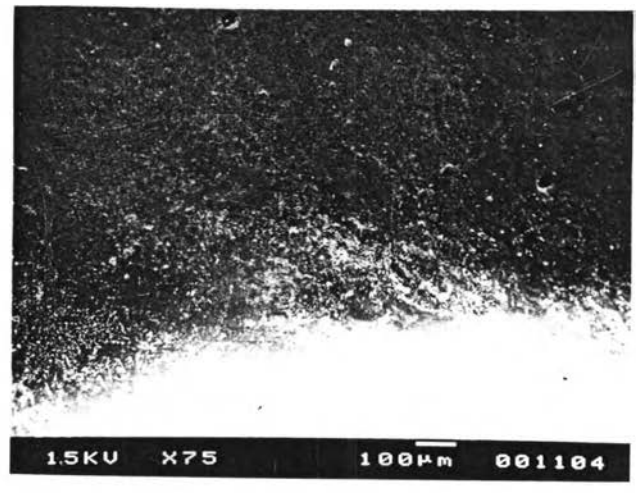

D

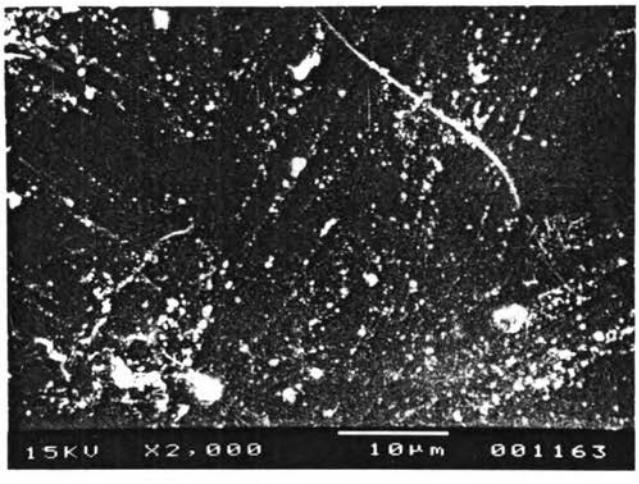

B

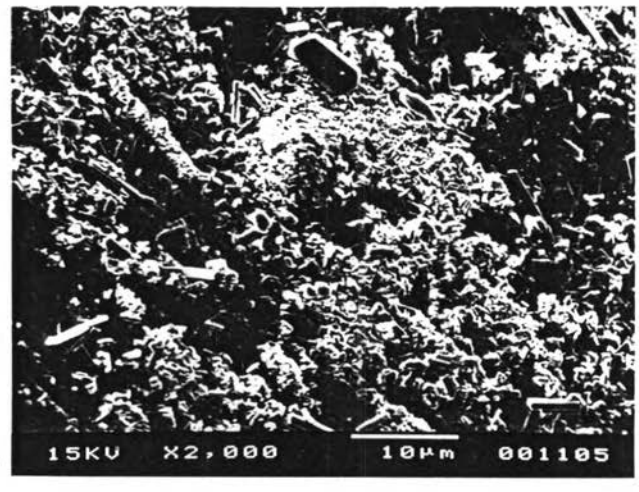

E

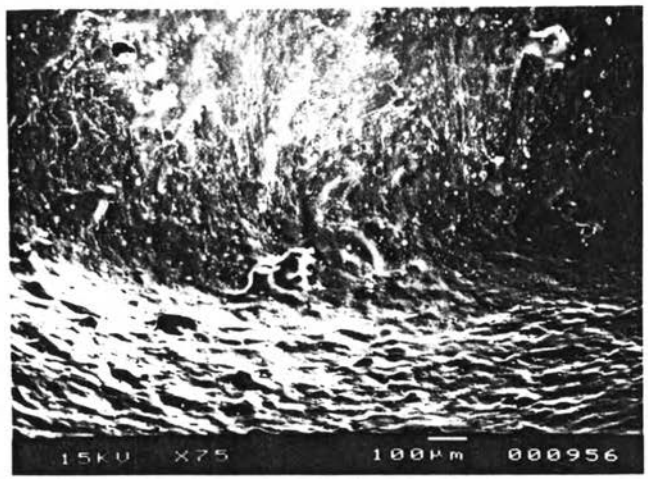

C

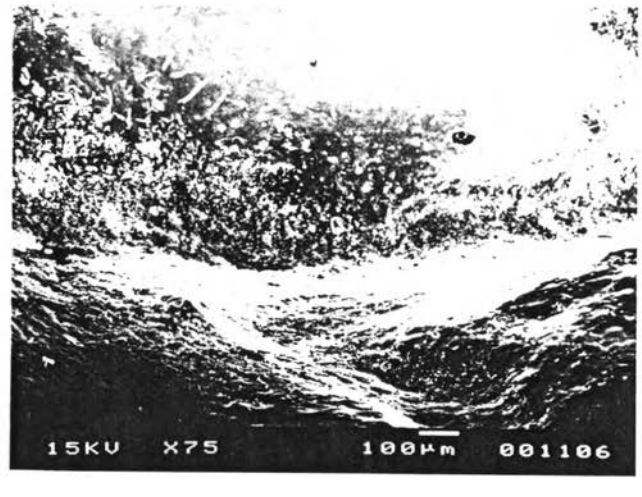

F

Figure 52 The photomicrographs of coated tablet(key:A-C(L0 S) (A-crown*75, B-crown*2000, C-edge*75), D-F(L0 S after dissolution test)(D-crown*75, E-crown*2000, F-edge*75)).

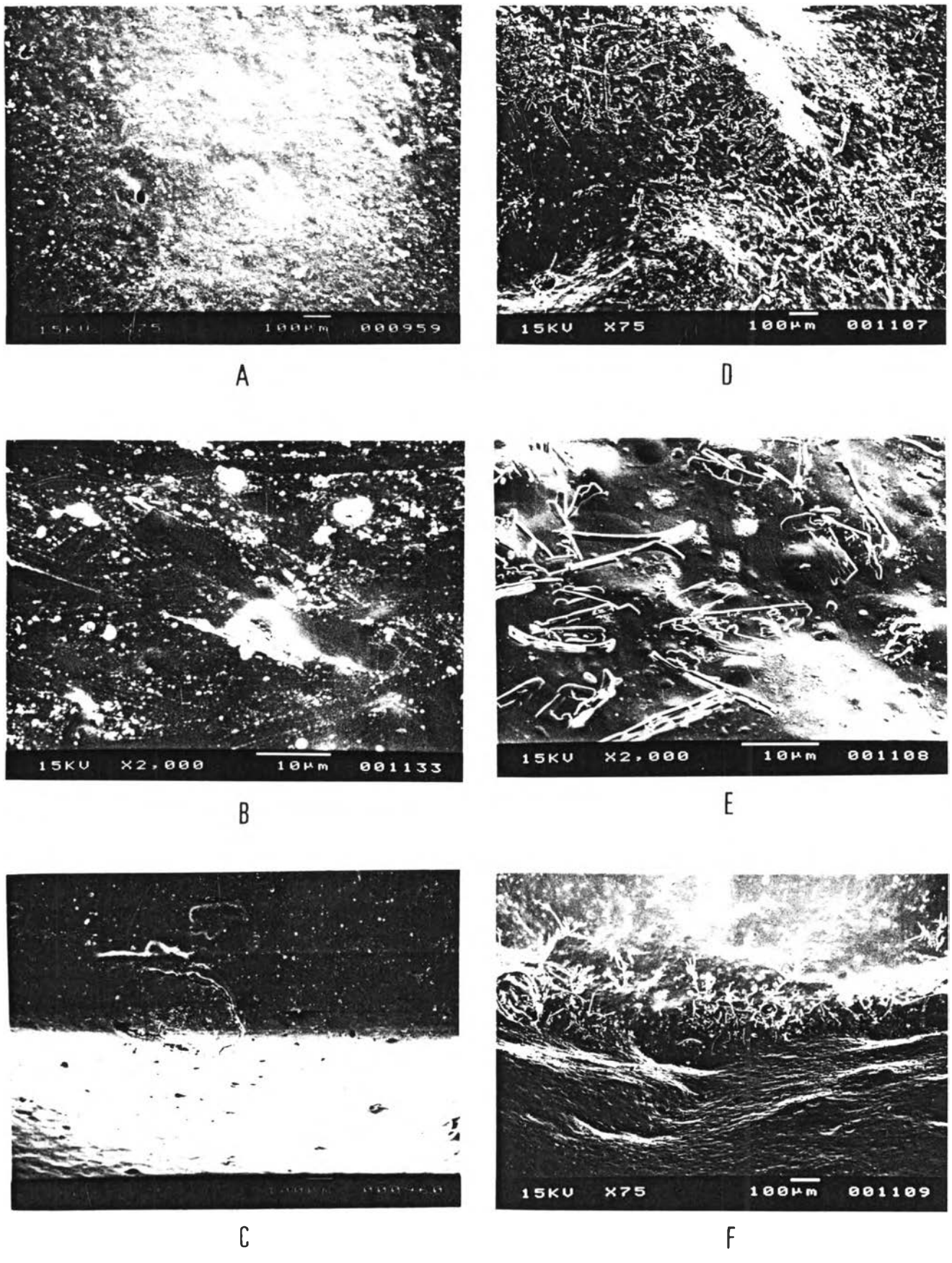

Figure 53 The photomicrographs of coated tablet(key:A-C(LA10 S) (A-crown*75, B-crown*2000, C-edge*75), D-F(LA10 S after dissolution)(D-crown*75, E-crown*2000, F-edge*75)).

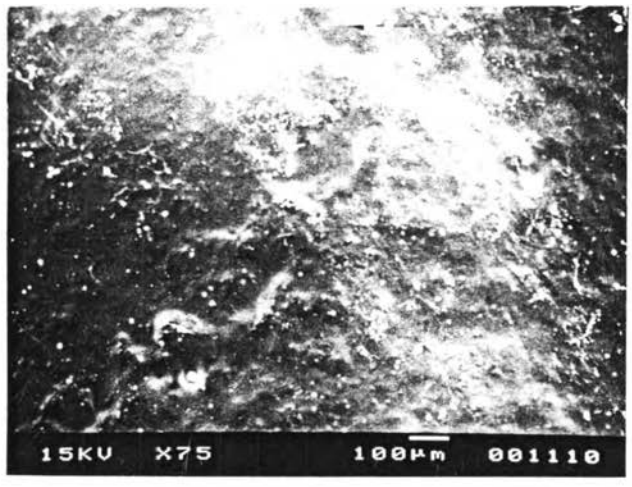

A

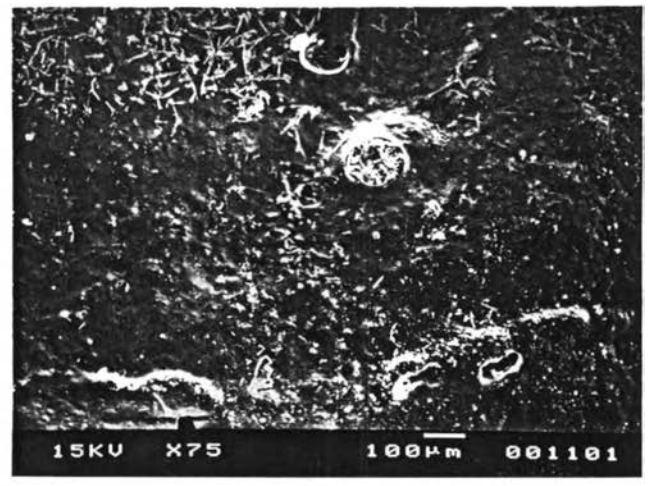

D

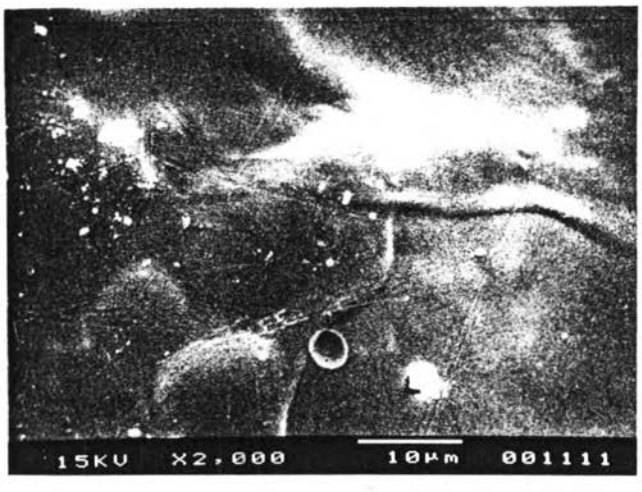

B

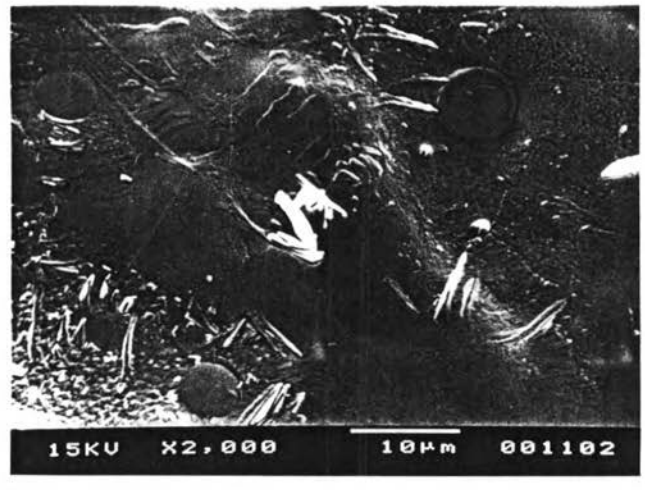

E

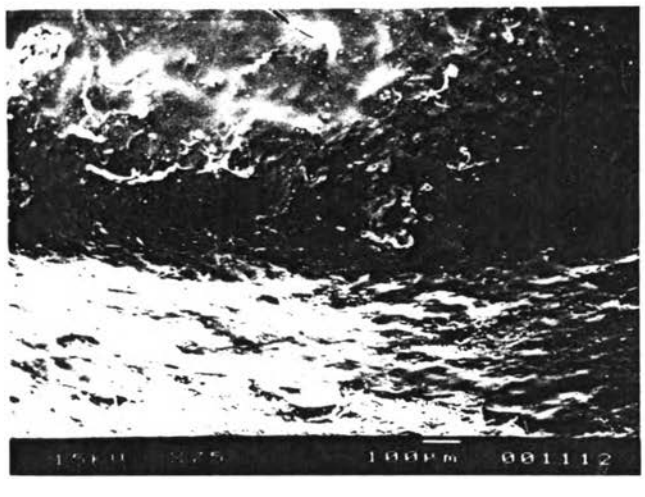

C

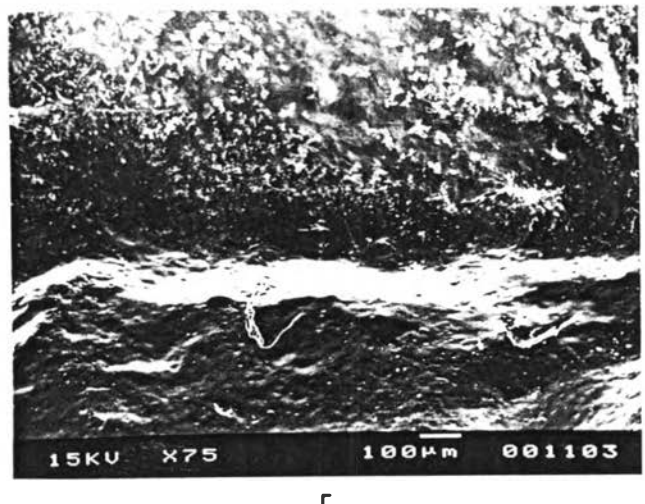

F

Figure 54 The photomicrographs of coated tablet(key:A-C(M0 S) (A-crown*75, B-crown*2000, C-edge*75), D-F(M0 S afterdissolution)(D-crown*75, E-crown*2000, F-edge*75)).

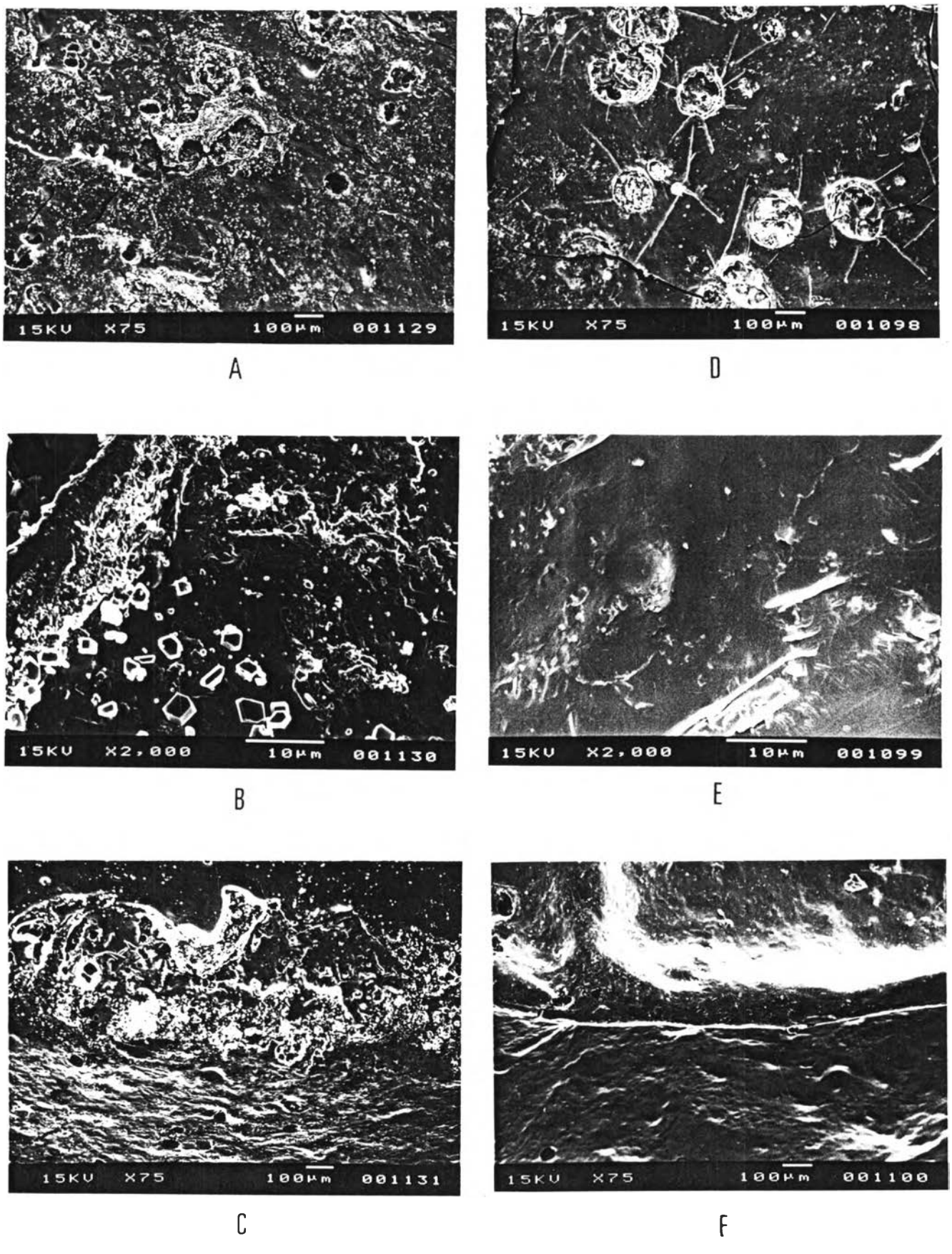

Figure 55 The photomicrographs of coated tablet(key:A-C(H0 S) (A-crown*75, B-crown*2000, C-edge*75), D-F(H0 S after dissolution)(D-crown*75, E-crown*2000, F-edge*75)).

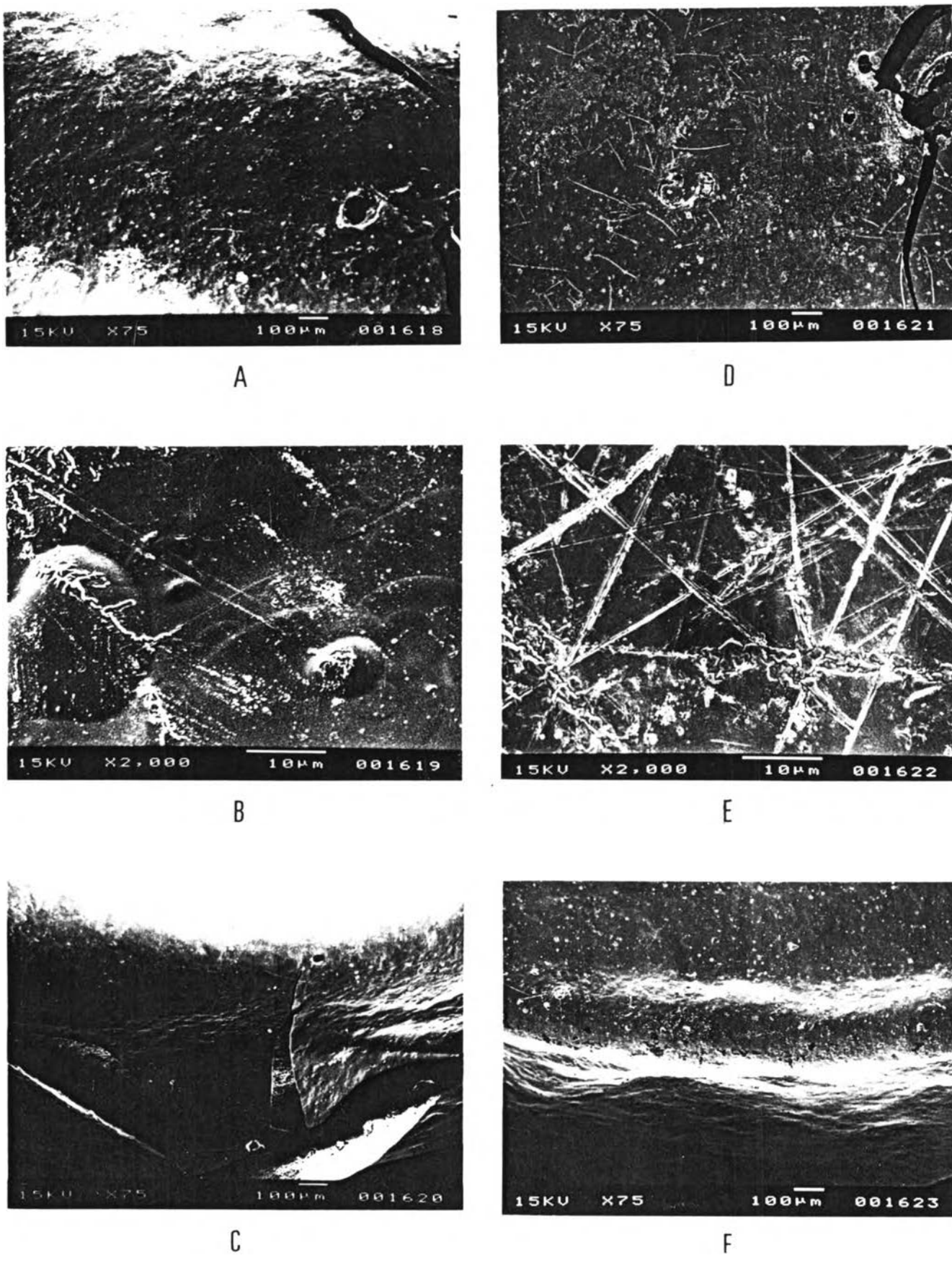

Figure 56 The photomicrographs of coated tablet(key:A-C(LH0 S) (A-crown*75, B-crown*2000, C-edge*75), D-F(LH0 S after dissolution)(D-crown*75, E-crown*2000, F-edge*75)).

be observed and some pores and large cracks could be clearly seen as found in LH0 S before dissolution test.

9. Assay of active ingredient.

The percentages of drug content are presented in Table 15. The percentages of drug content of core tablet, CORE S, L0 S, M0 S, H0 S and LH0 S were within the limit of BP. standard(92.5-107.5%).

Table 15 The drug content of core and coated tablets after exposure to accelerated condition.

FORMULA	SAMPLE			%DRUG CONTENT
	1	2	3	AVG(SD)(%)
CORE	98.84	97.54	96.54	97.64(1.15)
CORE S	94.22	96.25	94.54	95.01(1.09)
L0 S	100.33	99.76	97.94	99.34(1.25)
M0 S	98.99	99.31	98.99	99.10(0.18)
H0 S	99.39	100.61	98.38	99.46(1.12)
LA10 S	98.17	98.78	99.27	98.74(0.55)
LH0 S	97.61	95.77	96.31	96.56(0.95)

The Evaluations of Free Film

1. Physical apperance

The color, transparency, bleeding and detachability of prepared free films are shown in Table 16. The picture of prepared free films of L0, M0, and H0 is illustrated in Figure 57.

The color of L0, LH0, LA and LHA free films was yellow, the color of LB, LC, MA, HA and HB free films was yellowish, the color of MC and HC free films was white and the color of MB system, M0 and H0 was colorless.

The free films of LC, MC, HC , MB20, and MB30 were obviously translucent while the other free films were transparent. The degree of translucency increased with an increase in the concentration of plasticizer.

The bleeding, a separation of the plasticizer on a surface of the free film, could be observed on the surface of LB and MB systems, MC20, HB20, and HB30. The amount of bleeding of LB system increased with an increase in the concentration of PEG400. The bleeding of HB system at concentration of plasticizer 20 % w/w was equal to that of concentration 30 % w/w , but the bleeding of HB10 could not be observed, and the bleeding of MC20 was also observed.

All free films were rather easily detachable except those of LA30, MC30, HB20 and HB30 which were sticky. All these free films were rather tough and not brittle.

2. Infrared spectrometry

Infrared spectrometry was employed in this study to aid the determination of the chain length and degree of deacetylation of chitosan and to aid the determination of chitosan characteristic in free film.

The IR of obtained chitosan L, M and H were compared with that of imported chitosan powder as depicted in Figure 58. IR spectra of chitosan L, M and H were quite similar to that of chitosan L(J). All IR spectra could be divided into 3

Table 16 The color, transparency, bleeding and detachability of free films.

FORMULA	COLOR	TRANSPARENCY	BLEEDING	DETACHABLE
L0	YELLOW	R	(-)	E
M0	COLORLESS	R	(-)	E
H0	COLORLESS	R	(-)	E
LA10	YELLOW	R	(-)	E
LA20	YELLOW	R	(-)	E
LA30	YELLOW	R	(-)	S
LB10	YELLOWISH	R	(+)	E
LB20	YELLOWISH	R	(+ +)	E
LB30	YELLOWISH	R	(+ + +)	E
LC10	YELLOWISH	L(+)	(-)	E
LC20	YELLOWISH	L(++)	(-)	E
LC30	YELLOWISH	L(+++)	(-)	E
MA10	YELLOWISH	R	(-)	E
MA20	YELLOWISH	R	(-)	E
MA30	YELLOWISH	R	(-)	E
MB10	COLORLESS	R	(+)	E
MB20	COLORLESS	L(+)	(+ +)	E
MB30	COLORLESS	L(+)	(+ + +)	E
MC10	WHITE	L(+)	(-)	E
MC20	WHITE	L(++)	(+)	E
MC30	WHITE	L(+++)	(-)	S
HA10	YELLOWISH	R	(-)	E
HA20	YELLOWISH	R	(-)	E
HA30	YELLOWISH	R	(-)	E
HB10	YELLOWISH	R	(-)	E
HB20	YELLOWISH	R	(+ + +)	S
HB30	YELLOWISH	R	(+ + +)	S
HC10	WHITE	L(+)	(-)	E
HC20	WHITE	L(++)	(-)	E
HC30	WHITE	L(+++)	(-)	E
LH0	YELLOW	R	(-)	E
LHA10	YELLOW	R	(-)	E
LHA20	YELLOW	R	(-)	E
LHA30	YELLOW	R	(-)	E

R=TRANSPARENT E=EASILY DETACHABLE (-) NONE (+ -) MEDIUM
L=TRANSLUCENT S= STICKINESS (+) SMALL (+ - +) HIGH

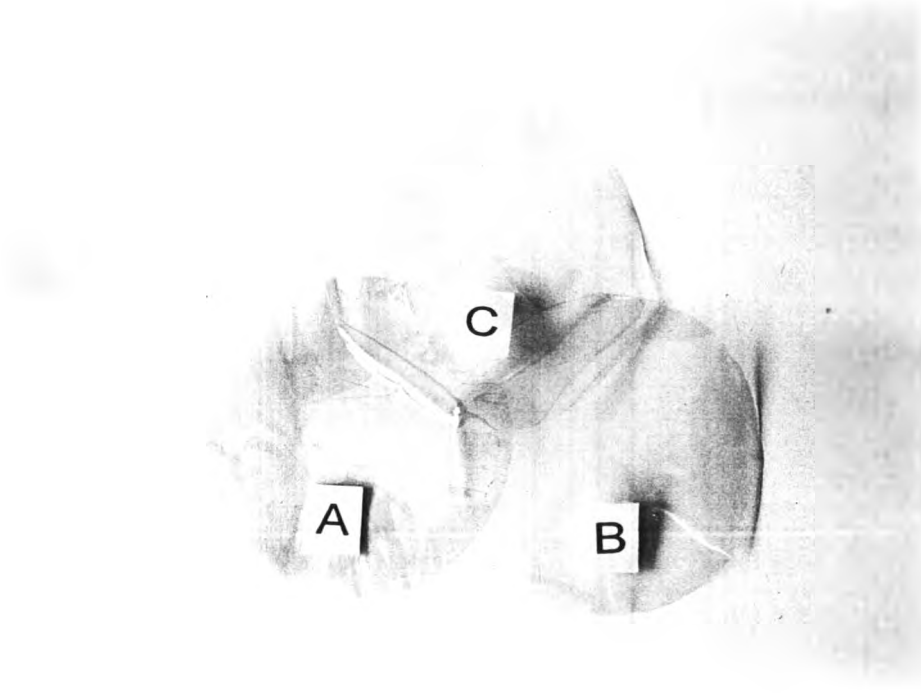

Figure 57 The prepared free films(key:A-L0, B-M0, C-H0).

cm-1), νOH (bending, 3550-3200 cm-1), νNH_2 (3500-3400 cm-1) and νNH (3520-3400 cm-1); between 1694-1515 cm-1 indicating ν C=0 (1694-1650 cm-1J) and NH (bending, 1650-1515 cm-1) and between 1170-1114 cm-1 indicating C-0-C stretching. The methyl group next to the C=O absorbs strongly near 1380 cm-1 due to symmetric CH_3 deformation. Since chitosan still had ν C=0 remaining in dthe molecule. It was suggested that lower peak of νC=0 or symmetric CH_3 deformation when compared to other peak such as peak between 3200-3600 cm-1, indicated higher degree of deacetylation.

In order to estimate the polymer chain length, the peak height ratio, particularly peak between 1170-1114 cm-1 to 3600-3200 cm-1 was conducted. Higher peak ratio indicated longer polymer chain.

IR spectra of acetic acid and triacetin (Fig.59) , and propylene glycol and PEG400 (Fig.60) were also used to characterize the mixture in free film.

IR spectra of LO, LA20, LB20 and LC20 are exihibited in Figure 61. IR spectra of LA20 and LB20 were similar to LO which showed a shoulder peak at about 1645 cm-1, and a main peak at about 1560 cm-1 and a peak at about 1412 cm-1. The peak at 1590 cm-1 was not found because of the occurrence of the main peak at about 1560 cm-1. The peak at 1412 cm-1 was shifted from 1423 cm-1 of L and its intensity was higher than the peak at about 1645 cm-1. The peak intensity at about 1380 cm-1 was also more than that of at about 1645 cm-1 and slightly less than that of the peak at 1412 cm-1. The IR spectrum of LC20 was similar to the other except that there were new peaks which were the combination peak between LO and triacetin at 1745 and 1225 cm-1.

IR spectra M and H systems, Figure 62 and 63 respectively, were similar to L system except that no shoulder at about 1645 cm-1. The peak at about 1350 and 1412 cm-1 had intensities nearly to that at about 1645 cm-1.

The differences of absorption bands observed in IR spectra of chitosan acetic, plasticizer, and mixture in free films are presented in Table 17 .

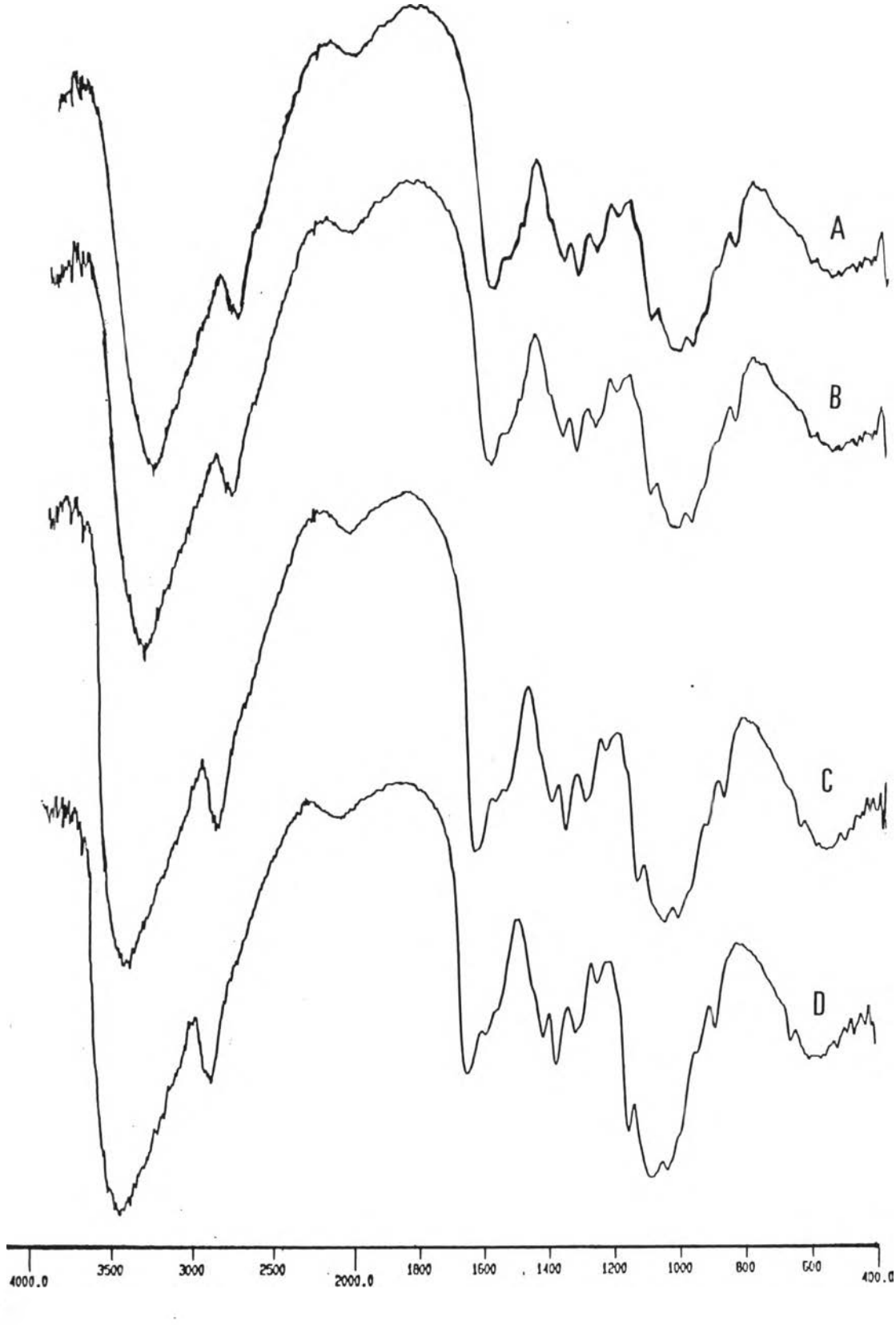

Figure 58 IR spectra or chitosan powders(key:A-L(J), B-L, C-M, D-H).

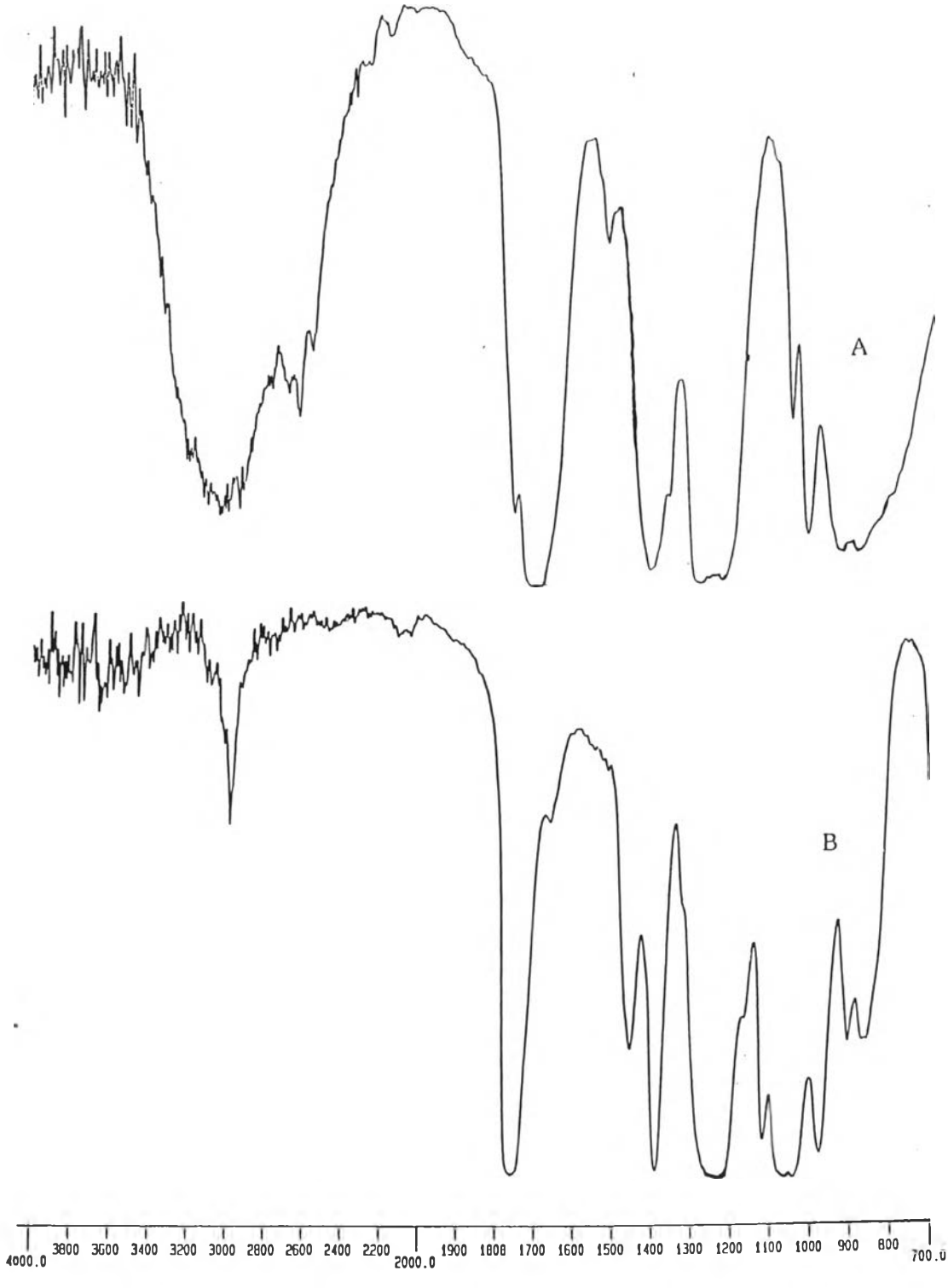

Figure 59 IR spectra(key:A-acetic acid, B-triacetin).

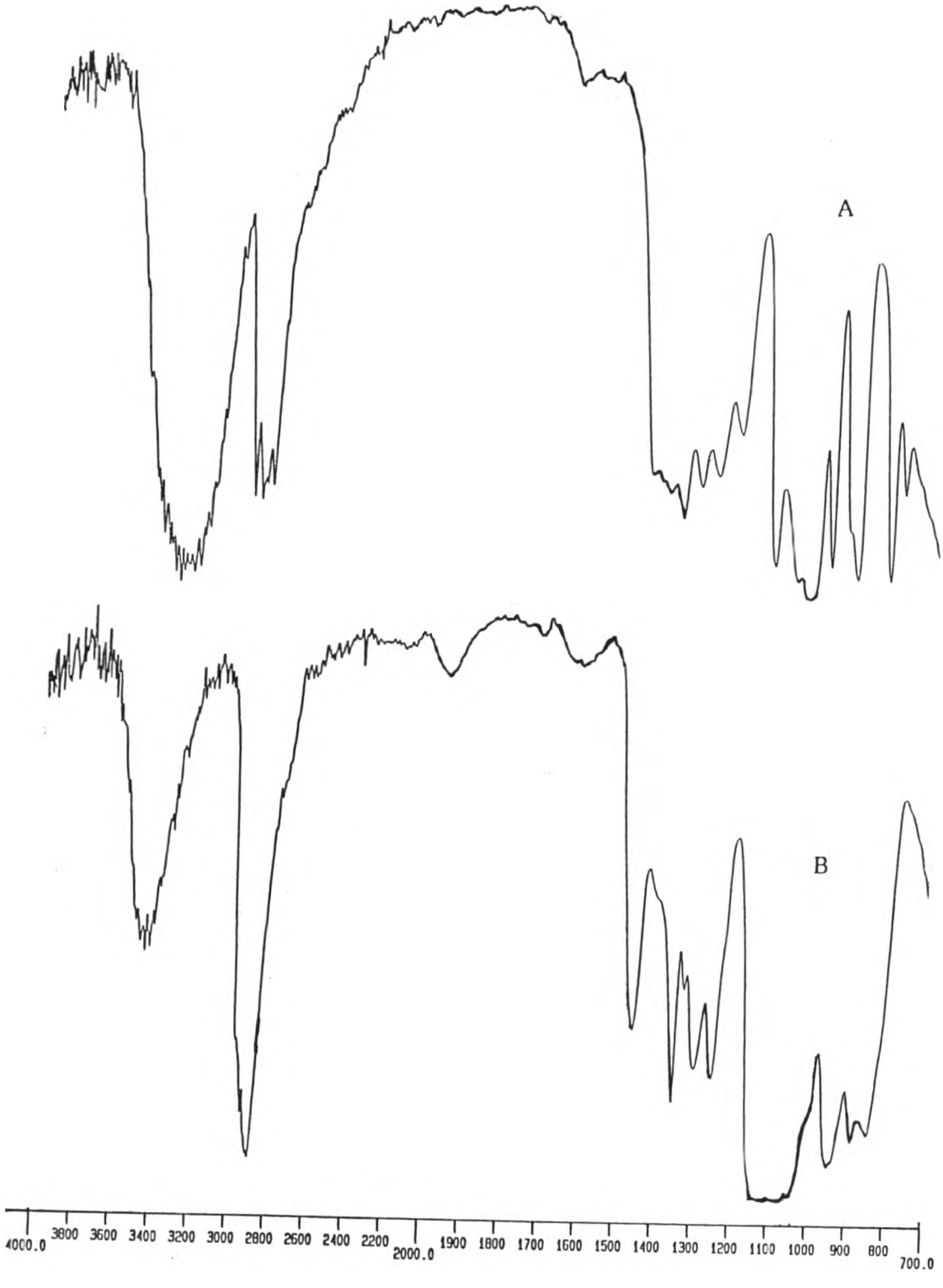

Figure 60 IR spectra(key:A-propylene glycol, B-PEG400).

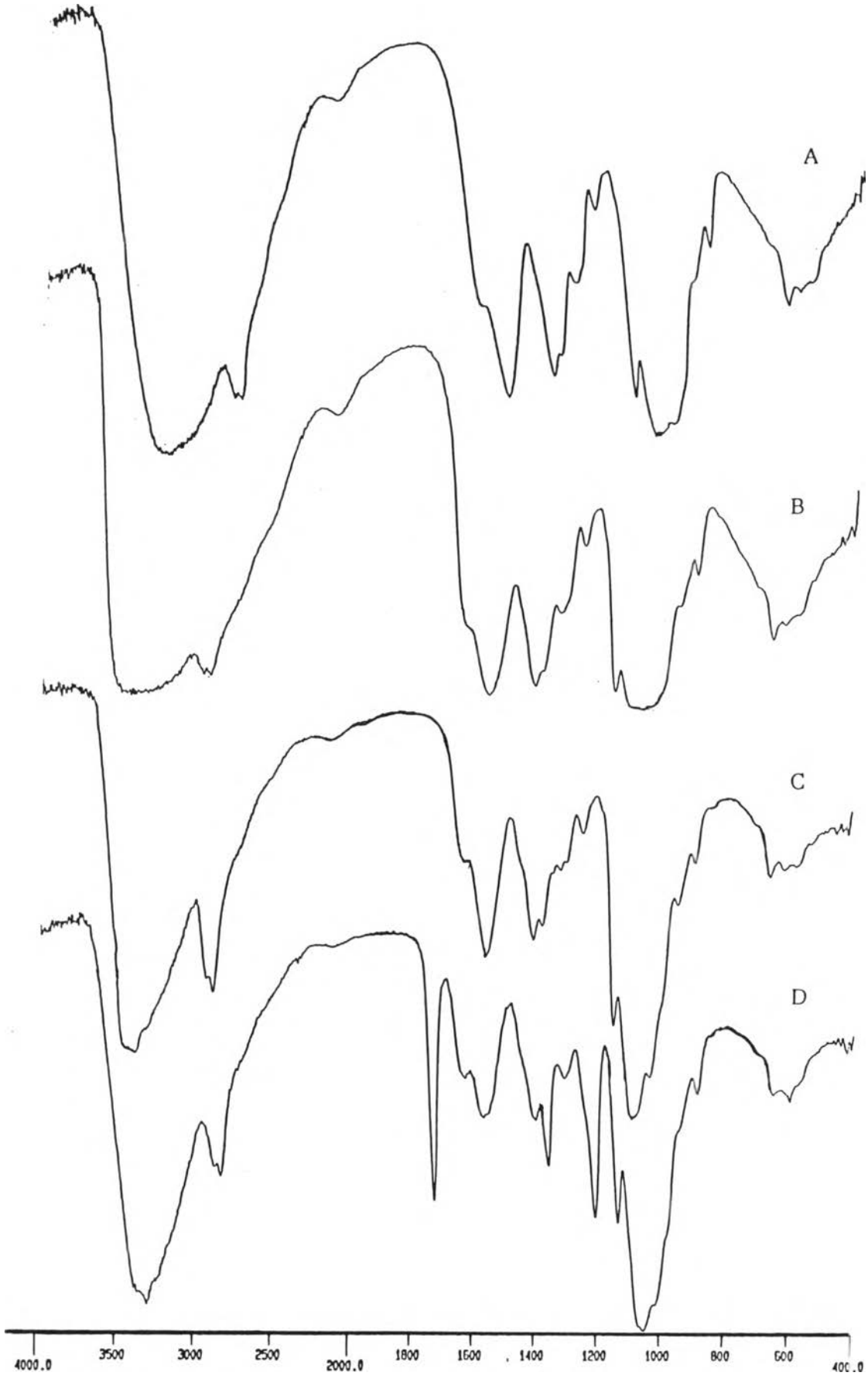

Figure 61 IR spectra of free films(key:A-L0, B-LA20, C-LB20, D-LC20).

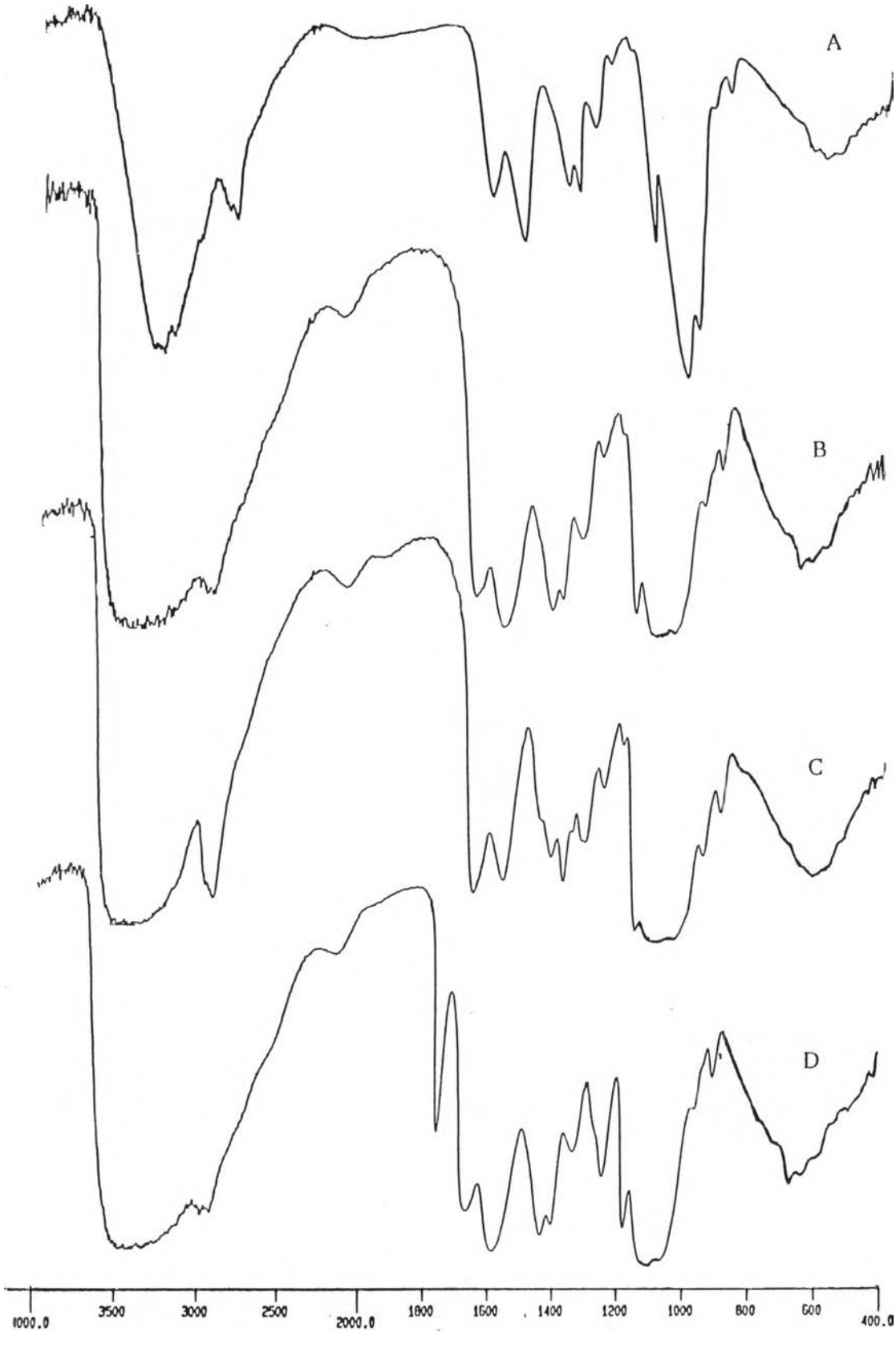

Figure 62 IR spectra of free films(key:A-M0, B-MA20, C-MB20, D-MC20).

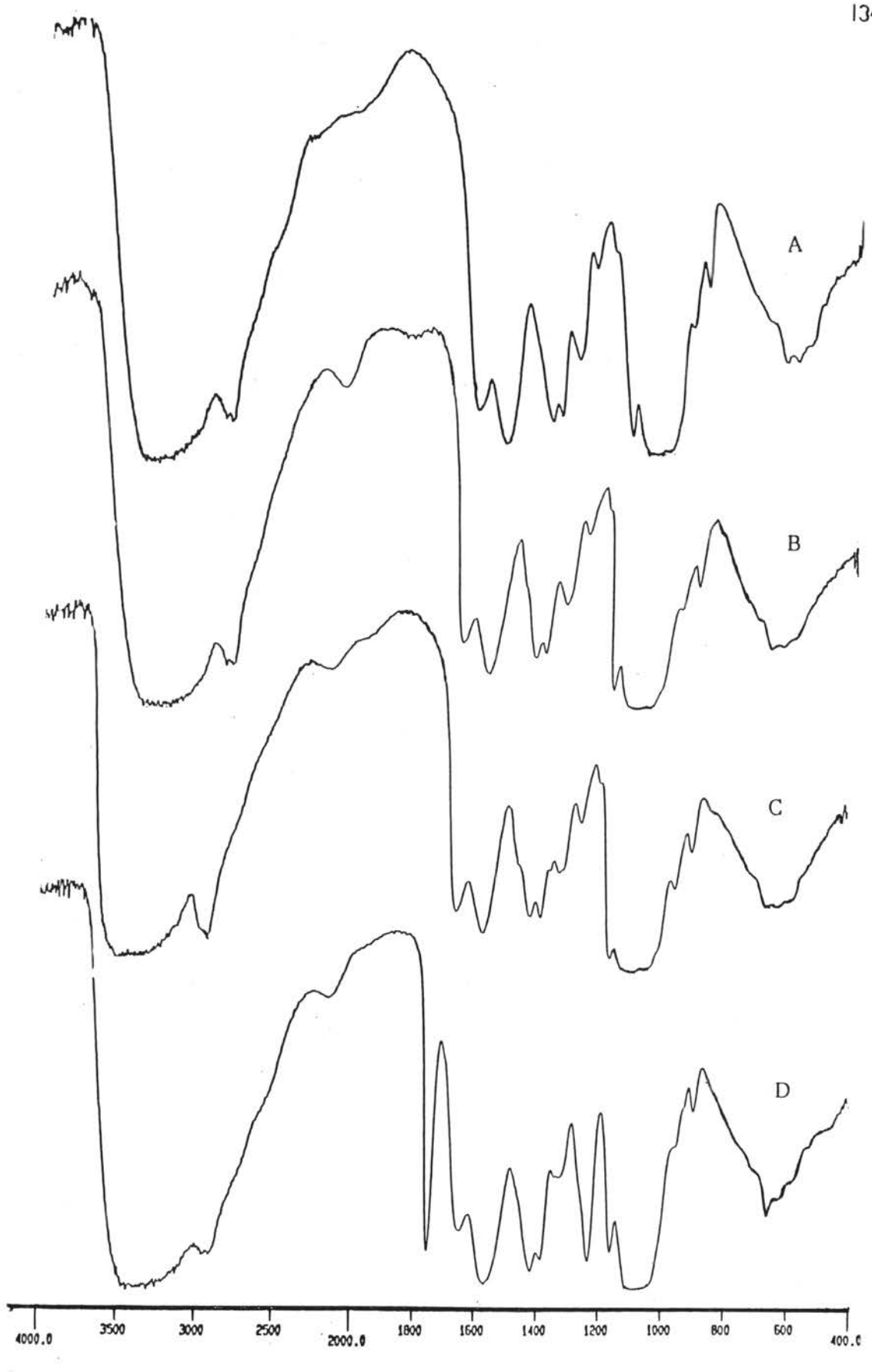

Figure 63 IR spectra of free films(key:A-H0, B-HA20, C-HB20, D-HC20).

Table 17 The differences of absorption bands observed in IR spectra.

ABSORPTION BANDS IN IR SPECTRA(CM -1)

ACETIC ACID	PD	PEO 400	TRIACETIN	LM	L	M	H	LA	M3	PP	LA20	LB20	LC20	MA20	LB20	MC20	HA20	HB20	HC20
3130	3346	3436	2963	3459	3436	3431	3422	3441	3414	3426	3444	3420	3420	3451	3440	3445	3466	3435	3450
2984	3276	2864	1745		3349	3374	3361	3352	3388	3392	3389	3369	3367	3381	3378	3385	3384	3385	3377
2664	2972	1456	1652	2907	2933	2917		2917	2920	2927	2918	2919	2921	2928	2930	2938	2928		2941
2628	2952	1360	1439	2882	2898	2897	2880	2881	2877	2890	2877	2874	2880	2875	2878	2879	2886	2879	2895
2558	2907	1325	1225	2145	2197	2133	2127	2150	2046		2140			2165	2149	2149	2130	2161	2149
1767	2877	1296	1370										1745			1745			1746
1696	2818	1250	1197	1644	1645	1660	1665	16505	1652	1651	16458	16455	16439	1651	1656	1646	1651	1651	1640
1517	1661	1119	1101	1590	1590	1590	1590												
1410	1450	994	1041	15503	15508	15508	15503	1569	1559	1559	1560	1564	1583	1565	1564	1559	1560	1561	1559
1378	1415	886	1020	1428	1423	1494	1491	1412	1412	1410	1411	1412	1414	1412	1418	1411	1413	1413	1410
1227	1377	884	858	1380	1381	1379	1379	13785	1379	1380	13798	1384	1375	1380	1378	1379	1381	1380	1370
1052	1331		892	1322	1322	1320	1322	1327	1319	1321	1334	1327	1322	1324	1312	1321	1322	1323	1323
1012	1289		856	1260	1258	1262	1259	1259	1263	1262	1258	1256	1225	1261	1256	1226	1263	1256	1226
924	1250			1154	1156	1158	1153	1154	1165	1155	1154	1152	1154	1164	1153	1155	1153	1152	1154
889	1156			1069	1067	1071	1069	1082	1078	1076	1068	1082	1077	1075	1070	1068	1063	1077	1076
	1077				1029	1032	1032		1035			1035		1032					
	1042									962		960		960	961		960	960	
	991			896	896	897	897	899	899	900	899	898	899	899	898	899	899	898	898
	929			686	600	663	667	656	650	656	656	659	658	656		656	657	657	655
	836						609	618	617	618	619	614	606	618	619	620	624	616	
	803			657		584													
						527	522												
				451	478	151	472	440	431	431	440	432	445	442	456	483		421	420
				418	402	410		408		412	409	415	412	409	411	407	409	407	

S=Shoulder peak

Table 18 Peak height ratios from the IR spectra.

	ABSORBANCE RATIOS OF BAND PAIR			
FORMULA	1155/3422 TO 3459	1655/3422 TO 3459	1423 OR 1412/3422 TO 3459	1380/3422 TO 3459
L(J)	0.26	0.44	0.21	0.22
L	0.29	0.47	0.21	0.23
M	0.31	0.50	0.21	0.26
H	0.41	0.51	0.25	0.31
L0			0.35	0.32
LA20			0.31	0.31
LB20			0.36	0.32
LC20			0.26	0.37
M0			0.33	0.36
MA20			0.31	0.30
MB20			0.32	0.38
MC20			0.32	0.30
H0			0.33	0.32
HA20			0.31	0.31
HB20			0.34	0.35
HC20			0.30	0.28

Peak height ratios used to determine the chain length and degree of deacetylation are summarized in Table 18.

A peak height ratio of the peak at about 1150 to 3422-3459 cm-1 was used to determine the chain length, as the result that a peak ratio of H was apparently higher than that of M, followed by that of L and L(J) respectively, however a peak height ratio of M was slightly higher than L.

The degree of deacetylation of chitosan used in this experiment could be compared by using the peak height ratio at about 1655 to between 3422-3459 cm-1. According to their peak height ratios the degree of deacetylation could be ordered as L(J)>L>M>H, however that of H was slightly less than that of M.

3. The X-ray diffractograms

The powder X-ray diffraction patterns of chitosan powders, non-plasticized and plasticized free films are illustrated in Figures 64-71. It revealed that they were mostly in amorphous form, but with a few diffraction peaks.

3.1 Chitosan powders

The X-ray patterns of chitosan powders are displayed in Figure 64. The same major X-ray diffraction peak of chitosan L, M and H was particularly observed at 19^{o} and the other smaller peak of chitosan powders could be clearly observed at 10.0^{o}, 9.0^{o} and 9.5^{o} respectively. The peak height ratio of the smaller to the major peak of chitosan powders was 0.38, 0.54 and 0.31 respectively.

3.2 Unplasticized free films

The X-ray patterns of unplasticized free films are shown in Figure 65. The diffractogram of LO displayed four peaks at 7.5^{o}, 10.5^{o}, 17^{o} and 23^{o}. The diffraction peaks of MO occurred near the same position at that of its powder, except that the peak of MO at 19^{o} was triplet. In the case of HO, it displayed the diffractogram similar to that of LO, except that the peak at about 19^{o} did not clearly separate to be douplet. LHO showed different pattern, it could not clearly obserbed the sharp peak and the peak at 19^{o} did not separate, and the peak occurred

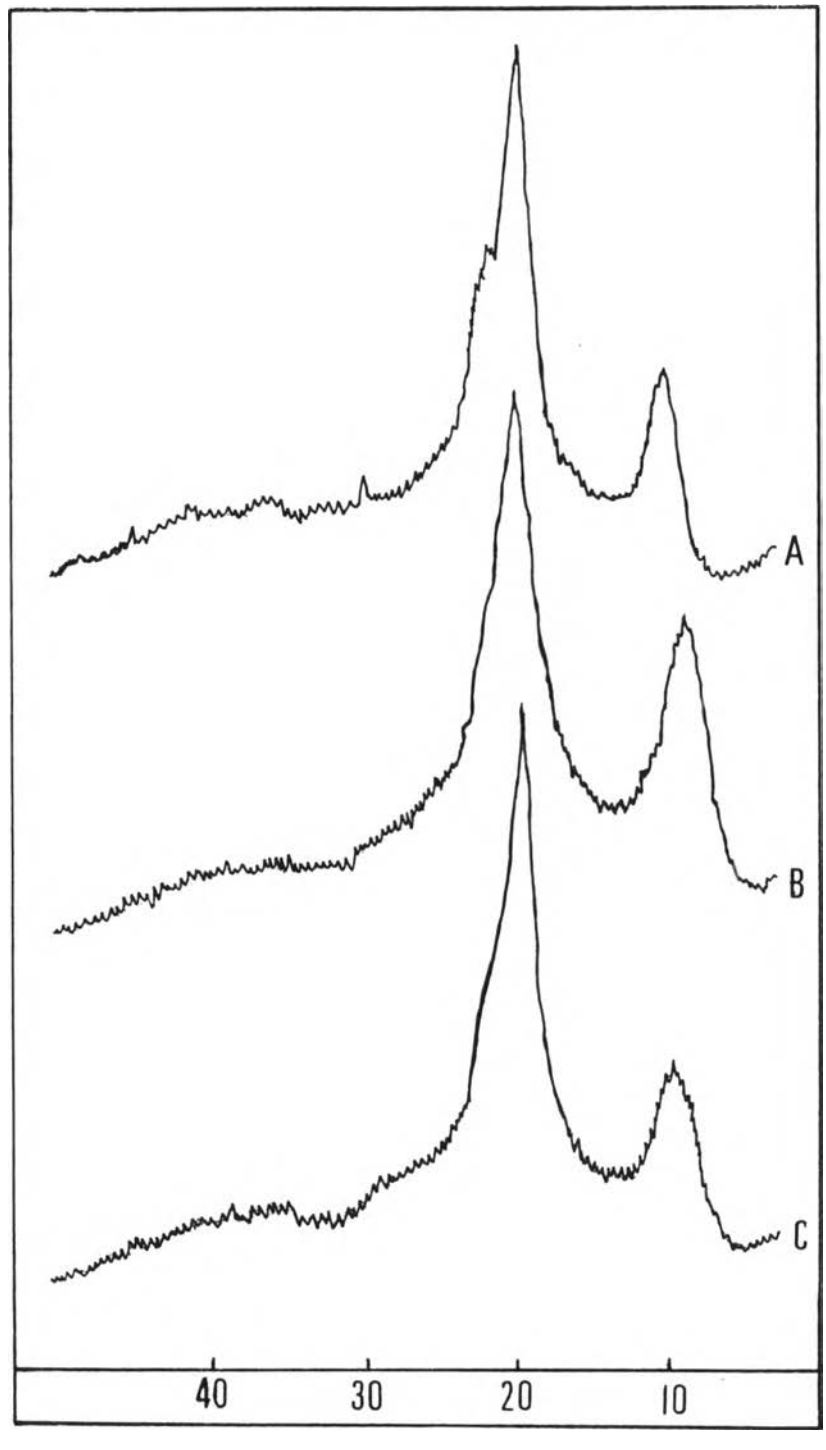

Figure 64 X-ray diffractograms of chitosan powders(key:A-L, B-M, C-H).

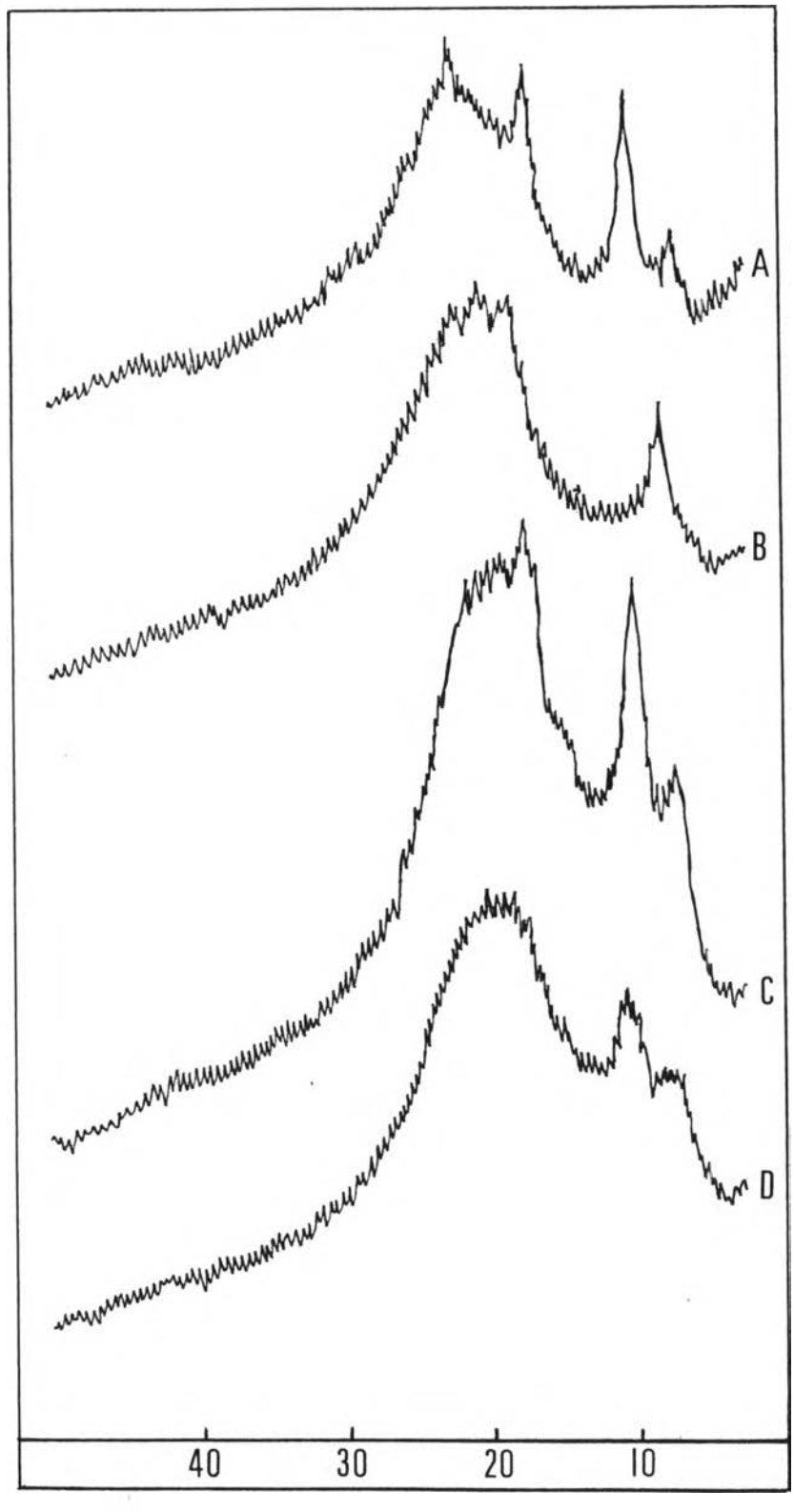

Figure 65 X-ray diffractograms of unplasticized free films (key:A-L0, B-M0, C-H0, D-LH0).

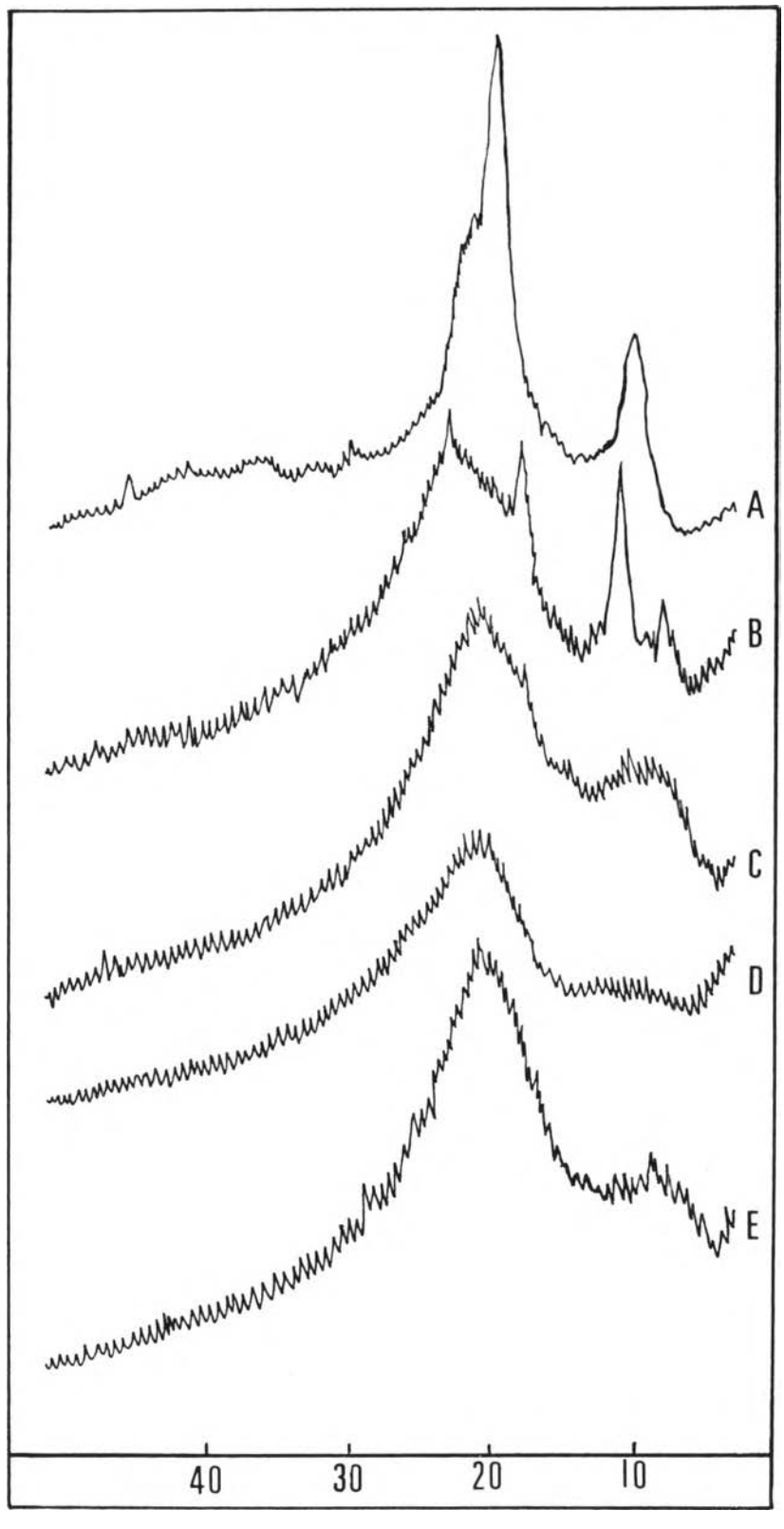

Figure 66 X-ray diffractrograms of chitosan L powder and unplasticized and plasticized free films with propylene glycol(key:A-L, B-L0,C- LA10, D-LA20, E-LA30).

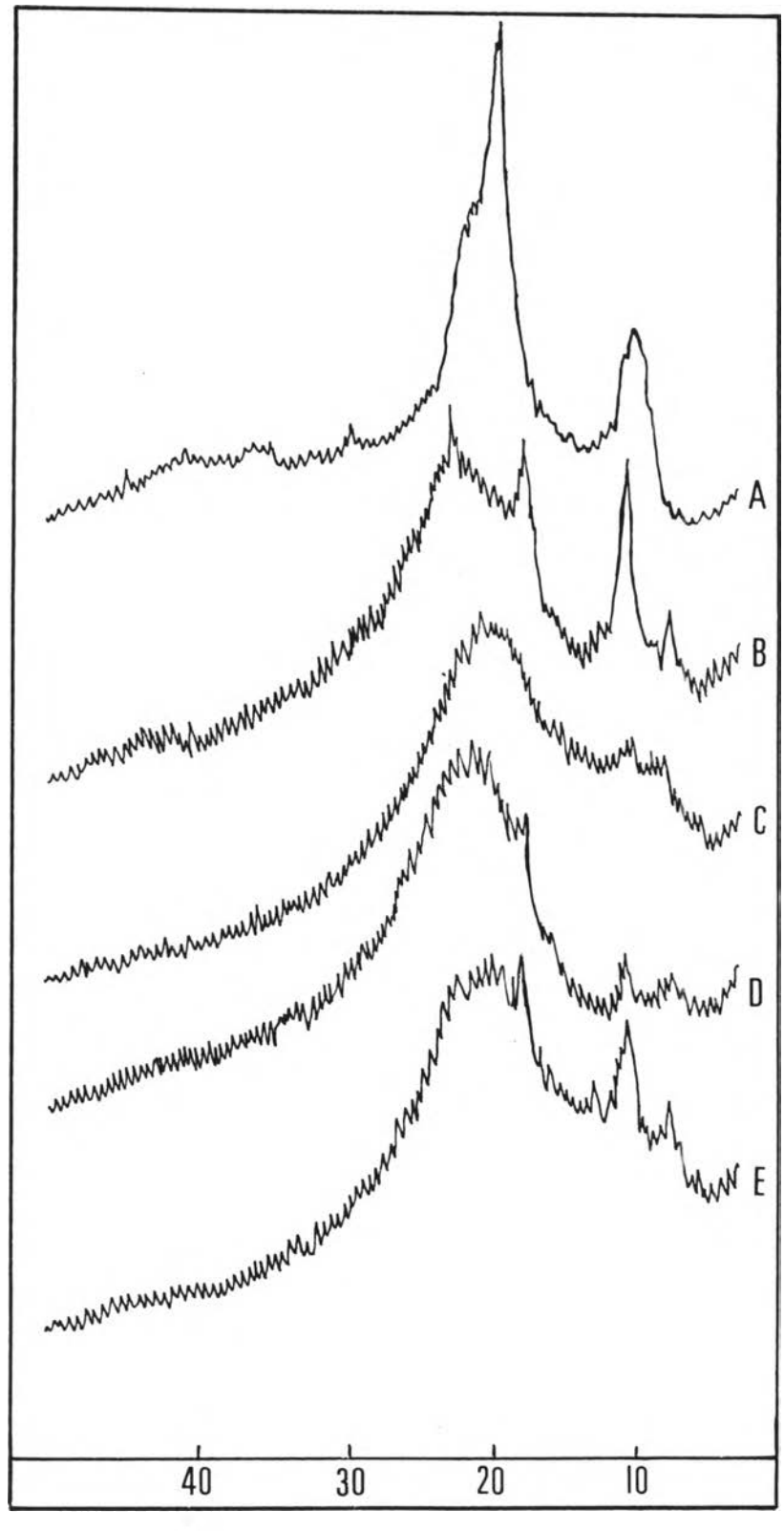

Figure 67 X-ray diffractrograms of chitosan L powder and unplasticized and plasticized free films with PEG400 (key:A-L, B-L0,C- LB10, D-LB20, E-LB30).

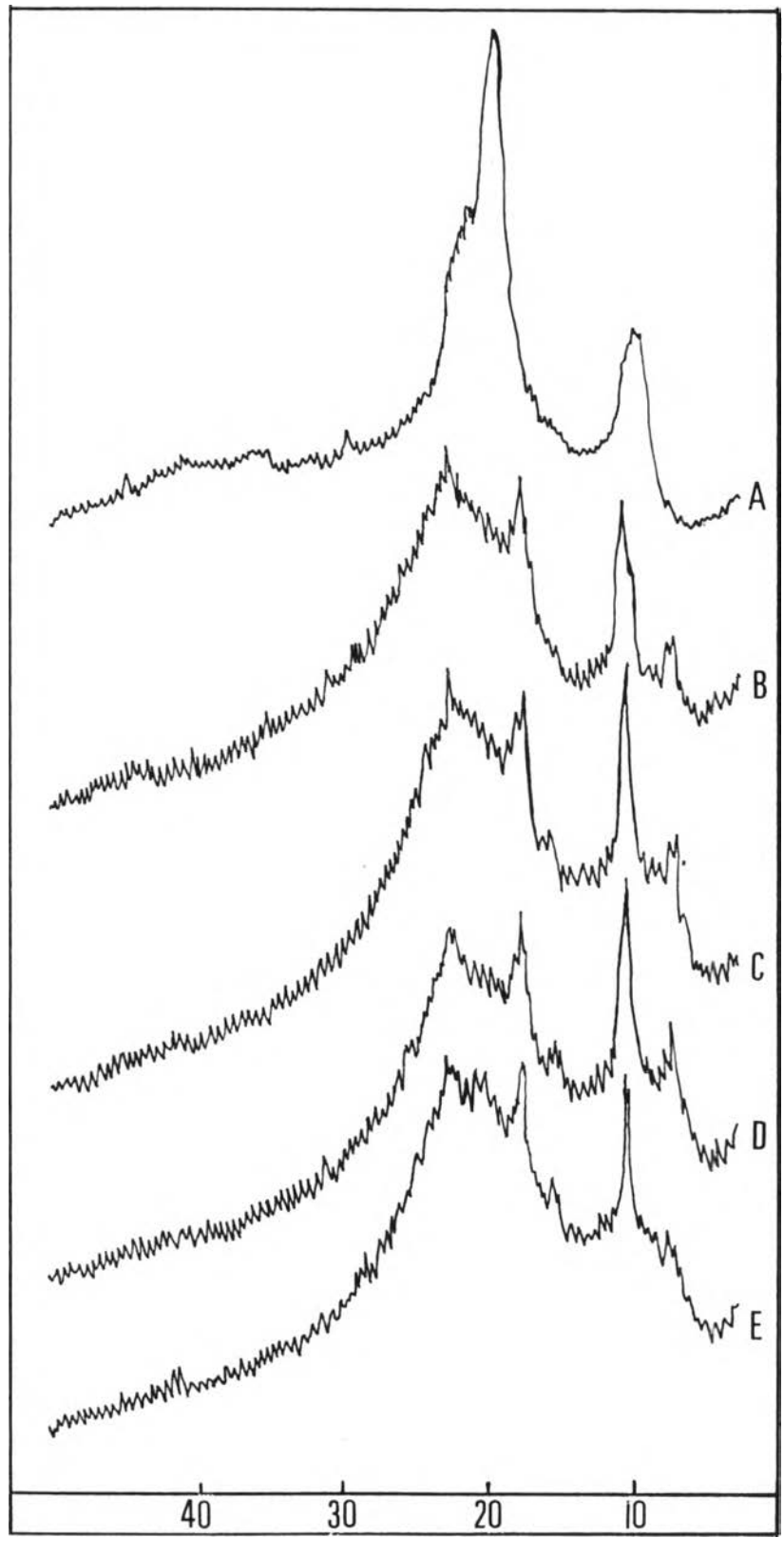

Figure 68 X-ray diffractograms of chitosan L powder and unplasticized and plasticized free films with triacetin (key:A-L, B-L0,C- LC10, D-LC20, E-LC30).

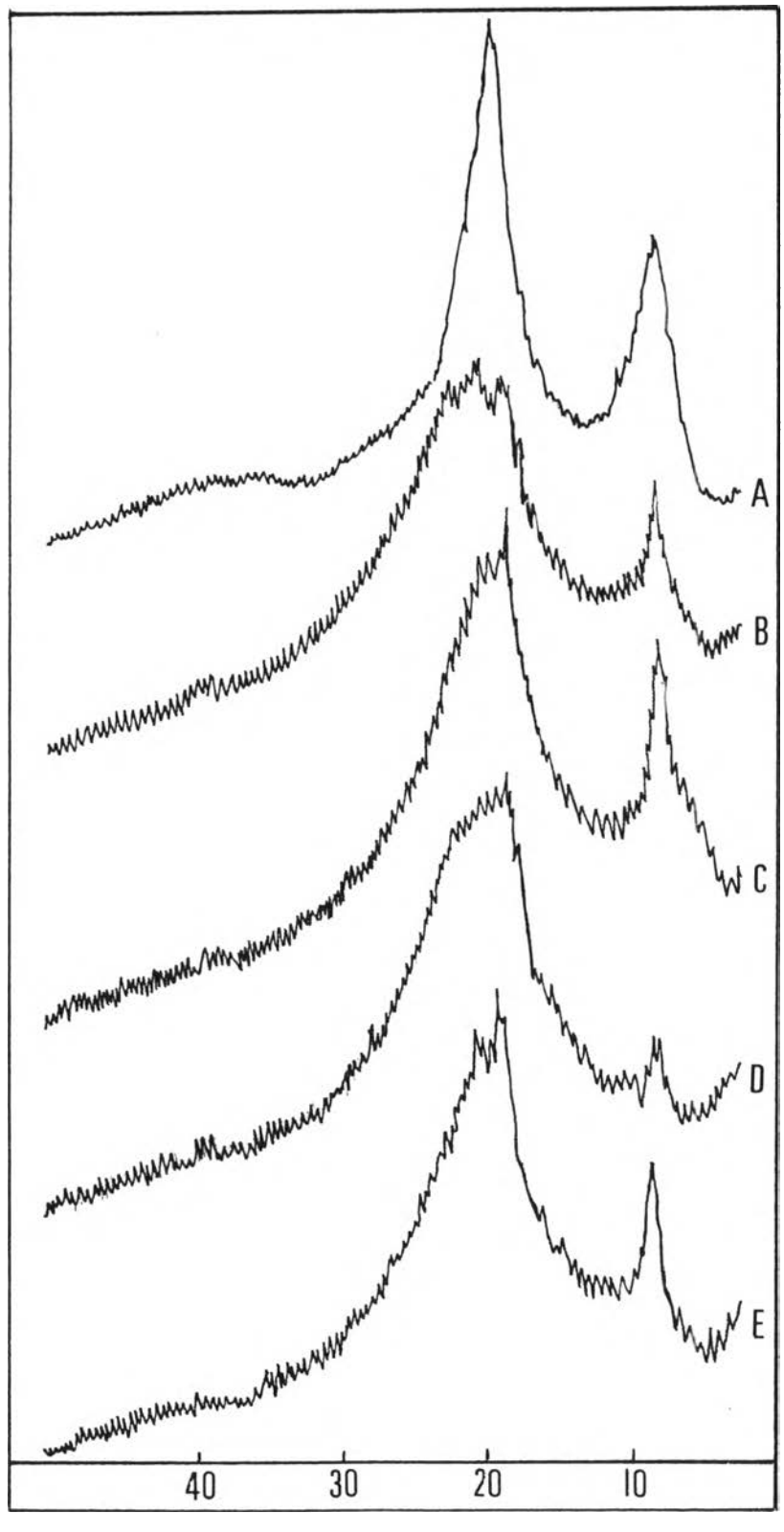

Figure 69 X-ray diffractograms of chitosan M powder and unplasticized and plasticized free films (key:A-M, B-M0,C- MA20, D-MB20, E-MC20).

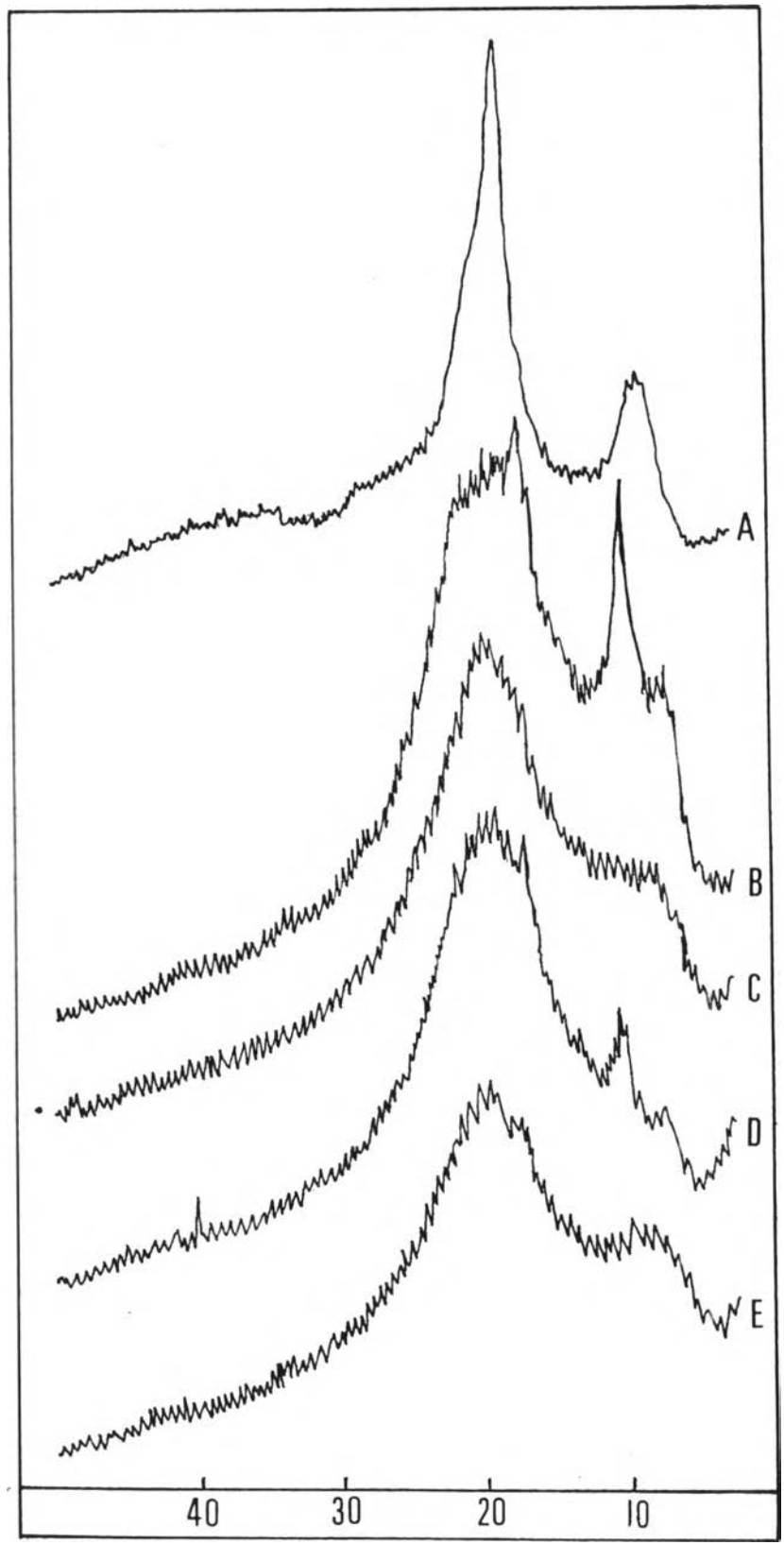

Figure 70 X-ray diffractograms of chitosan H powder and unplasticized and plasticized free films (key:A-H, B-H0,C- HA20, D-HB20, E-HC20).

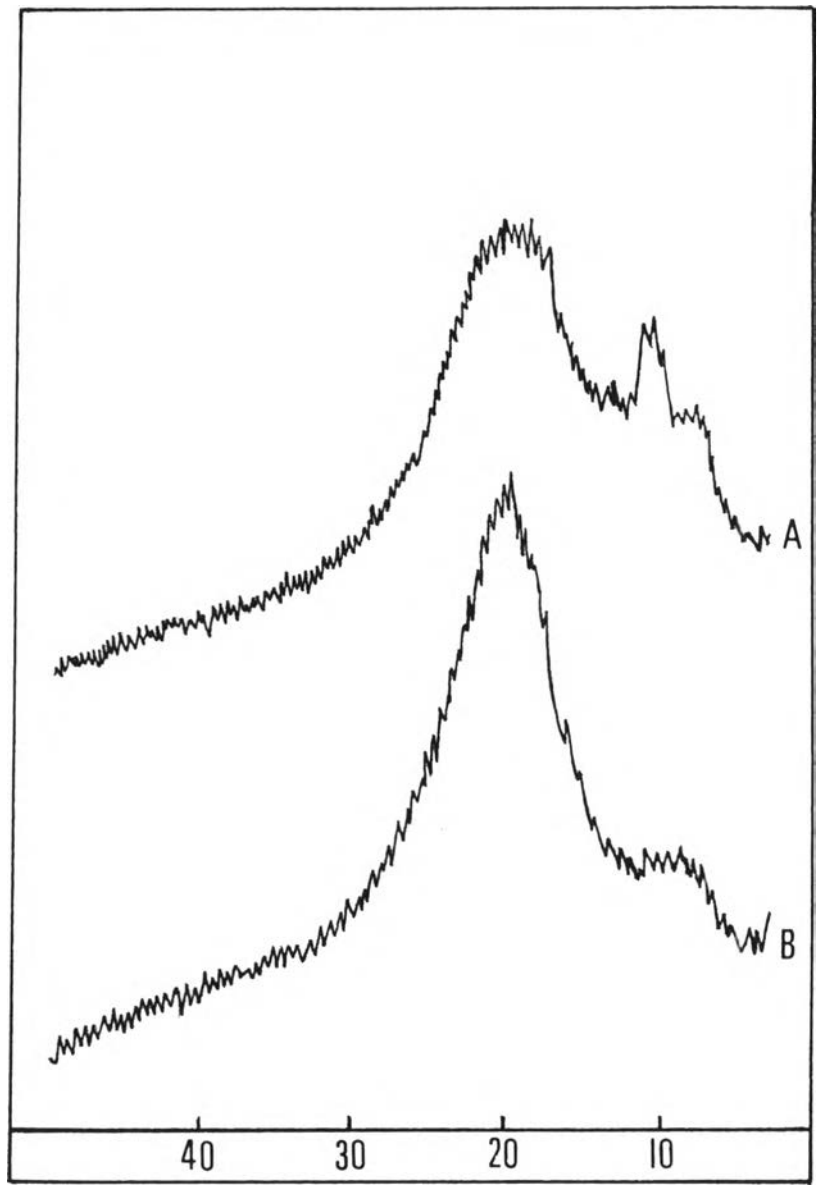

Figure 71 X-ray diffractrograms of chitosan LH free films (key:A-LH, B-LHA20).

at 8^{o}, 11^{o} and 19^{o}. Notification was detected the diffractogram of LO and HO showed higher peak intensity at about 10^{o} than that of MO and LHO, and could not observed the new peak at about 7.5^{o} in the diffractogram of MO.

3.3 The plasticized free films

3.3.1 Chitosan L

The X-ray diffraction spectra of chitosan L free film plasticized with propylene glycol at concentration of 10, 20 and 30 % w/w (LA10, LA20 and LA30) are demonstrated in Figure 66. The diffractogram of LA free films was similar to that of chitosan L powder, but showed lesser intensity. The new peaks occurred in L0 at 7.5^{o}, 17.0^{o} and 23.0^{o} could not observed in LA system. The diffractogram of LA20 showed lesser intensity of both peaks than that of LA10 and followed by that of LA30.

The X-ray diffractograms of free films of chitosan L plasticized with PEG400 at concentration of 10, 20 and 30 % w/w (LB10, LB20 and LB30) are illustrated in Figure 67. The more amount of PEG400 was increased, the diffractograms of LB free films were more similar to that of L0, however, the diffractograms of LB free films were not be clearly observed a douplet at 19^{o}.

The X-ray diffractions spectra of free films of chitosan L plasticized with triacetin at concentration of 10, 20 and 30 % w/w (LC10, LC20 and LC30) are presented in Figure 68. The diffractograms of LC free films were very similar to that of L0, but the intensities of the peak at 10^{o} were higher than that of L0, which the peak height ratios of the peaks at 10^{o} to 23^{o} could be ranked as: LC20>LC30>LC10>LO (1.10, 0.85, 0.81 and 0.69) respectively.

3.3.2 Chitosan M

The X-ray diffraction spectra of free films of chitosan M plasticized with propylene glycol, PEG400 and triacetin at concentration of 20 % w/w (MA20, MB20 and MC20) are illustrated in Figure 69.

The diffractograms of MA20, MB20 and MC20 were similar to M0, except that the peak at 9° of M0 had lesser intensity than that of MA20, but higher than that of MB20 and slightly higher than that of MC20. Notification was detected, the peak height ratios of the peaks at 9.0° to 19° of M0, MA20 MB20 and MC20 were 0.53, 0.61, 0.21 and 0.49 respectively. The diffractograms of unplasticized and plasticized free films of chitosan M could not be observed the new peak near the peak at 9°.

3.3.3 Chitosan H

The diffractogram of HA20, HB20 and HC20 are shown in Figure 70. The diffractograms of HA20 and HC20 were different from that of H0, since the intensities of the peak at 9.5° were apparently lesser than that of H0; this peak intensity of HA20 was also slightly lesser than HC20. Moreover, they could not be clearly observed the new peak at 7.5° like that of H0. In the case of HB20, the diffractogram was similar to that of H0, but with lesser peak intensity. The peak height ratios of the peaks at 9.5° to 19.0° of H0, HA20, HB20 and HC20 were 0.75, 0.26, 0.30, 0.29 respectively.

3.3.4 Combined chitosan L and H

The diffraction spectrum of LHA20 compared to that of LH0 is shown in Figure 71. The peak intensity at 11° of LHA20 diffractogram was lesser than that of LHO, but the main peak at 19° was higher than that of LHO.

In conclusion, The peak at about 10° of difractograms of chitosan M system shifted to the right side more than those of chitosan H system, followed by that of chitosan L, and combined chitosan L and H systems respectively. The diffraction spectra of unplasticized free films of L0, H0 and LH0 showed some new peaks occurrence and peak intensities at about 10° of L0 and H0 were higher than those of M0 and LH0. For plasticized free films, the free films of L, H and LH plasticized with propylene glycol showed the lower intensities of peak at about 10° than those of free films plasticized with PEG400, triacetin or unplasticized free film. For LB free films, the more amount of PEG400 added, the diffractograms were similar to L0. For LC free films, the diffractogram was similar to

that of L0, but the peak height ratio of the peaks at 10^{o} to 23^{o} was higher than that of L0. But for HC20, the peak intensity at 9.5^{o} and the peak height ratio of the peaks at 9.5^{o} to 19^{o} was lesser than H0 and that of MC20 was slightly lesser than that of MC.

4. DTA thermograms

The thermograms of chitosan powders, non-plasticized free films and plasticized free films are displayed in Figures 72-74, and melting points and weight loss of these materials are summarized in Table19.

Chitosan powder (L) showed the melting endothermic peak at 165^{o}c. L0 displayed endothermic peak at 168^{o}c and a small exothermic peak at 271^{o}c. While LA20 also showed a melting endotherm at 168^{o}c, but a small exothermic peak at 235^{o}c. LB20 showed the endothermic peak at 174^{o}c and a small indothermic peak at 97^{o}c, and LC20 showed the endothermic peak at 169^{o}c.

Chitosan powder (M) showed the melting endotherm at 171^{o}c and a small endotherm at 98^{o}c. M0 showed the endothermic peak at 170^{o}c and two small endothermic peaks at 98^{o}c and 253^{o}c. MA20 exhibited the endothermic peak at 178^{o}c; MB20 exhibited the endothermic peak at 171^{o}c and small endothermic peaks at 90^{o}c and 253^{o}c; and MC20 exhibited the endothermic peak at 175^{o}c and a small endothermic peak at 90^{o}c. The weight loss of this system could be ordered as followed :M0>MC20>MA20<MB20>M.

Chitosan powder (H), and free films of H0 and HA20 showed the endothermic peak at 181^{o}c, 167^{o}c and 175^{o}c respectively. HB20 exhibited the endothermic peak at 170^{o} and small endothermic peaks at 98^{o}c and 145^{o}c, while HC20 displayed the endothermic peak at 164^{o}c and a small endothermic peak at 94^{o}c. The weight loss of this system could be ranked as followed : HC20>H0>HA20>HB20>H.

In summary, the endothermic peak of chitosan L occurred at lower temperature than chitosan M and chitosan H exhibited the highest endothermic temperature. The non-plasticized free films of three chitosan grades showed a similar

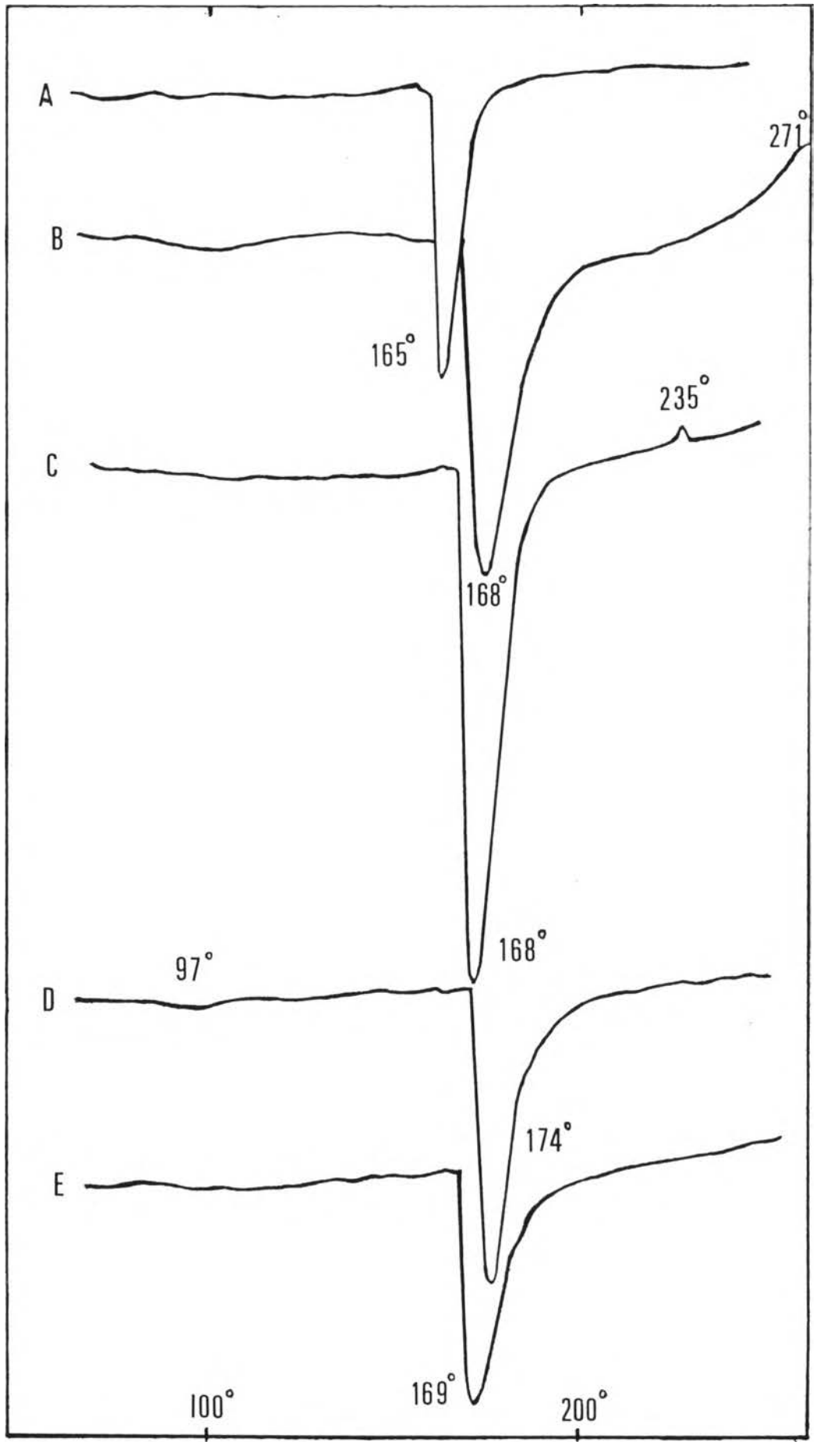

Figure 72 DTA thermograms of chitosan L powder and free films (key:A-L, B-L0, C-LA20, D-LB20, E-LC20).

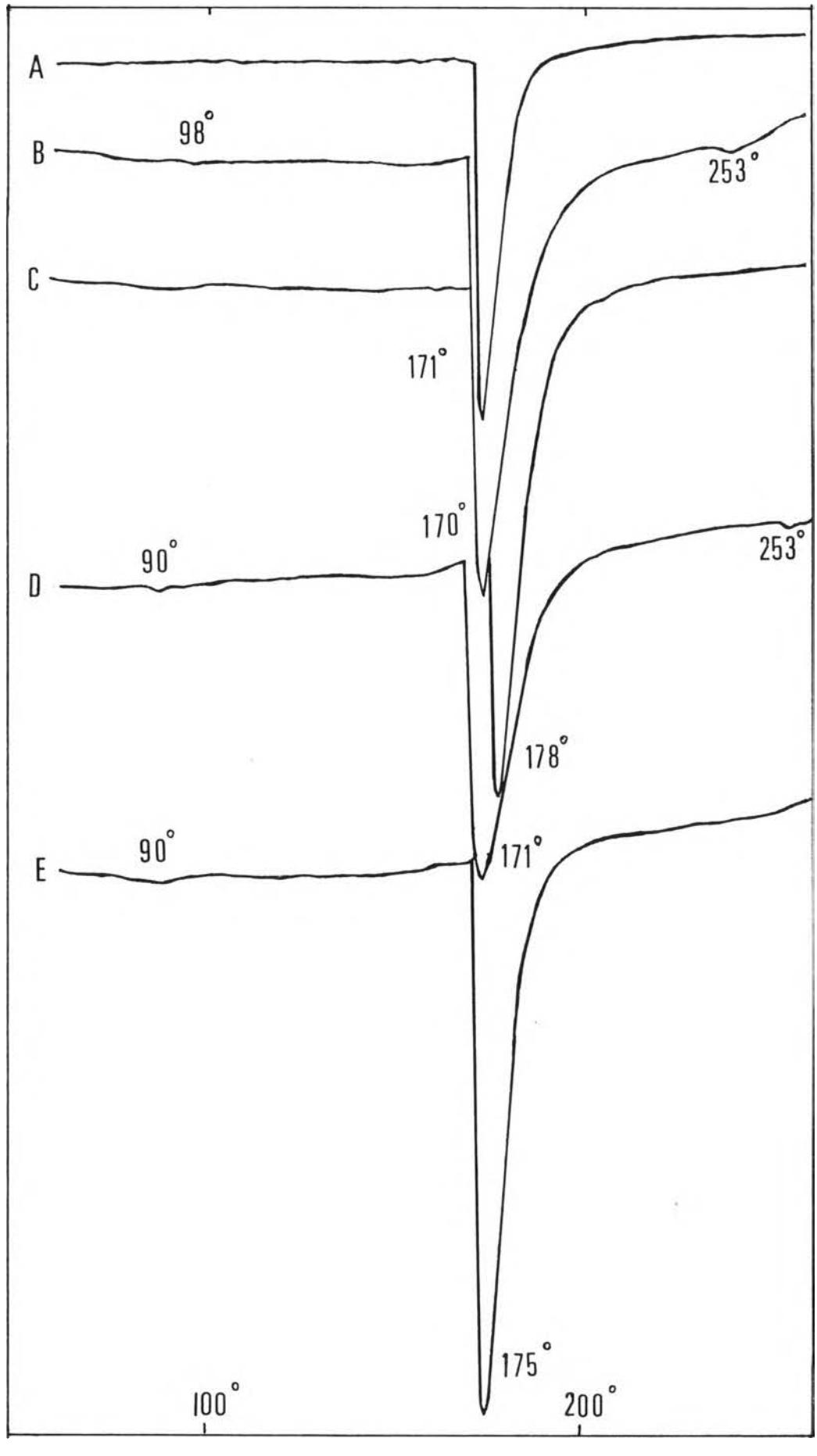

Figure 73 DTA thermograms of chitosan M powder and free films (key:A-M, B-M0, C-MA20, D-MB20, E-MC20).

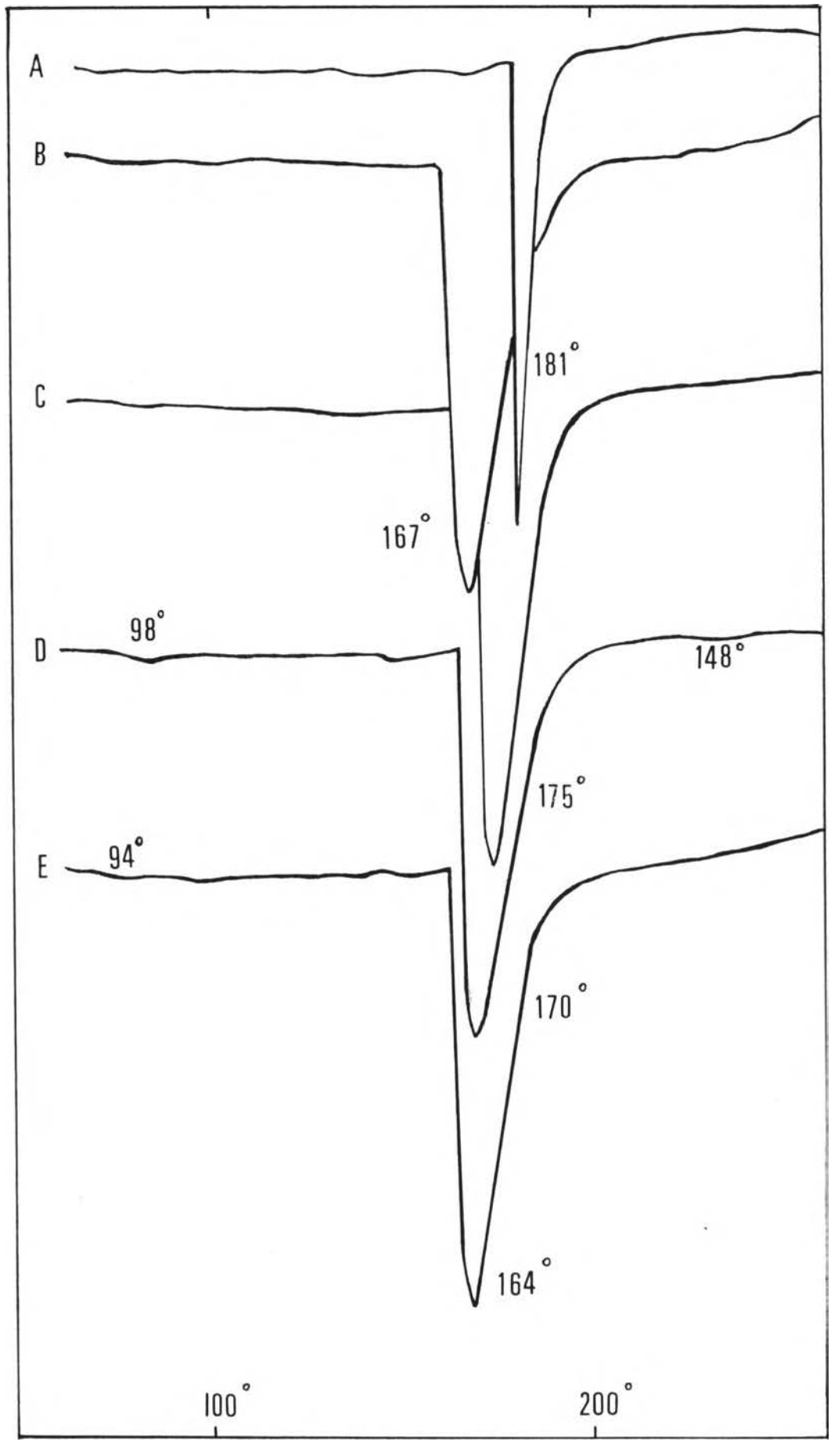

Figure 74 DTA thermograms of chitosan H powder and free films (key:A-H, B-H0, C-HA20, D-HB20, E-HC20)

Table 19 The summary of melting point peaks and weight loss of chitosan powders and free films.

FORMULAR	MELTING POINT PEAK (CELCIUS DEGREE)	OTHER PEAK (CELCIUS DEGREE)	WEIGHT OF SAMPLE(mg)BEFORE TEST	WEIGHT OF SAMPLE(mg)AFTER TEST	WEIGHT LOSS(mg)
L	165		7.5	(-)	*
L0	168	271 EX	10.8	(-)	*
LA20	168	235 EX	9.2	(-)	*
LB20	174	97 EN	9.9	(-)	*
LC20	169		10.1	(-)	*
M	171	98 EN	8.5	7.5	1
M0	170	98 EN, 235EN	10	6.6	3.4
MA20	178		10.1	7	3.1
MB20	171	90 EN, 253 EN	9.8	7.3	2.5
MC20	175	90 EN	10.2	7	3.2
H	181		7.5	6.6	0.9
H0	167		10.1	6.6	3.5
HA20	175		10	6.8	3.2
HB20	170	98 EN, 148 EN	10	7.5	2.5
HC20	164	94 EN	10.1	6.4	3.7

EN =Endothermic peak

EX =Exothermic peak

* =no measurement

melting endothermic temperature. The plasticized free films showed different endothermic peaks which were not much more different. The resultant of a weight loss displayed that chitosan powder showed the lowest, followed by the free films which was plasticized with PEG400 and propylene glycol respectively. The highest weight loss could be observed from M0 in the chitosan M free films and HC20 in chitosan H free films.

5. The moisture sorption.

Alteration of the film weight represented the moisture sorption ability are presented in Table 20.

The moisture sorption of L0 was nearly equal to that of H0 and was greater than that of M0, however those of L0, M0 and H0 were less than that of LH0. The moisture sorption of chitosan free films plasticized with propylene glycol was rather greater than those plasticized with triacetin, but rather less than those plasticized with PEG400, however the relationship between the amount of plasticizer and degree of moisture sorption could not be clearly observed. Almost moisture sorptions of free films slightly gradually reduced upon longer storage time.

6. Swelling of free films

6.1 Weight swelling index (w)

The data of film swelling which was determined by the weight difference in deionized water and in dilute HCl(1:100) solution are shown in Table 31 and 32 respectively in Appendix III.

The swelling index of free films which was determined by measurement the weight difference between before and after submersion in deionized water and dilute HCl (1 : 100) solution are illustrated in Figure 75 A and B respectively.

After submersion in deionized water, unplasticized free films exhibited rather higher swelling index(w) than plasticized free films except MC10 , LHA10 and LHA30 which showed reversed results. For unplasticized free films, MO exhibited higher swelling index(w) than HO, followed by LO and LHO respectively. Similar results appeared in the plasticized

Table 20 The moisture sorption of free films.

FORMULA	INCREASED WEIGHT AVG(SD)(%)		
	7 DAYS	10 DAYS	15 DAYS
L0	16 89(0 92)	17.21(1 02)	16 22(1 10)
M0	12 92(0 34)	14 02(0 70)	12 62(1 46)
H0	17 07(0.14)	16 80(0 82)	15 25(1 06)
LA10	18 89(0 61)	19 54(0 35)	17 55(0 52)
LA20	18 37(0 43)	17 64(0 510	16 08(0 25)
LA30	19 55(2 41)	17 27(2 65)	16 49(2 82)
LB10	17 05(0 54)	15 22(0 58)	15 53(0 84)
LB20	24 44(0 85)	22 82(0 95)	24 38(1 30)
LB30	22 03(0 76)	21 70(0 05)	20 47(0 72)
LC10	17 45(1 69)	16 89(1 41)	16 89(1 30)
LC20	15 54(0 93)	14 91(0 89)	13 66(1 11)
LC30	9 63(1 21)	8 60(1 44)	7 76(1 57)
MA10	16 73(1 64)	14 02(1 24)	12 80(1 17)
MA20	11 72(0 64)	9 17(0 60)	8 43(0 91)
MA30	19 96(1 32)	17 28(1 30)	15 36(1 51)
MB10	22 77(1 07)	21 26(0 78)	20 39(0 66)
MB20	20 11(0 13)	20 57(1 69)	23 66(4 68)
MB30	21 18(1 02)	21 41(2 300	18 40(2 23)
MC10	12 16(1 73)	10 45(1 27)	9 67(1 56)
MC20	16 68(0 54)	19 66(0 77)	15 28(0 34)
MC30	15 36(1 14)	10 87(0 83)	6 94(1 14)
HA10	14 86(0 60)	13 78(0 87)	13 68(0 98)
HA20	12 22(1 05)	10 51(1 03)	12 78(2 35)
HA30	13 50(0 66)	11 43(0 69)	11 75(1 08)
HB10	20 45(0 18)	18 06(0 58)	19 13(0 16)
HB20	21 62(0 84)	19 51(1 09)	20 75(0 82)
HB30	25 05(1 99)	17 12(1 24)	15 13(1 58)
HC10	10 48(2 25)	9 28(1 97)	8 26(2 38)
HC20	14 85(0 85)	14 53(1 01)	14 34(0 94)
HC30	13 43(0 16)	13 01(0 46)	13 85(0 81)
LH0	20 11(1 00)	19 66(1 10)	19 80(1 31)
LHA10	14 66(0 82)	13 24(0 34)	14 10(0 46)
LHA20	18 98(1 09)	15 83(0 65)	12 92(0 69)
LHA30	20 83(0 86)	17 96(1 29)	14 32(1 47)

films that M free films showed rather higher swelling index(w) than H free films, followed by L and LH free films.

For LA, MA, MB and MC free films, as the percentage of plasticizer increased, the swelling index (w) had a tendency to decrease. For LB and LC free films, the highest weight swelling index (w) could be observed in the free films of 20% plasticizer, followed by those of LB10 and LB30 and those of LC30 and LC10 respectively.

HA free films exhibited the highest swelling index in HA30, followed by that of HA10 and HA20 respectively. For HB free films, the highest swelling index could be obsered in HB20, followed by that of HB10 andHB30 respectively. HC free films exhibited the highest swelling index in HC20, followed by HC30 and HC10 respectively.

For LHA system, the highest weight swelling index (w) could be observed in the free film of LHA10, followed by LHA30, LH0 and LHA20.

LB free films exhibited rather higher swelling index than LC and LA systems respectively. For M free films, MB showed rather higher swelling index (w) than MA free films, but less than MC10 and MC20. The swelling of the film of MC10 was apparently higher than that of M0, and that of MC20 was slightly less than that of M0.

After submersion in dilute HCl (1:100) solution, unplasticized free films showed rather higher swelling index than plasticized free films except that the weight swelling index (w) of the free films of LB20,LB30,LC20 and LC30 was higher than that of L0, and that of MC10 was higher than that of M0. In the case of the free film of H0, the weight swelling index (w) was apparently higher than that of M0, followed by that of LH0 and L0 respectively.

For LA and LHA free films, as the percentage of plasticizer increased, weight swelling index (w) had a tendency to decrease. For LB,MB, MC and HB free films, as the percentage of plasticizer increased, weight swelling index (w) had a tendency to increase. For LC, HA and HC free films, the highest weight swelling index (w) could be observed in the free film containing

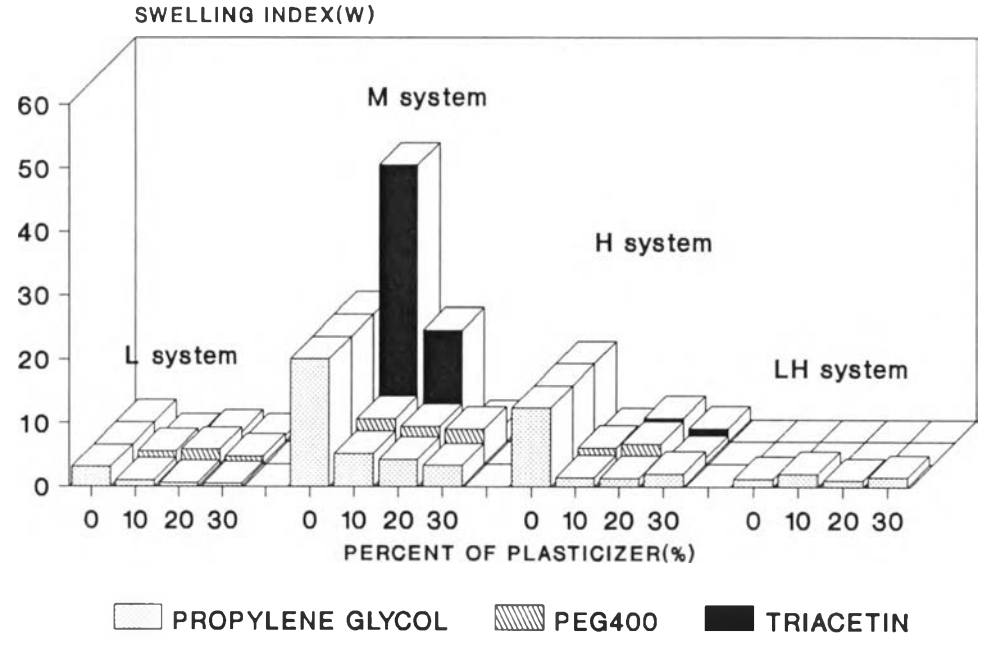

A

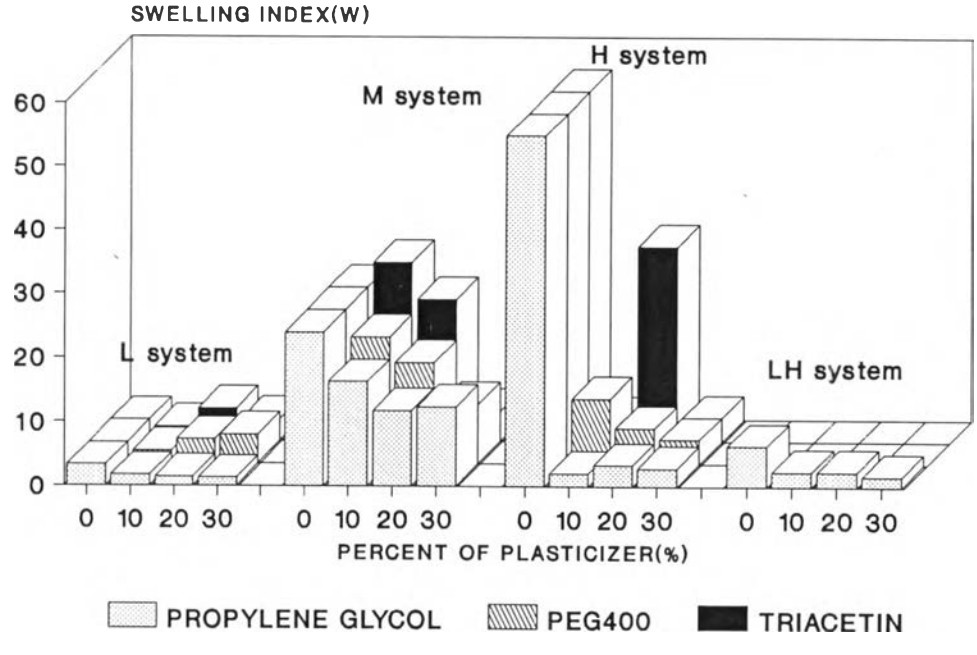

B

Figure 75 The weight swelling index(w) of free films determined by measurement the weight difference(key:A-indeionized water, B-in dilute HCl(1:100) solution).

the plasticizer at 20 % w/w , followed by that containing the plasticizer at 30 % w/w and 10 % w/w respectively.

For MA system, MA10 showed the highest weight swelling index(w), followed by MA30 which slightly higher than MA20.

LA free films exhibited rather less swelling index than that of LB and LC systems. For M free films, the swelling index of free films submerged in dilute HCl (1 : 100) solution was similar to that of the free films which was submerged in deionized water. HB tablets showed rather greater weight swelling index (w) than HA free films, but apparently less than HC20.

The weight swelling index (w) of free films submerged in dilute HCl (1:100) solution was rather greater than that of the free films submerged in deionized water.

6.2 Volume swelling index (v)

The swelling index of free films determined by the volume difference is illustrated in Figure 76 A and B respectively and the data are presented in Table 33 and 34.

After submersion in deionized water, the volume swelling index(v) of free films had a similar pattern to that determining using weight difference, except that the volume swelling index (v) was higher than weight swelling index (w). For HB free films, as the percentage of plasticizer increased,volume swelling index (v) had a tendency to decrease and for LB free films, LB30 exhibited the highest volume swelling index(v), followed by LB10 which was nearly to LB20.

After submersion in diluted HCl (1 : 100) solution, the swelling index of free films had a similar pattern to that determining using weight difference, except that M0, H0 and MC10 showed very high swelling and could not be measured, and the swelling index of the free film of MB20 was higher than that of MB10 and MB30 respectively.

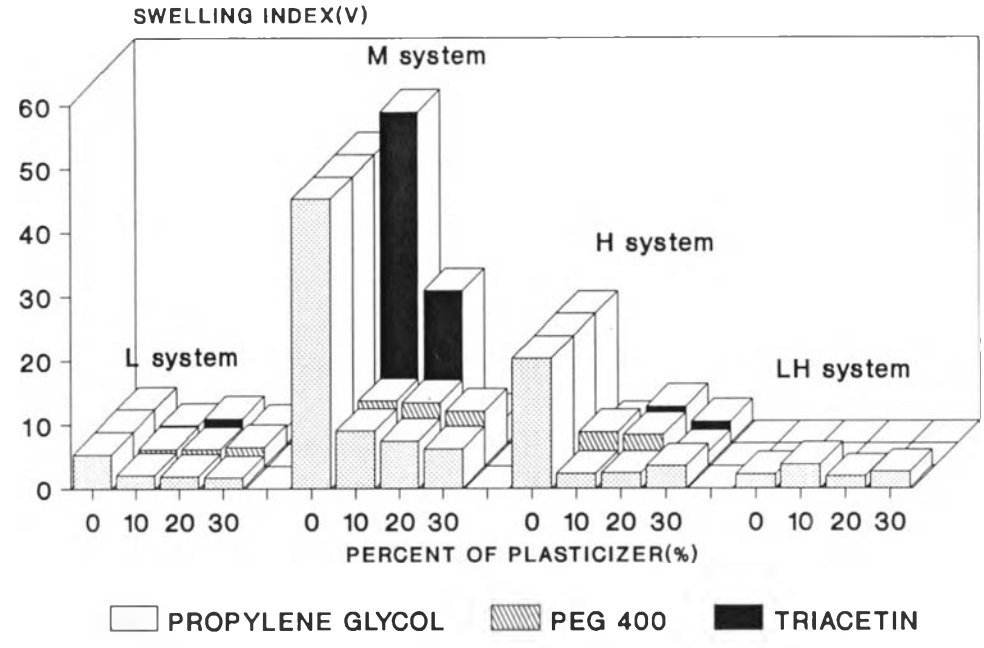

A

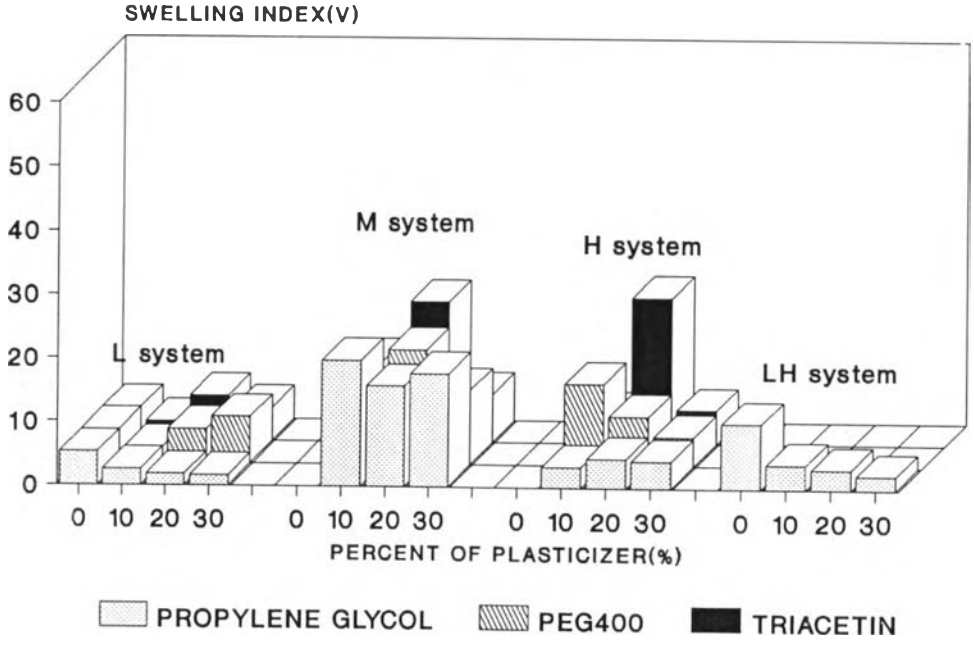

B

Figure 76 The volume swelling index(v) of free films determined by measurement the volume difference(key:A-in deionized water, B-in dilute HCl(1:100) solution).

7. Tensile properties

The ultimate tensile strength and percentage of elongation of prepared free film are presented in table 35 in Appendix III and graphically shown in Figure 77 A and B and Figure78 A and B.

For unplasticized free films, L0 showed the lowest ultimate tensile strength, followed by M0 and H0 respectively, and LH0 showed slightly higher than H0. L0 exhibited the highest percentage of elongation, followed by M0, LH0, and H0 respectively, however LH0 exhibited slightly higher percentage of elongation than that of H0, and L0 showed slightly higher percentage of elongation than M0, but apparently higher than H0 and LH0.

The relationship between the ultimate tensile strength and percentage of elongation, and the type and amount of plasticizers could not be clearly observed, but might be mentioned that L free films exhibited rather less ultimate tensile strength than M free films, followed by H free films. MC free films showed apparently higher ultimate tensile strength than MB, MA and L free films, and HC free films showed higher ultimate tensile strength than HA, HB and LH system. As the percentage of propylene glycol increased, LH free films had tendency to decrease the ultimate tensile strength and increase the percentage of elongation.

The stress strain curves of free films of L0, M0 and H0 are portrayed in Figures 79 A, B and C respectively The ultimate tentile strenght of the free films of L0, M0 and H0 was 5.186, 7.522, 8.805 kg/mm^2, and the percentage of elongation was 11.28, 20.24 and 25.18 respectively. From the stress strain curves, the tensile property of these free films was similar to the plastic like material which could be more stretched whenapplying the force .

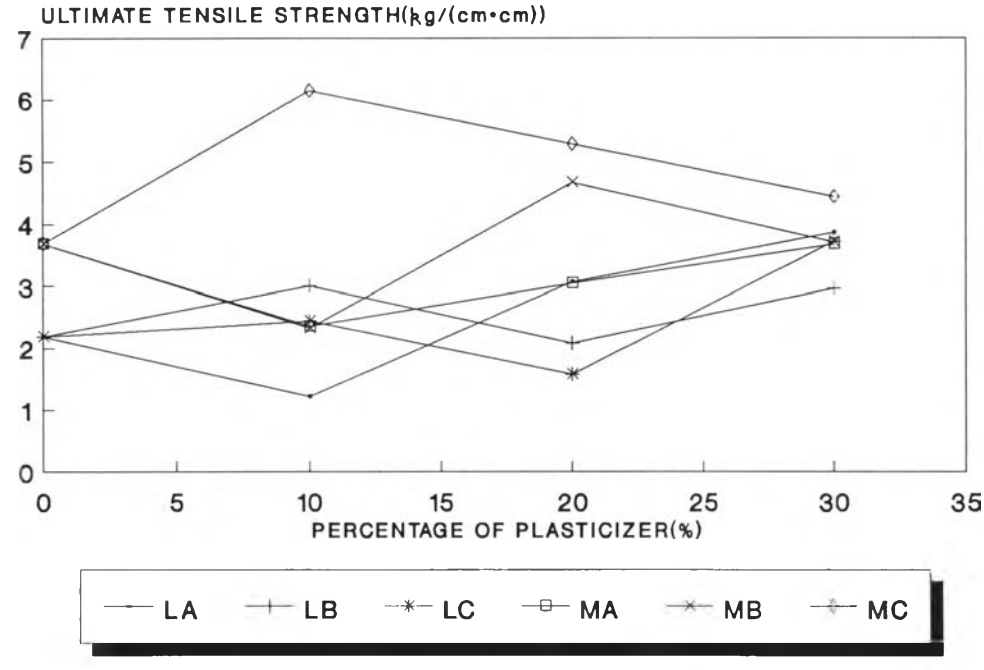

A

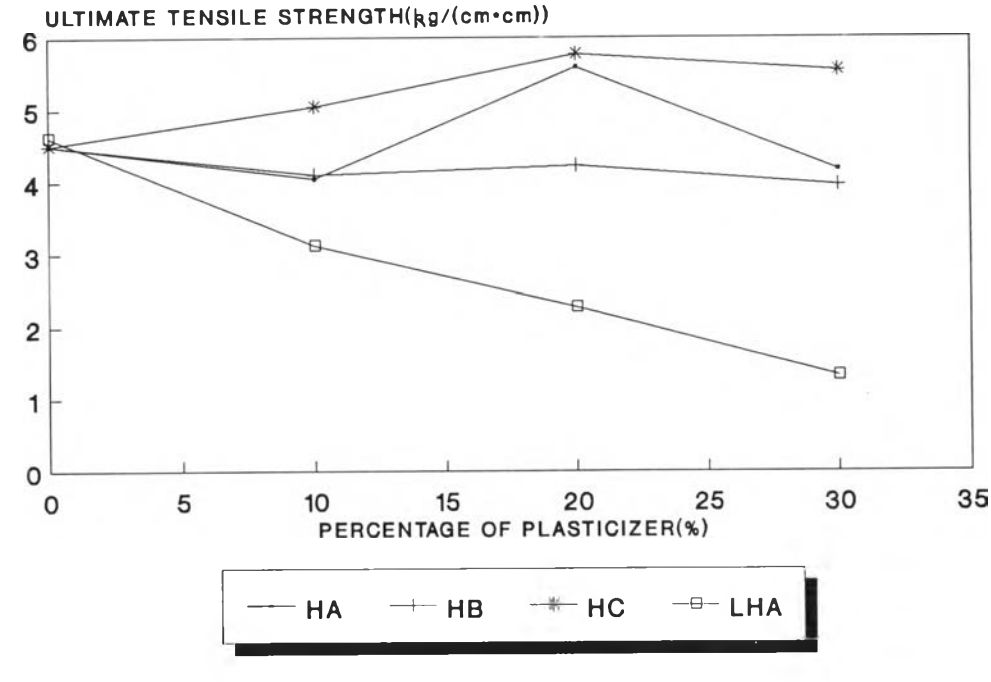

B

Figure 77 The ultimate tensile strength of free films(key:A - LA,LB,LC, MA, MB, MC free films, B-HA, HB,HC, LHA free films).

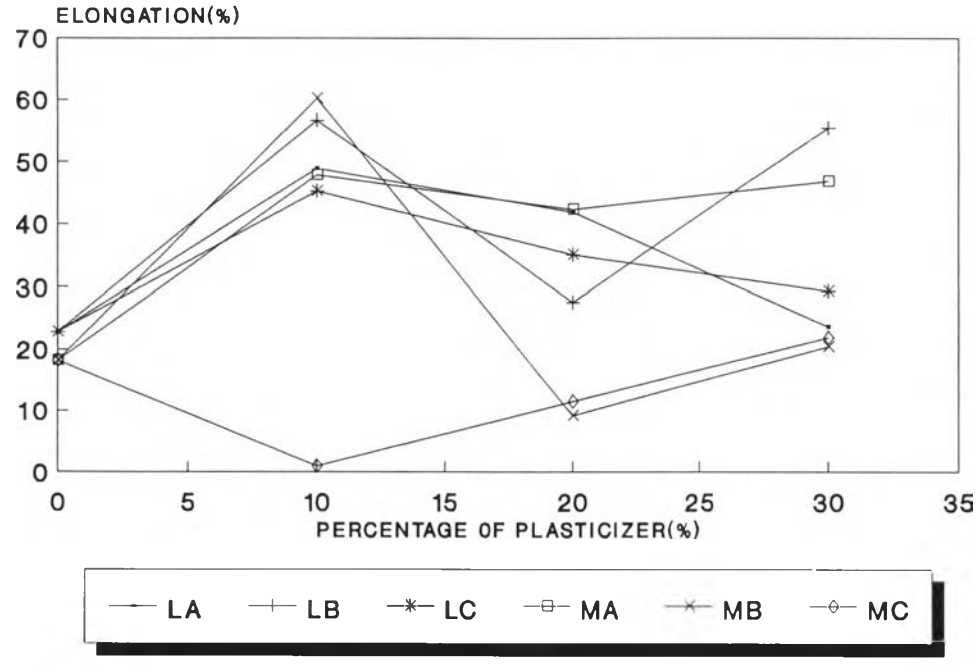

A

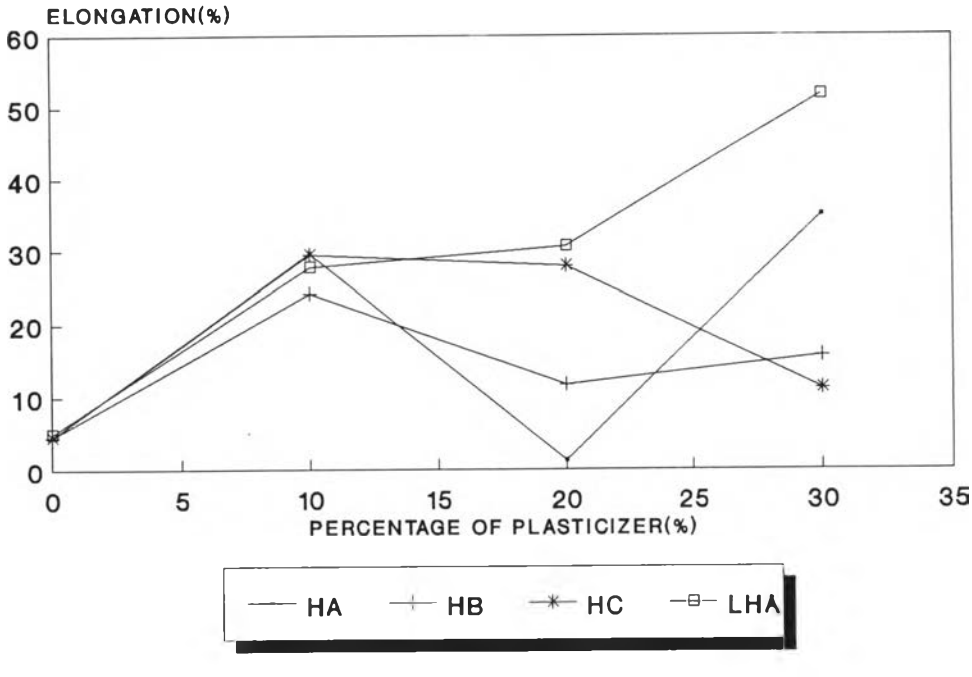

B

Figure 78 The percentage of elongation of free films(key:A-LA, LB,LC, MA, MB, MC free films, B-HA, HB,HC,LHA free films).

Figure 79 The stress-strain curves of free films(key:A-L0, B-M0, C-H0).

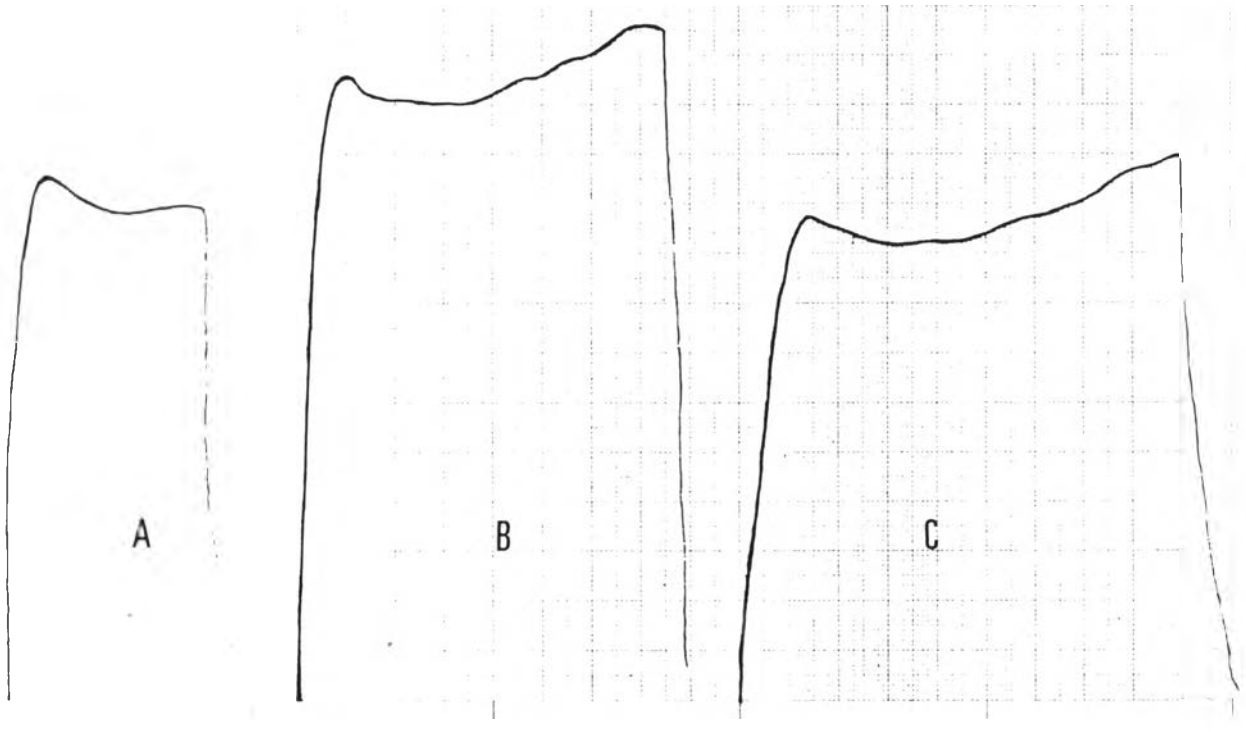

	FORMULAR		
	L0	M0	H0
THICKNESS(mcm)	69	66	50
	73	68	45
	72	65	46
	68	64	47
	71	64	48
AVG(SD)	70.60(2.07)	65.40(1.67)	47.20(1.92)
BREAKING FORCE(Kg)	2.087	2.804	2.369
ULTIMATE TEN.(Kg/mm*mm)	5.186	7.522	8.805
%ELONGATION	11.28	20.24	25.18

Table 21 The ultimate tensile strength and percentage of elongation of free film.